Optimization of heterogeneous bio-based catalysts and synthesis of inorganic equivalent for large-scale biodiesel production

A Thesis

Submitted to the Faculty of Graduate Studies and Research

in Partial Fulfillment of the Requirements

for the Degree of

Master of Applied Science

in

Process Systems Engineering

University of Regina

by

Mariam Hanson

Regina, Saskatchewan

January 2025

UNIVERSITY OF REGINA

FACULTY OF GRADUATE STUDIES AND RESEARCH

SUPERVISORY AND EXAMINING COMMITTEE

Mariam . Hanson, candidate for the degree of **Master of Applied Science in Process Systems Engineering,** has presented a thesis titled, ***Optimization of heterogeneous bio-based catalysts and synthesis of inorganic equivalent for large-scale biodiesel production,*** in an oral examination held on **December 11, 2024**. The following committee members have found the thesis acceptable in form and content, and that the candidate demonstrated satisfactory knowledge of the subject material.

External Examiner:	Dr. Farshid Torabi, Energy & Process Systems Engineering
Supervisor(s):	Dr. Raphael Idem, Industrial & Process Systems Engineering
Committee Member:	Dr. Teeradet Supap, Adjunct, Faculty of Engineering and Applied Science*
Committee Member:	Dr. Hussameldin Ibrahim, Industrial & Process Systems Engineering
Chair of Defense:	Dr. Abu Bockarie, Adult Education & Community Engagement and Human Resource Development (AHRD)

*Unable to attend

ABSTRACT

This research focuses on optimizing the production of biodiesel to reduce overdependence on fossil fuels by utilizing waste resources. In recent years there have been concerns on the use of fossil fuels in the increasing demand of energy and its drawbacks. Fossil fuels, unlike biodiesel, are carbon rich and hence on combustion, releases excessive amounts of CO_2, NO_X and SO_X leading to global warming.

In this research, waste cooking oil (WCO) and ethanol were used as the main raw materials to produce biodiesel known to have net zero carbon emission potential to meet Canada's commitment to attain net zero carbon emissions by 2050. In providing alternative use for waste resources, waste eggshells, cow bones, fish scales and banana peels were investigated, characterized and optimized to manufacture high performing Lewis base catalysts to obtain high biodiesel yield in a transesterification reaction.

Initially eggshell, fish scale and cow bone catalysts all of which are primarily calcium based were studied and optimized by varying mix procedure, mix ratio as well as impregnating 1%, 5% and 10% by weight of potassium promoters. Physical mixing, 1:6:3 (ES: FS:CB) mix ratio, 10% potassium impregnation were the obtained optimum and a 75% biodiesel yield was obtained when 1:6:3 + 10% K catalyst was used.

Due to the low biodiesel yields obtained there was a need to investigate other biobased materials with Lewis base potential. This led to the shift to potassium based biobased material, banana peels for optimization and use as transesterification catalyst. The banana peels were calcined at 600℃ (BP600), 800℃ (BP800), 900℃ (BP900) and 1000℃ for optimization. The yield on calcining at 1000℃ was not

enough to carry out a reaction. BP900 had the best performance yielding up to 96.16% biodiesel.

An inorganic replica of the optimum biobased catalyst BP900 was prepared using inorganic precursors due to the drawbacks of the biobased catalyst (low calcination yield of 10%, not available in large commercial quantities) via co-impregnation (BPIn1) and coprecipitation methods (BPIn2). BPIn 2 had a biodiesel yield of 84.58% and was used for further studies.

The effect of reaction time, temperature, catalyst amount and ethanol to oil ratio (E:O) on the biodiesel yield were checked and the optimum conditions were 6 hours, 70℃, 2wt%, 21:1 respectively. The viscosity, acid value and density were determined according to ASTMD, and results were within acceptable standards. TGA, XRD, SEM/EDS, N_2 Physisorption and CO_2 TPD analysis were performed on catalysts to determine their characteristics. Kinetic data was obtained for BPIn2 catalyst by varying the E:O, reaction time and reaction temperature for 2wt% catalyst dose runs to obtain various biodiesel yields. NLReg software was used to regress the data to obtain an activation energy (Ea) of 39.07kJ/mol, collision factor (k0) of $1.5*10^6$ $/g_{cat}.h.\ mol^{5.6}$, an order with respect to ethanol (e) of 3, and an order of reaction with respect to oil (o) of 2.

ACKNOWLEDGEMENT

My utmost appreciation goes to the almighty God for grace and strength in seeing me through to the completion of both my master's degree coursework and thesis.

I am thankful to Dr. Raphael Idem for the opportunity to work under his supervision and guidance throughout my thesis as well as Dr. Natewong Paweesuda, Dr. Teeradet Supap, Mr. Foster Appiah, Ms. Jessica Naarku Tetteh and all CETRI members for their selfless contributions during my research journey.

Special acknowledgement to Mr. Ebenezer Ekow Hanson for financial support towards my master's tuition and to the Natural Sciences and Engineering Research Council of Canada (NSERC) through the Discovery Grant of Dr. Raphael Idem, the Faculty of Graduate Studies and Research (FGSR), and the Clean Energy Technologies Research Institute (CETRI).

DEDICATION

I dedicate this research work to God almighty, my father Mr. Ebenezer Ekow Hanson, my mother Mrs. Umuhani Iddrisu Hanson, my sister Irie Nana-Esi Hanson and my brother Surajdeen Hanson.

TABLE OF CONTENTS

LIST OF TABLES

LIST OF FIGURES

TRANSPARENCY STATEMENT

I made use of ChatGPT open AI in summaries, paraphrasing and generating some ideas for aspects of my thesis especially with the introduction, literature review and a bit of the experimental section.

The use of the mentioned technology is approved by my supervisor and supervisory committee for the stated purposes. No other AI- technologies were used in the writing of this thesis. I acknowledge that output from AI sources can be discriminatory, incomplete, inaccurate or bias and I have taken necessary action to curb such occurrence. The academic integrity and accuracy of this thesis are entirely my responsibility.

CHAPTER 1: INTRODUCTION

1.1 World energy demand and related CO_2 emissions

It is essential to view energy as a basic human necessity equal with food, air, water and earth. According to (World Energy outlook, 2023) there was a 1.3% increase in the 2022 energy demand globally. This growth in energy demand is mostly attributed to population growth and expanding economies. Fossil fuels (Figure 1) are reported to represent approximately 80% of the global supply of energy (World Energy outlook, 2023) due to its high energy content, availability and advancement in technology for harnessing its energy.

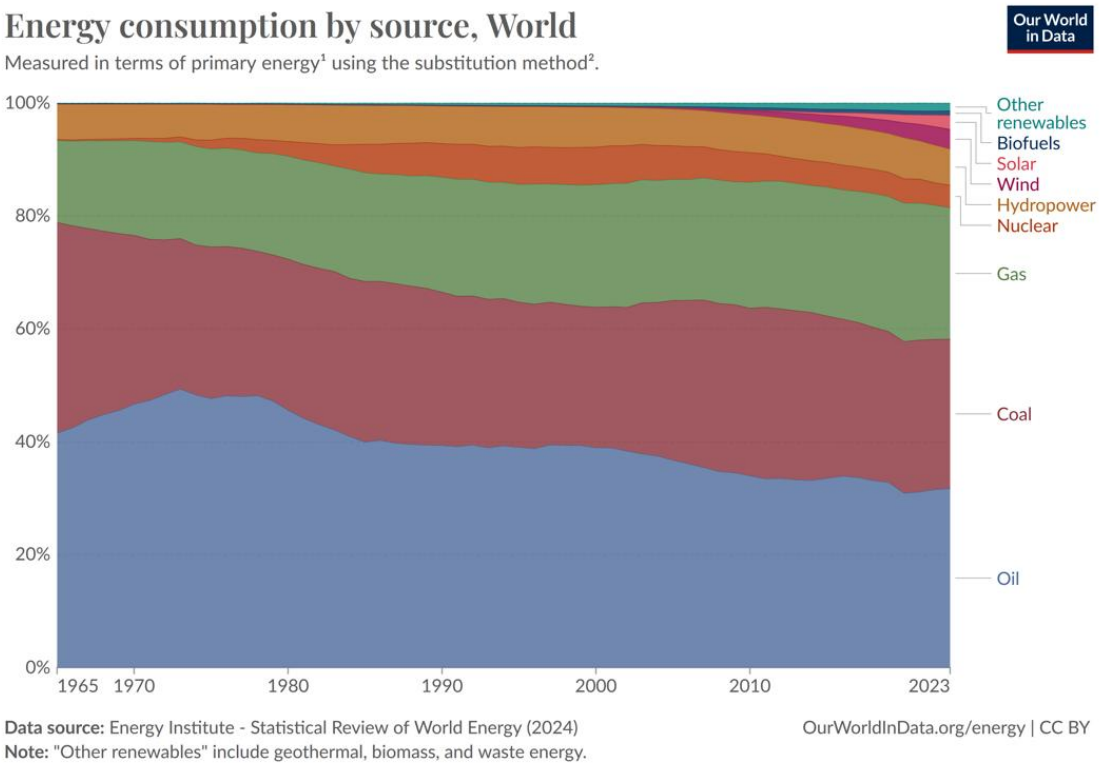

Figure 1: *Global energy consumption by Energy source (Our world in data, 2024)*

The world faces a drawback in fossil fuels control due to the high amounts of greenhouse gases released into the atmosphere during its processing as shown in

Figure 2 and Table 1. The year, 2022, saw a 1% increment in CO_2 release because of a 1.8% rise in the use of fossil fuel energy (U.S. EPA, 2024). Despite the challenges, the coal combustion sector observed a 6.1% decrease in its CO_2 emissions between 2021 and 2022. Per projections, it is salient to enhance low carbon emission energy sources; hydropower(Bertassoli et al., 2021), wind energy(Ghenai, 2012), solar energy(Ludin et al., 2018) and biofuels(Jeswani et al., 2020) to cater for the increasing energy requirement. Environmental concerns on climate change and global warming impact have also imposed restrictions on fuel combustion emissions(Borges & Díaz, 2012),(Leung et al., 2010a)

Gas	1990	2005	2018	2019	2020	2021	2022
CO_2	4,752,232	5,744,134	4,988,198	4,852,631	4,341,710	4,654,265	4,699,403
CH_4	602	467	445	453	376	379	401
N_2O	229	255	161	156	138	147	156

Table 1: *CO_2, CH_4 and N_2O Emissions from fossil fuel combustion(kt)* (U.S. EPA, 2024)

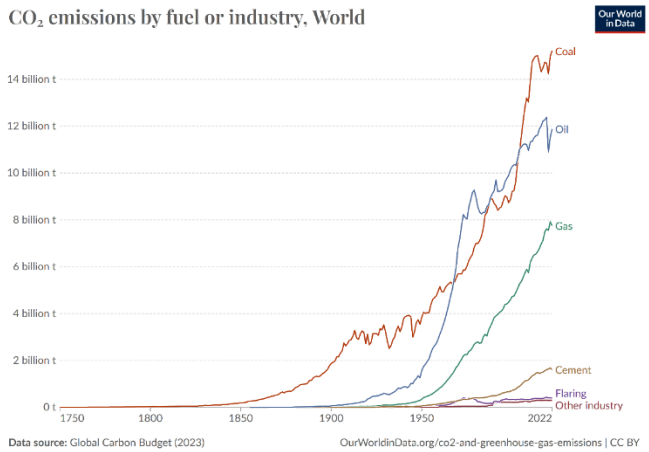

Figure 2: *CO_2 emissions by fuel type and industry (data, 2024)*

1.2 Role of biodiesel in world energy supply

Biodiesel, a renewable energy source, is an alternative fuel for conventional fossil produced diesel such that no engine modification is required in its use(Enweremadu &

Mbarawa, 2009). Typically, it is produced via an organic reaction known as transesterification. In transesterification, an ester is transformed into a new ester based on the type of alcohol used. This transformation is due to the exchange of alkoxy moiety between the reacting ester and alcohol(Schuchardt et al., 1998). In biodiesel production, the original ester usually has a long chained alkoxy group (high molar mass, high density, high fatty acid content and is unsuitable for use in diesel engines) while the original alcohol is mostly short alkoxy chained. Through the reaction which is hastened by using a base or an acid catalyst to increase biodiesel yields, a shorter alkoxy ester and a long alkoxy chained alcohol are produced. The combustion profile of biodiesel is such that relatively low amounts of carbon monoxide, particulate matter and unburnt hydrocarbons are emitted relative to diesel derived from petroleum sources (Y. Chen et al., 2009). There is no sulfur compound emitted in its use(Osman et al., 2021) and due to its excellent lubricating properties, engine wear is reduced by 30%(Agarwal et al., 2003).

Biodiesel is produced in a variety of purity levels; 100% pure biodiesel, B100 as well as in a blend with petroleum diesel. B5 (5% biodiesel), B2 (2% biodiesel) and B20 (20% biodiesel) blends are the most common.

1.3 Increasing yield of biodiesel

Biodiesel is regarded as an environmentally friendly and renewable alternative to fossil fuels, and is synthesized from animal fats, vegetable oils, or recycled greases through transesterification. The economic viability and sustainability are crucially dependant on the efficiency of the biodiesel production pathway. These strategies to enhance biodiesel production yield, focusing on feedstock optimization, process improvements, and technological advancements are discussed below.

1.3.1 Optimization of biodiesel Feedstock

Feedstock choice significantly influences biodiesel production yield. High oil content feedstocks, such as algae, waste cooking oils and jatropha are being studied to enhance their potential. Algal biomass can be cultivated on non-arable land and offers high lipid yields (up to 60% of its dry weight) (Chisti, 2007a). Cheap feedstocks, including animal fats and waste cooking oils, not only reduce costs but also enhance sustainability (Chhetri et al., 2008). Additionally, genetically modified organisms (GMOs) that produce higher lipid contents are being explored, though their use is subject to regulatory and public acceptance issues (Yuan, 2019).

1.3.2 Process improvement

Enhancing the transesterification process can significantly increase biodiesel yield. Traditional processes typically require catalysts (alkaline or acidic) that can lead to soap formation and reduce yield. Employing enzymatic transesterification can improve yield by minimizing side reactions, especially when using high free fatty acid (FFA) feedstocks (Hahn-Hägerdal, 2006). Moreover, optimizing conditions of transesterification, such as pressure, temperature, and time, can maximize yield. For instance, using supercritical methanol conditions has shown to increase yield by overcoming mass transfer limitations (Díaz et al.,2012).

1.3.3 Technology advancement

Innovative technologies are pivotal in boosting biodiesel production. Membrane technology, such as pervaporation, can separate glycerol from biodiesel in situ, shifting equilibrium towards biodiesel production and improving overall yield (Díaz

et al., 2012). Furthermore, the application of microwave and ultrasonic technologies has the potential to increase transesterification reaction rates, resulting in shorter reaction times with higher yields (Muthu & Priya, 2017).

1.3.4 Integration of waste management

Utilizing waste materials not only provides an economical feedstock but also addresses waste disposal issues. The integration of biodiesel production with existing waste treatment facilities can further enhance yield and efficiency. For example, integrating biodiesel production with anaerobic digestion systems can utilize glycerol produced as a byproduct, maximizing resource use (Berglund & Börjesson, 2006). Increasing biodiesel production yield is a multifaceted challenge that can be addressed through feedstock optimization, process enhancements, and the adoption of advanced technologies.

1.4 CO_2 emission reduction in the use of biodiesel

Vegetable oils, animal fats, and algae derived biodiesel are increasingly recognized as a sustainable substitute for fossil derived fuels. The major environmental benefits biodiesel provides is its low Carbon dioxide (CO_2) emission potential. Biodiesel contributes to CO_2 emission reduction, comparing it to conventional diesel and examining its lifecycle impacts.

1.4.1 Carbon neutrality of biodiesel

The primary argument for biodiesel's role in CO_2 emission reduction is its potential for carbon neutrality. When biodiesel is burned as fuel, it emits CO_2; however, the feedstocks used to produce biodiesel which is primarily plants sourced oil and

alcohol, absorb CO_2 during their growth phase for photosynthesis. This cycle of carbon absorption and emission can lead to a net-zero carbon footprint over the lifecycle of the fuel (A. Demirbas, 2007). Studies show that the net CO_2 emissions from biodiesel can be significantly lower than those from fossil diesel. For instance, a lifecycle assessment of biodiesel from soybeans indicated a reduction of greenhouse gas emissions by up to 57% compared to petroleum diesel ((USDA), 2016).

1.4.2 Reduction in fossil fuel dependency

By substituting fossil fuels with biodiesel, countries can reduce their reliance on fossil fuel, which is a significant source of CO_2 emissions. This transition not only diminishes the overall carbon footprint but also enhances energy security. Biodiesel can be blended with petroleum diesel, allowing for immediate reductions in fossil fuel consumption while utilizing existing infrastructure (Y. Zhang et al., 2003).

1.4.3 Improved combustion properties

Biodiesel has different combustion characteristics compared to petroleum diesel, often resulting in lower particulate matter and soot emissions. Although both biodiesel combustion and diesel derived from fossils combustion led to direct CO_2 emissions, the cleaner burn can significantly reduce greenhouse gases, such as carbon monoxide and unburned hydrocarbons, which can indirectly contribute to a lower overall greenhouse gas profile (Biodiesel.org, 2021). The reduction in these pollutants further enhances the climate benefits associated with biodiesel use.

1.4.4 Lifecycle Emissions considerations

While biodiesel significantly reduces CO_2 emissions compared to fossil fuels, it is essential to consider the entire lifecycle, including land use changes, agricultural practices, and processing emissions. Some studies indicate that land-use changes associated with biodiesel crop production can lead to increased CO_2 emissions, offsetting some benefits (Searchinger, 2008). However, sustainable agricultural practices and the use of waste feedstocks can mitigate these effects, emphasizing the importance of sourcing and production methods in evaluating overall emissions. (R. Chen et al., 2018) reported in a life cycle assessment of biodiesel that 76% GHG emission reduction is attainable relative to petroleum diesel without considering indirect land use change (ILUC) and 66% to 72% when ILUC is considered. A Life cycle analysis completed by Argonne National Laboratory found that emissions for 100% biodiesel (B100) are 74% lower than those from petroleum diesel (US Department of energy, 2008)

1.4.5 Policy and market Implications

The potential for CO_2 emission reduction through biodiesel has led to various policy incentives globally, promoting the adoption of biofuels. Governments are increasingly implementing mandates and subsidies to encourage the use of biodiesel, aiming to reduce greenhouse gas emissions and meet renewable energy targets (Nikolina, 2016). These policies can enhance market stability and encourage technological advancements in biodiesel production, further contributing to emission reductions. The use of biodiesel presents a viable strategy for reducing CO_2 emissions when considered within a comprehensive lifecycle framework. Its carbon-neutral potential,

combined with improved combustion properties and reduced reliance on fossil fuels, highlights its significance in addressing climate change.

1.5 Scope and Objectives of this Research

This research focuses on exploring the heterogeneous catalytic potential of bio-based waste resources to produce biodiesel through a base catalyzed transesterification reaction. Eggshells, fish scale, cow bone and banana peel all which are waste are to be optimized by selecting the best calcination temperature, best mix procedure, best mix ratio, best promoter and its amount to be impregnated on the bio-based catalyst to obtain high biodiesel yield. An inorganic replica of the best performing biobased catalyst will be prepared by different procedures to provide an alternative for situations where the waste resources are in low supply for large scale biodiesel production. The effect of the reaction conditions (temperature, time, ethanol to oil ratio, catalyst dosage) on biodiesel yield will be checked. Kinetic analysis will be performed to determine the activation energy, and order of reaction in the use of one of the catalysts in transesterification reaction.

The main objectives of this research are as follows.

1. Optimize eggshell, fish scale and cow bone in a tri-blend and banana peel (individually) to produce heterogeneous biobased catalyst with high biodiesel production yield in the use of waste cooking oil and ethanol as feedstock.
2. Synthesize best performing biobased catalyst with inorganic precursors (an inorganic replica) and check how the various rection conditions affect its biodiesel yield.
3. Perform kinetic studies on the best performing inorganic replica catalyst

This thesis consists of five main chapters.

Chapter 1: this is the introduction section, and it introduces the purpose, scope and objectives of this work. Its basis is rooted in the world energy demand, supply and alternative clean energy requirements for a sustainable future. It also selects biofuels specifically biodiesel as its target alternative clean energy and discusses ways of boosting biodiesel production.

Chapter 2: this chapter is the literature review section, and it reviews existing literature on biomass to renewable and clean energy pathways. It delves deeper into the biodiesel production methods, transesterification catalysts, sourcing transesterification catalysts from waste sources, characterizing catalysts and maximizing biodiesel yield.

Chapter 3: this is the experimental section. It outlines the materials and step by step methods taken to prepare the catalysts and conduct the experimental run. It provides a pictorial illustration of the experimental setup, and the conditions utilized in the experimental runs.

Chapter 4: this is the results and discussion section. Here, the results obtained from experimental runs are provided with observations and trends discussed. Procedures for the analysis of the data obtained are also explained.

Chapter 5: this is the conclusion and recommendation section. It summarizes the research results and ensures that all set objectives for this work were achieved. Recommendations on areas to explore in future research about the findings of this work are given in this section.

CHAPTER 2: LITERATURE REVIEW

2.1 Energy Generation Pathway Using Biomass

The world is gradually seeking for the need to substitute fossil fuels with sources of renewable such as solar energy, wind energy, geothermal energy, biomass energy, and hydroelectric energy (Figure 3) to mitigate the inevitable effects in the long term overdependence on fossil derived fuels (climate change, global warming and air pollution) and provide a sustainable development (Owusu & Asumadu-Sarkodie, 2016) alongside attaining sustainable development goal (SDG) 7 i.e. affordable and clean energy (Gebara & Laurent, 2023), SDG 9 i.e. industry, innovation and infrastructure (Kynčlová et al., 2020), and SDG 13 i.e. Climate action (Prag, 2017). Alternative energy sources which are sustainable, renewable and have environmentally benign potential to meet Canada's commitment to attain net zero carbon emissions by 2050 (Canadian net zero accountability act/law, 2021) are required.

In the year 2020, 7669TWh of renewable electricity was produced globally(global bioenergy statistics report, 2023).

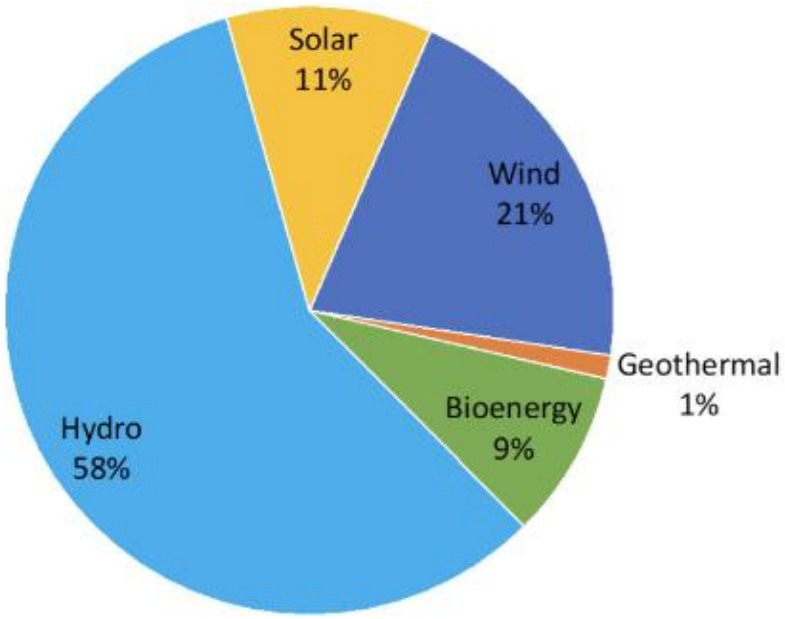

Figure 3: Renewable power generation (GLOBAL BIOENERGY STATISTICS REPORT, 2023b)

Due to these fossil fuel drawbacks, biomass is taking over as the most widely used alternative renewable energy source since its use especially in the transportation industry e.g. Biodiesel does not require engine modifications (Enweremadu & Mbarawa, 2009), (Owusu & Asumadu-Sarkodie, 2016).

Studies have shown that the only renewable energy source that allows storage and release when the need arises is biomass (Moriarty & Honnery, 2019b). The remaining renewable energy sources only exist as energy flows(Moriarty & Honnery, 2019a). This therefore makes it more desirable for use as transportation fuel.

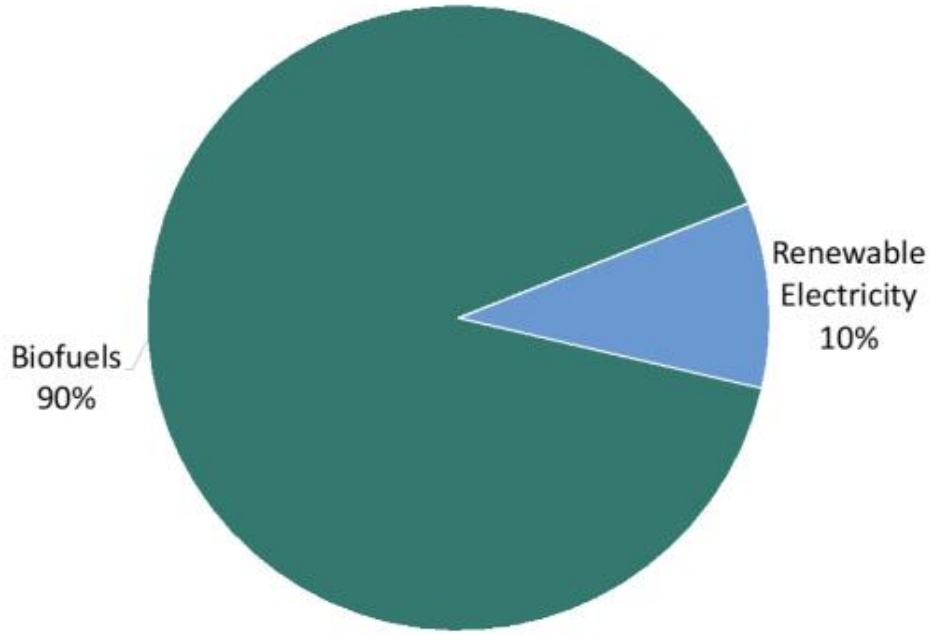

Figure 4: Renewable energy use in transport (GLOBAL BIOENERGY STATISTICS REPORT, 2023a)

As per the most recent global data from the (global bioenergy statistics report, 2023), renewable energy is responsible for 20% of the globally consumed energy from which biofuels account for 90% of renewable energy use in the transportation sector globally (Figure 4) but 99% in the Americas (Global bioenergy statistics report, 2023).

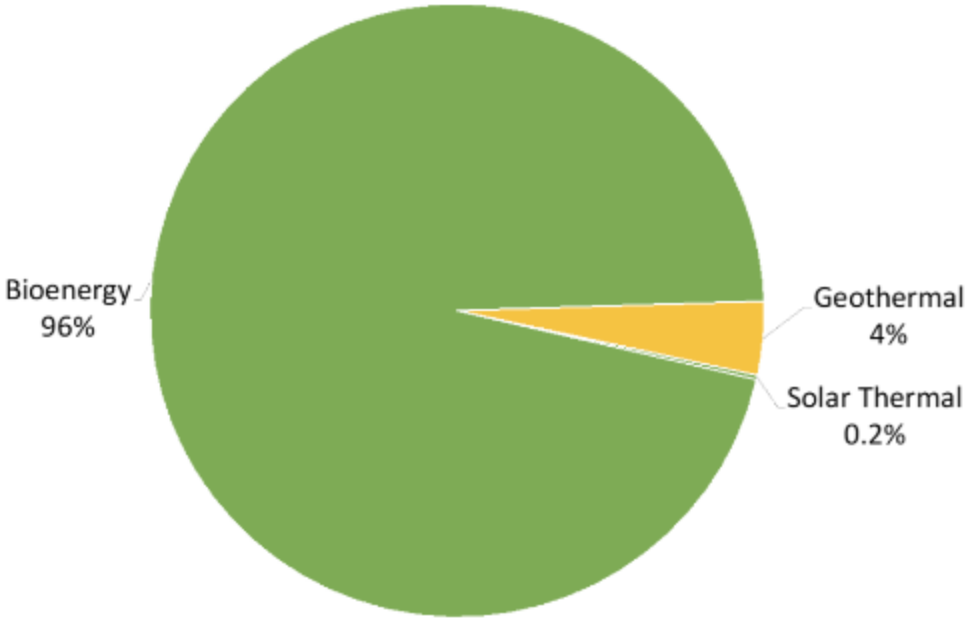

Figure 5: Renewable heat production (GLOBAL BIOENERGY STATISTICS REPORT, 2023b)

Biomass is renewable organic matter originating from animals and plants. It remains a salient source of fuel in numerous countries, especially for household heating (Figure 5) and cooking in developing countries (Martínez-Patiño et al., 2017). In developed nations, the use of biomass for electricity generation and transportation is on the rise in curbing the impacts of carbon dioxide emissions from fossil fuels. Biomass sources of energy (Figure 6 and Figure 7) include a variety of materials such as municipal waste materials, waste from wood and wood processing, animal manure, human sewage and residues and agricultural crops (Perea-Moreno & Kalak, 2023). The main sources are illustrated in figure 6.

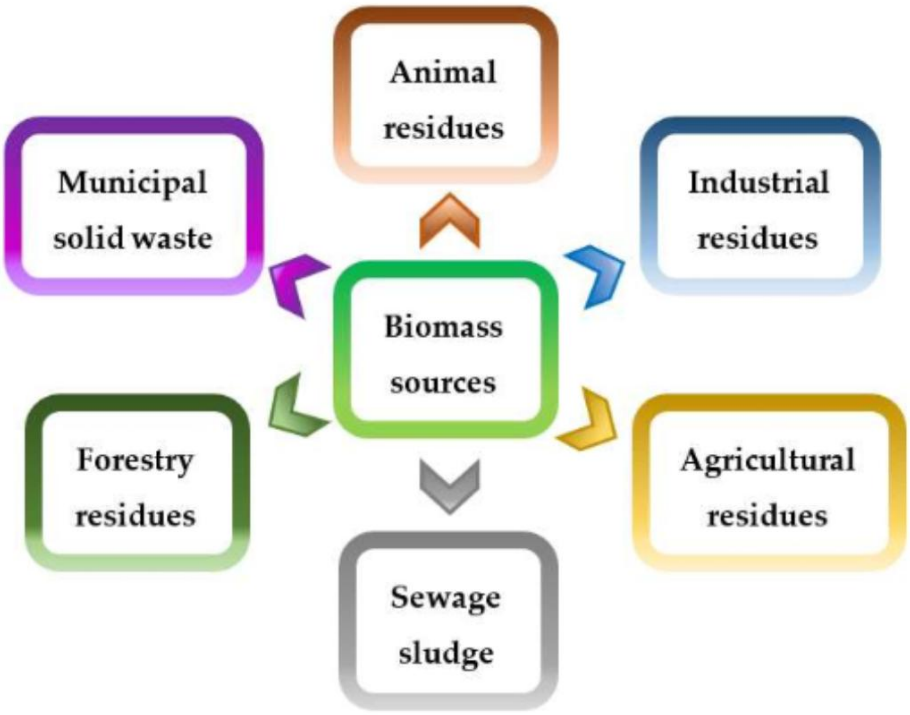

Figure 6: Biomass energy sources (Perea-Moreno & Kalak, 2023)

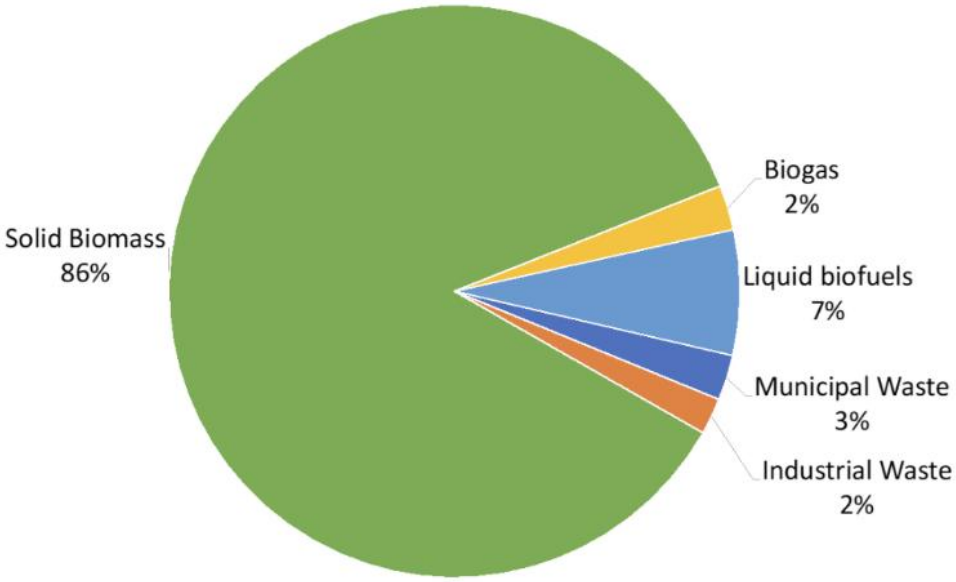

Figure 7: Domestic supply of biomass (GLOBAL BIOENERGY STATISTICS REPORT, 2023b)

Biomass stores chemical energy originally obtained from the sun. Through photosynthesis, plants produce biomass. Utilizing biomass simply accelerates the

release of carbon dioxide (CO_2), which plants subsequently absorb to create more biomass (Tursi, 2019a). Figure 8 shows the cycle carbon follows from biomass generation to its utilization (Owusu & Asumadu-Sarkodie, 2016; Tursi, 2019a)

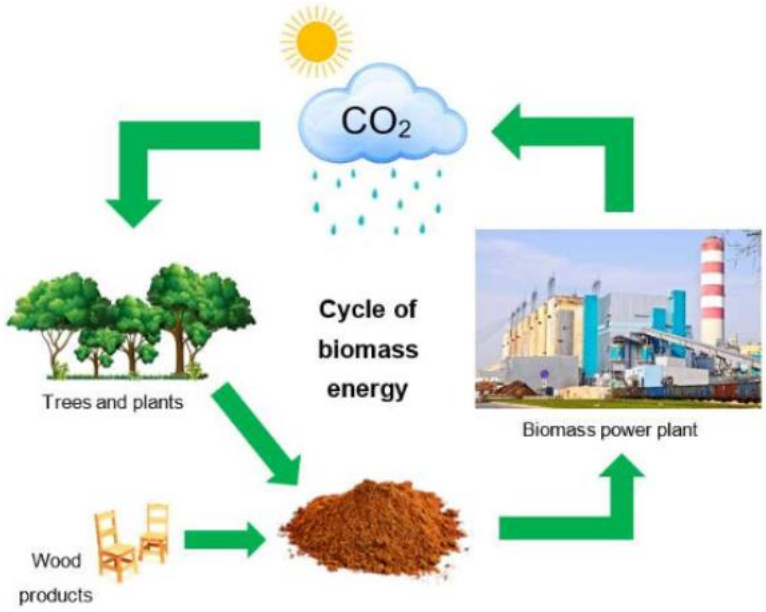

Figure 8: Cycle for carbon flow of biomass from production to use in power generation (Perea-Moreno & Kalak, 2023)

Biomass is from plant and animal resources and has the potential to be used as an energy source. The abundance, affordability and availability of biomass is an incentive to reduce energy dependance on fossil-based fuels. Countries with technological advancement utilize large amounts of firewood, animal waste, and agricultural waste for heating and cooking. However, the unsustainable commercial utilization of biomass can pollute the environment via air pollution. Locally, ducks, pigs, chickens and ducks are fed with agricultural and food waste(Sivabalan, 2021) . Biomass waste is produced in significant quantities worldwide that is; corn stover (128.02 million tons), rice straw (about 731.3 million tons), sugarcane bagasse (180.73 million tons), and wheat straw (354.34 million tons) are the most produced agricultural waste yearly (Sarkar et al., 2012).

Asia leads in the production of wheat and rice straw, while America remains the world's largest producer of sugarcane bagasse and corn stover (Saini et al., 2015). According to statistics, the annual biomass production in Europe is about 950 million tons. This has the potential to supply fuel of about 300 million tons to substitute petroleum derives fuel (Perea-Moreno & Kalak, 2023). Approximately 65% of Europe's total oil consumption can be supplied from waste biomass resources potentially (Stout, 2012).

A variety of energy carriers can be gotten from biomass depending on the conversion process utilized. These processes include chemical conversion, direct combustion, biochemical conversion, and thermochemical conversion (Bhatia et al., 2021). While several factors impact the choice of conversion method, the biomass quantity and quality, the processing cost and sustainability of the targeted product are salient factors to consider (Dalena et al., 2017; Tursi, 2019a).

2.2 Converting Biomass to Energy

There are three major processes used in the conversion of biomass to energy.

1. Biochemical conversion
2. Thermochemical conversion
3. Chemical conversion

2.2.1 Biochemical conversions

This technology utilizes enzymes, bacteria and other biological agents to degrade biomass to produce carbohydrates and later convert it to biogas, liquid fuels and other bio products (Mahalaxmi, 2014). Fermentation and anaerobic digestion are amongst the common biochemical technologies in use (Brethauer & Studer, 2015). The action

of biological organisms is slow, and this influences the nature of biochemical processes leading to a reduced temperature requirement and slow reaction rate while higher temperatures and fast reactions occur in thermochemical processes (Rabaçal et al., 2012)

2.2.1.1 Anaerobic digestion

This process involves four individual stages, namely acidogenesis, hydrolysis, methanogenesis and acetogenesis and contributes to effective breakdown of waste there by serving as a waste management pathway for renewable energy production(Zamani Abyaneh et al., 2022) . Microorganisms facilitate chemical reactions in series in an oxygen deprived environment making use of natural metabolic processes to produce simpler molecules such as methane, carbon dioxide and traces of gases (biogas) and a slurry digestate from the breakdown of large organic macromolecules (Zamani et al., 2019. Agricultural residues and animal manure from farms, sewage sludge, and municipal solid waste are among the feedstock often utilized (M. K. Sharma & Kazmi, 2015). Figure 9 shows a process flow diagram in the generation of renewable energy via anaerobic digestion.
Although there is a decrease in the energy content by 20% to 40% in the production, biogas has the potential to be used in numerous applications such as gas turbines and ignition gas engines. It is more effective when used on organic waste feedstock consisting of 80% to 90% moisture (Sreekrishnan et al., 2007).

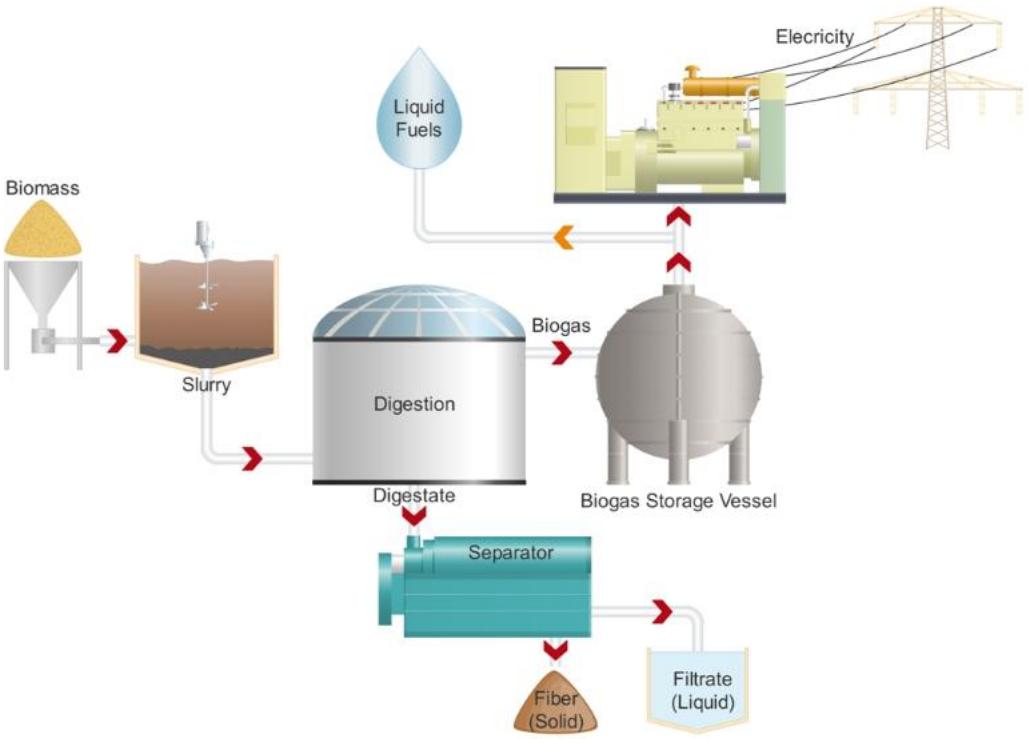

Figure 9: Biomass anaerobic digestion flow diagram (Tursi, 2019a)

Hydrolysis is the first stage of the process during which relatively small molecules (simple sugars, amino acids and fatty acids) are produced from the digestion of huge organic polymers (proteins, fats and carbohydrates) (Horan et al., 2018). Hydrogen and acetate are the byproducts produced (Rabaçal et al., 2017).

Acidogenesis is characterized by the further digestion of simple sugars, amino acids and fatty acids facilitated by fermentative bacteria (acidogenic microorganisms) yielding ammonia, carbonic acids, hydrogen gas, fatty acids, lighter volatile fatty acids, alcohols, carbon dioxide, and hydrogen sulfide. This process only carries out a partial decomposition reaction leading to the requirement of one more step to obtain the desired methane gas (Tursi, 2019a).

Acetogenesis involves the production of acetic acid, carbon dioxide and hydrogen gas from the further breakdown of acidogenesis stage products via acetogenic

microorganism action. The decomposition process is finally completed in this step by acetogens making methane production possible(Tursi, 2019a).

Methanogenesis is the last step of the oxygen deprived process where methane is obtained as the main product. Acetic acid and carbon dioxide undergo either acetolactic methanogenesis or hydrogenotrophic methanogenesis to form methane (Tursi, 2019a).

2.2.1.2 Fermentation

Fermentation biochemical process as shown in Figure 10 uses yeast under anaerobic conditions to undertake series of organic biochemical reactions to convert hexoses and pentoses (simple sugars) to alcohol (mostly ethanol) and carbon dioxide. The most used microorganism for this process is Saccharomyces cerevisiae. The feedstocks for this process fall into three categories: starches, lignocellulosic substrates and sugars. Theoretically, 100g of feed hexose or pentose produces 48.86g of carbon dioxide and 51.14g of ethanol. Carboxylic acids and glycerol are the byproducts in this reaction. The reaction temperature, microorganism, fermentation time and feedstock type affect the yield and quality products(Katrin Thommes, 2014).

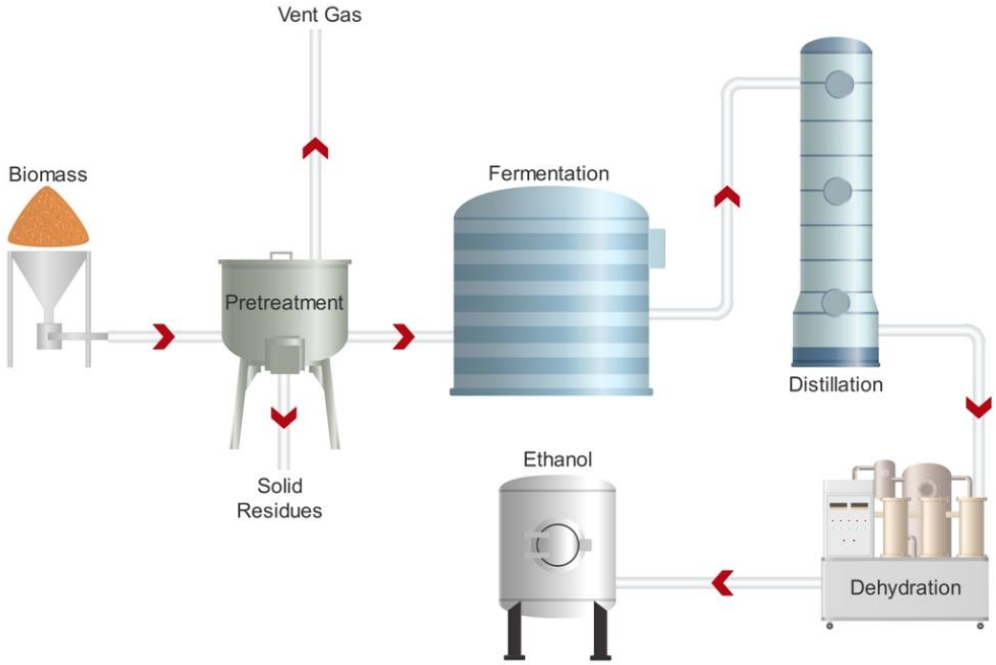

Figure 10: Biomass fermentation flow diagram (Tursi, 2019a)

The substrate plays a major role in the metabolic pathway to obtaining ethanol from sugar conversion (Taherzadeh & Karimi, 2008), glycolysis is used to convert hexoses including glucose whereas the pentose phosphate pathway is used for pentose conversions. Hexose gives faster rates ethanol conversions relative to its pentose counterpart.

The produced ethanol undergoes separations (distillation and dehydration) to enhance purity. The remaining solid product is either fed to livestock or used to produce gas by powering boilers (Mariod, 2016).

2.2.2 Thermochemical conversions

Elevated temperatures and rapid conversion rates distinguish thermochemical conversion. The three primary methods are partial oxidation (gasification), thermal decomposition in the absence of oxygen (pyrolysis) and complete oxidation

(combustion). Other examples include Fischer–Tropsch synthesis and liquefaction(Tursi, 2019b).

This process involves the biomass subjected to controlled heating (oxidation), synthesis gas is the intermediate produced, is further processed to obtain high value products(A. Demirbas, 2004; Tanger et al., 2013). Interconnected steps are involved in thermochemical refinery including pretreatment of feedstock (crushing and dehydration), feeding into reactor, conversion of feedstock into valuable products, separation of product to obtain high purity and conditioning, and finally to its end use (Tursi, 2019b).

Through thermochemical technologies, we obtain chemicals, fuels, and power form biomass. Factors including but not limited to pressure, feed rate, temperature, heating time, quenching processes and the biomass properties dictate the product quality and respective amounts. Figure 11 illustrates the biomass conversion that is based on thermochemical processes.

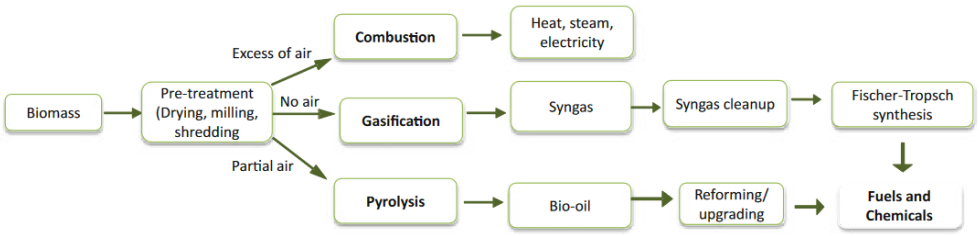

Figure 11: Flow diagram of thermochemical conversion process (Rabaçal et al., 2017)

2.2.2.1 Combustion

Biomass combustion is the by far the most established power and heat generation thermochemical conversion method. It accounts for over 97% of global bioenergy

production (A. Demirbas, 2004). The conversion of hydrocarbon content of biomass into water and carbon dioxide is via an exothermic combustion reaction with oxygen (Linan, 1993). Water is released directly through biomass drying and indirectly when volatiles undergo oxidation. Electricity and heat are the primary types of energy produced from combustion od hydrocarbons in biomass Basu et al.,2012a.

Significant particulate matter (PM) emissions, especially PM smaller than 1 µm, which is a key factor in relation to health impact of air pollution is produced (Fernandes & Costa, 2012)(Tanger et al., 2013). Incomplete combustion releases harmful intermediates like large oxygenated organic carbon species, NO_x, SO_x, volatile organic compounds (VOC), methane, carbon monoxide, and particulate matter (Tanger et al., 2013)

Due to the matured nature of this technology, further advancements are likely to provide only incremental improvements. Moreover, combustion produces heat, a challenging form of energy to store. While conversion efficiency is high when heat is the desired output, storing it remains difficult. When electricity is generated, the process efficiency is lower, and storing electricity in batteries is still not fully developed.

Large, medium, and small-scale commercial applications are available in energy generation via biomass combustion. EnSny is a large-scale bio-oil co firing plant implemented into existence (Tursi, 2019b).

2.2.2.2 Gasification

An oxygen deprived condition is salient in undertaking gasification reactions (Figure 12). This process uses one third of the oxygen required in complete combustion to carry out a biomass partial oxidation reaction thereby releasing energy. The product

of this exothermic reaction is syngas composed of a hydrogen carbon dioxide mix. This gas can function as a biofuel. There is an alternative where the syngas undergoes further processing to obtain other fuels and chemicals through Fischer Tropsch method to yield high grade organic acids, ammonia, alcohols and other products (Cherubini et al., 2010; Tanger et al., 2013)

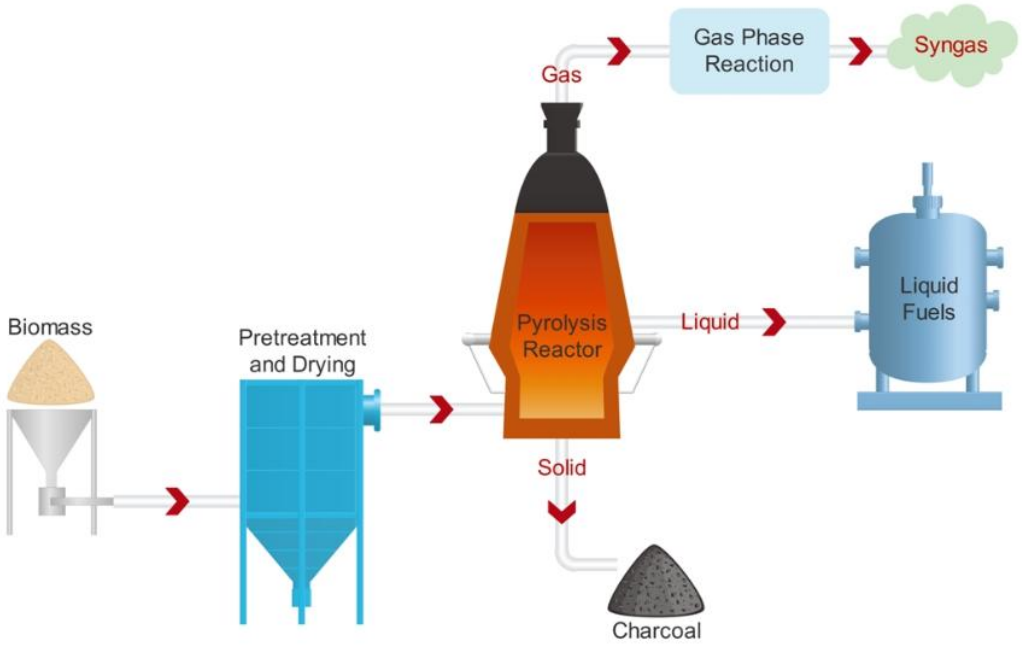

Figure 12: Biomass gasification flow diagram (Tursi, 2019b)

One of the main challenges in biomass gasification is the formation of "tars" (Milne and Evans, 1998). These “tars”, along with some contaminants, need to be removed before fuel synthesis as they pose both operational difficulties and environmental pollution risks (Basu et al., 20122012a; Foust et al., 2009).

There is a recent springing interest in biomass gasification technique although it has limitations for commercial success due to competition with more established conversion processes. Its economic potential is low (Mitchell et al., 1995); (Bridgwater, 2012)

2.2.2.3 Pyrolysis

In this technique there is absence of oxygen while biomass is heated in such condition at relatively low temperatures as shown in Figure 13. In these recent decades, it has gained many interests because of its bioenergy production potential, converting biomass into valuable energy products and waste management (Liew et al., 2014). During pyrolysis, raw biomass is transformed into several products: gaseous products, solid biochar and liquid bio-oils (Fernández & Menéndez, 2011). Pyrolysis oil and gas and serve as cleaner, more efficient fuel types than solid biomass. There is the alternative where they are used as intermediates for other chemicals.

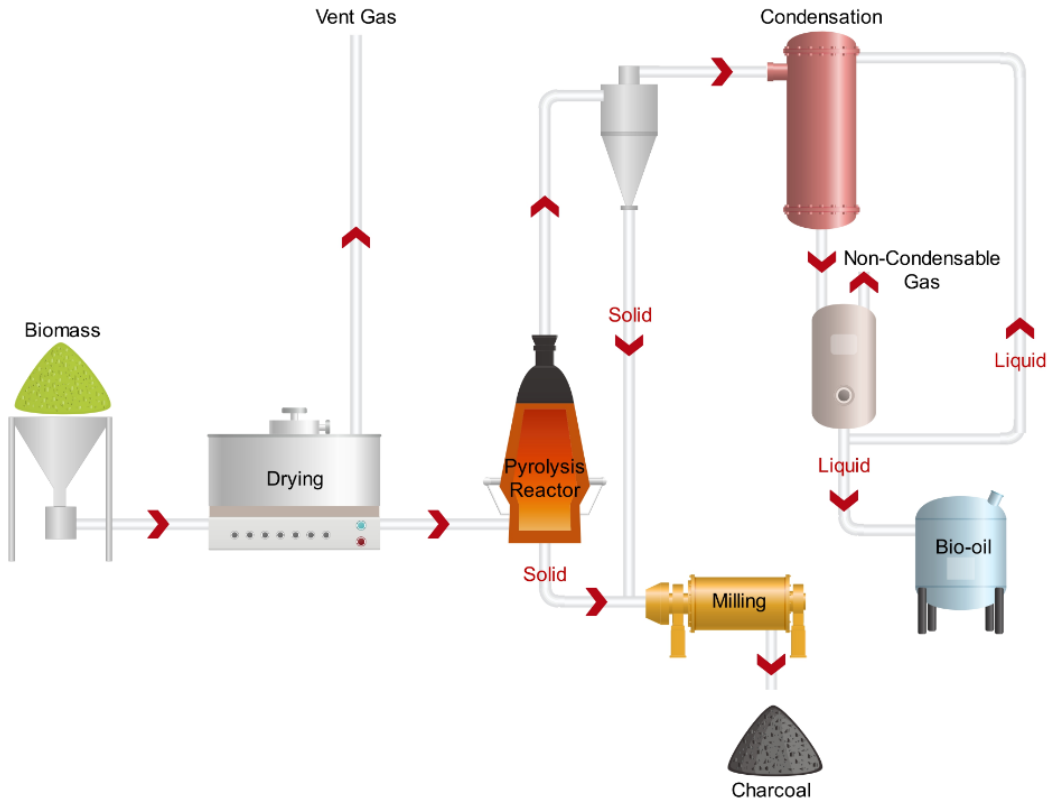

Figure 13: Biomass pyrolysis flow diagram (Tursi, 2019a)

The solid biochar contains varying amounts of inorganic materials, unconverted organic matter, and carbonaceous residues. When applied to soils, biochar offers

benefits and may reduce atmospheric carbon dioxide over time. Organic chemicals exist in a complex mixture in bio-oil (liquid component) ((Simões Da Silva, 2016). Pyrolysis has been used commercially transform biomass to produce solvents, other chemicals, and fuels. Traditionally, a relatively slower pyrolysis is used for char production, involves the gradual decomposition of biomass, while fast pyrolysis, with short residence times at moderate temperatures, is used to maximize liquid product yields (Yaman, 2004). (Bridgwater, 2012; Mitchell et al., 1995) With properly maintained storage conditions and product quality, biofuels have good storage lengths for future use unlike combustion.

Though still under development, bio-oil from pyrolysis shows promising, potential to lowering gasification costs compared to using a gasifier for solid biomass conversion (Bridgwater, (Mitchell et al., 2012; Mitchell et al., 1995). Thermo-catalytic conversion, including processes like liquefaction and Fischer–Tropsch synthesis, can also be considered. Liquefaction occurs at even lower temperatures with the help of catalysts, converting biomass into liquid fuel. This can be done through pyrolysis, gasification, or hydrothermal processes, where biomass is exposed to high temperatures (300–350°C) and pressures (12–20 MPa), resulting in oil production (Basu et al., 2012b).

Fischer–Tropsch synthesis is widely used to convert syngas from gasification into liquid transportation fuels. While this process is well-established, large-scale production may face catalyst shortages unless catalyst regeneration improves. This technology is commonly employed in commercial electricity generation and the production of synthetic fuels from conventional fossil fuels (Jeswani Balch et al., 2016)

2.2.2.4 Liquefaction

Liquefaction is a biomass conversion process (Figure 14) carried out in water at moderate temperatures between 280 and 370°C and high pressures of 10-25 MPa. This process produces a liquid bio granulate like crude oil, along with gaseous, aqueous, and solid by-products ((López Barreiro et al., 2013). The resulting product has a high heating value and low oxygen content, making it a chemically stable fuel. The main goal of liquefaction is to produce oil with a high hydrogen-to-carbon (H/C) ratio. There are two main types of liquefaction based on the raw material: lignocellulosic biomass (dry) and algal biomass (wet) liquefaction.

Both processes require pretreatment of the raw material, involving the removal of woody contaminants and the creation of a stable suspension. Alkaline treatments are typically used to reduce the particle size, allowing for easier pumping into reactors (Gollakota et al., 2018). The most common method utilizes lignocellulosic biomass processed at around 350°C and 150 bar for approximately 15 minutes. Under these conditions, phase separation naturally occurs, resulting in the formation of a gaseous CO_2 phase, solid residues, bio-crude, and a small aqueous phase (Rowbotham et al., 2012)

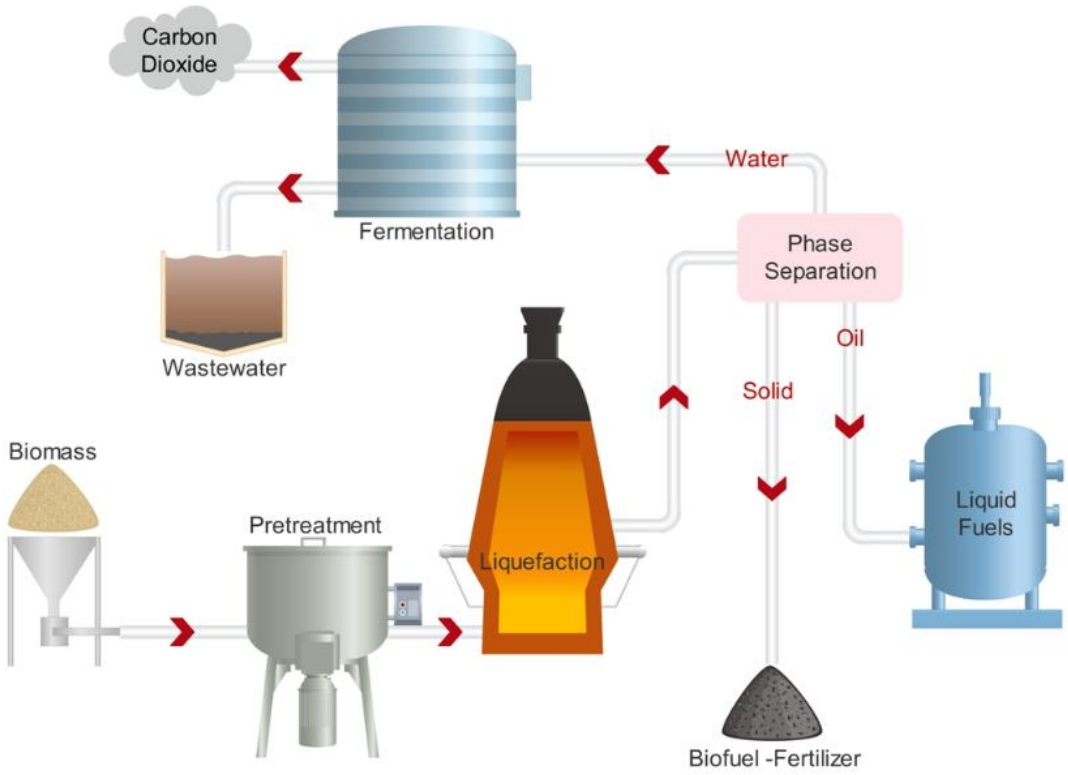

Figure 14: Biomass liquefaction flow diagram (Tursi, 2019a)

The solid residues can be directly used as biofuel or fertilizer, while the aqueous phase can be utilized within the plant for water-dependent processes or anaerobic digestion. The bio-crude, which has low oxygen content, requires additional refining for commercial use(Yu, 2011).

2.2.3 Chemical conversions

Physico-chemical conversion processes of biomass result in the production of high-density biofuels (Figure 15). Specifically, vegetable oils and animal fats are converted into biodiesel through esterification and/or transesterification(Tursi, 2019b). The primary vegetable oils used for first-generation biodiesel production include rapeseed oil, accounting for 80-85% of total global production, and sunflower oil, which contributes 10-15% (Fukuda et al., 2001a). Waste oils, such as used cooking oil

(WCO), and microbial oils, such as algal oil, are utilized for second and third-generation biodiesel production, respectively.

Vegetable oils primarily consist of triglycerides, which are not suitable as fuel in their raw form due to issues like incomplete combustion and residue buildup in engines. To address this, raw oils must undergo transesterification to break down triglycerides into fatty acids and glycerol, the latter contributing to the high viscosity of vegetable oils. During transesterification, triglycerides are converted into methyl or ethyl esters (biodiesel) by reacting with an excess of methanol or ethanol in the presence of an alkaline catalyst, such as NaOH or KOH

Oil + Short-chain alcohol → Biodiesel + Glycerol.

The transesterification reaction takes place at low temperatures (50°C -70°C) and atmospheric pressure. After the reaction, the product is neutralized and purified, particularly to remove glycerol (Leung et al., 2010b). Since glycerol is denser than biodiesel, it is separated using a phase separator, and excess alcohol is removed by distillation or evaporation. Biodiesel is further purified through water washing (liquid-liquid extraction) to remove residual catalysts and soaps, followed by drying and storage.

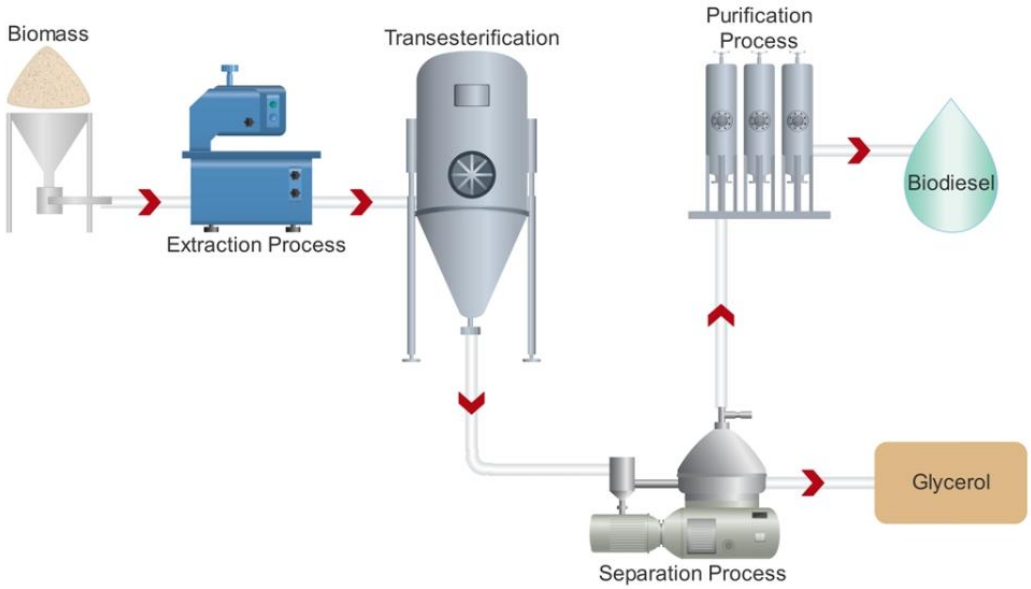

Figure 15: Biomass pysico-chemical conversion flow diagram (Tursi, 2019a)

Biodiesel is a renewable, biodegradable, and non-toxic fuel with physicochemical properties like diesel. Its high oxygen content and lubricating properties make it efficient for combustion in diesel engines. Glycerol, a by-product, can be utilized in value-added industries like food and pharmaceuticals, rather than being treated as waste(Canakci, 1999).

2.3 Feedstock, Methods of production and Reactor Configurations for Biodiesel Production

Biodiesel, a renewable biofuel, is primarily composed of fatty acid esters, which are derived from vegetable oils or animal fats. These esters result from the transesterification process, where oils or fats (triglycerides) react with alcohol (usually methanol or ethanol) to produce mono alkyl esters (biodiesel) and glycerol as a by-product.

Biodiesel has become a widely recognized and standardized fuel for various applications such as transportation fuels, heating, and electricity generation (Fukuda et al., 2001a). It is particularly favored due to its renewable and biodegradable nature, making it an environmentally friendly alternative to traditional petroleum-based diesel.

The chemical structure of biodiesel includes a long carbon chain, typically derived from the fatty acids in vegetable oils or animal fats, with a methyl ester functional group at one end. This ester group contributes to the biodiesel's characteristic chemical properties, such as its reduced viscosity compared to raw oils, and its improved combustion properties, making it suitable for use in diesel engines without major modifications.

In essence, the typical structure of a biodiesel molecule consists of:

- A long hydrocarbon chain, which is responsible for the fuel's energy content.
- A methyl ester group, which results from the transesterification reaction and helps ensure compatibility with engine systems.

The ester group is critical for the fuel's ability to reduce emissions, improve lubricity, and provide a clean-burning alternative to fossil diesel.

2.3.1 Feedstocks for Biodiesel

Biodiesel production can utilize various types of biological materials. These feedstocks are categorized into three main types: first second and third-generation feedstocks. Examples include recovery oil, animal oils, fresh vegetable oils, waste vegetable oils, and municipal and industrial waste organic recovery oil.

2.3.1.1 First-Generation Feedstocks

Vegetable oils such as rapeseed oil, sunflower oil, palm oil, soybean oil, and corn oil are the most common. Rapeseed oil alone accounts for about 80-85% of global biodiesel production, followed by sunflower oil (10-15%) (Fukuda et al., 2001a) Animal fats like tallow, lard, and poultry fat are also used but require more extensive processing due to impurities.

2.3.1.2 Second Generation Feedstocks

Waste cooking oils (WCO) are becoming more popular due to their cost-efficiency and sustainability, though they require additional purification steps (Canakci, 1999).

2.3.1.3 Third GenerationFeedstocks

Microbial oils, particularly algal oil, represent promising feedstocks for biodiesel due to high lipid content and rapid growth rates (Chisti, 2007b).

2.3.1.4 Recovery oil

These are generally oils extracted from oil-rich seeds or fruits. The biodiesel production process using these feedstocks involves pretreating the oil seeds or fruits and then extracting the oil. Initially, the seeds are stored in a manner that prevents problems such as mold growth and the activation of lipolytic enzymes. The pretreatment stage is carried out to remove certain impurities, ensuring that only suitable seeds proceed to the extraction process (Lim et al., 2015).; Rezania et al., 2022).

Oil extraction methods include mechanical, chemical, and enzymatic techniques. Mechanical extraction involves applying a pressure of 30–40 bar and temperatures near 95°C (Valladares-Diestra, 2020). When extracting oils from seed cells is difficult and leads to slow diffusion, chemical extraction with solvents is used. The enzymatic method aids in breaking down cell walls, facilitating the recovery and extraction of oils for biodiesel production and other uses (Mercer & Armenta, 2011).

2.3.1.5 Waste Vegetable Oil

Vegetable oil that has been used in food production and is no longer suitable for that purpose is known as "waste vegetable oil" (WVO). This type of waste oil can originate from various sources, including industrial, commercial, and household settings (El Sherbiny et al., 2010a)The pretreatment process involves filtering to remove suspended solids and then heating to dry the oil before it is used for biodiesel production.

2.3.1.6 Animal Oil

Animal fats are commonly obtained as byproducts from rendering processes and meat processing facilities. Major animal fats and oils include tallow from cows, lard from pigs, white grease, and poultry fat from chickens, turkeys, or other birds (Adewale et al., 2015). These fats are typically very viscous, but the processes used to convert them into biofuels reduce their viscosity, resulting in a less viscous product known as biodiesel (Norjannah et al., 2016; Rezania et al., 2019a).

2.3.1.6 Municipal and Industrial Waste Organic Recovery Oil

Municipal sewage sludge is increasingly being used worldwide as a lipid feedstock for biodiesel production due to its abundance and high lipid content, which makes biodiesel production from sludge economically feasible (Kargbo, 2010). Sewage sludge is classified into two types: primary and secondary. Primary sludge is obtained after screening and grit removal, consisting of floating grease and solids collected from the primary clarifier in a wastewater treatment plant. Secondary, or activated sludge, is mainly composed of microbial cells and suspended particles produced during the aerobic biological treatment of wastewater and collected in the secondary clarifier(Wu et al., 2016). After extracting and recovering the lipids from the sludge, they are used in transesterification reactions to produce biodiesel.

2.3.1.7 Chemical Constitution of Feedstock

Natural oils and fats are primarily composed of esters of glycerol and fatty acids, known as glycerides or triglycerides. Fatty acids are categorized into two types: saturated and unsaturated. Unsaturated fatty acids have one or more double carbon-to-carbon bonds, while saturated fatty acids have only single carbon bonds and are typically polar. Common fatty acids include stearic, oleic, linolenic, and palmitic acids. The chemical structure of triglycerides, which comprise 98% of the composition, along with monoglycerides and diglycerides.

2.3.2 Methods of Producing Biodiesel

The primary components of various biodiesel feedstocks, known as triglycerides, are converted into biodiesel through four main processes: pyrolysis (thermal cracking), micro emulsification, dilution, and transesterification.

2.3.2.1 Micro emulsification Method

Micro-emulsification is the process of forming microemulsions, which helps address the high vegetable oil viscosity issue. A microemulsion is a colloidal, optically isotropic fluid made up of microscopic structures, typically ranging from 1 to 150 nm, formed spontaneously by mixing two normally immiscible liquids and one or more ionic or non-ionic amphiphiles (F. Ma & Hanna, 1999a; Schwab et al., 1987). These fuels are sometimes called "hybrid fuels," although blends of conventional diesel with vegetable oils are also termed hybrid fuels (Balat & Balat, 2010). Microemulsions are clear, and stable, and consist of three components: an oil phase, an aqueous phase, and a surfactant.

Various solvents, such as methanol, ethanol, and 1-butanol, have been studied for creating microemulsions. Microemulsions with butanol, hexanol, and octanol meet the maximum viscosity requirements for diesel engines (Jain & Sharma, 2010). For example, a microemulsion created from a blend of soybean oil, methanol, 2-octanol, and a cetane improver in a ratio of 52.7:13.3:33.3:1.0 has successfully passed a 200-hour EMA test(Abbaszaadeh et al., 2012). While microemulsions of vegetable oils reduce oil viscosity, they have led to issues such as irregular injector needle sticking, heavy carbon deposits, and incomplete combustion during a 200-hour laboratory endurance screening test (Fukuda et al., 2001b).

2.3.2.2 Dilution Method

The use of vegetable oils as alternative fuels dates to 1900 when Dr. Rudolph Diesel, the inventor of the diesel engine, first tested peanut oil in his compression engine (Abbaszaadeh et al., 2012; Leung et al., 2010). However, using vegetable oils directly in diesel engines presents several challenges and limitations. While research on this topic has expanded significantly over the last few decades, experimentation with vegetable oils has been ongoing for nearly a century. To address the issues caused by the high viscosity of pure vegetable oils in compression ignition engines, crude vegetable oils can be mixed or diluted with diesel fuel to improve viscosity (Koh & Tinia, 2011). Studies have shown that energy consumption with pure vegetable oils is comparable to that of diesel fuel (F. Ma & Hanna, 1999b). Short-term usage ratios of 1:10 to 2:10 (oil to diesel) have been found to be effective (Fukuda et al., 2001b). Nevertheless, the direct use of vegetable oils or their blends has generally been considered unsatisfactory and impractical for both direct and indirect diesel engines. Major issues include the high viscosity of vegetable oils, their acidic composition, free fatty acid content, and the formation of gum due to oxidation and polymerization during storage and combustion. These factors lead to carbon deposits and thickening of lubricating oil (F. Ma & Hanna, 1999b). While heating and blending vegetable oils can reduce viscosity and enhance volatility, their molecular structure, including the polyunsaturated nature, remains unchanged (M. F. Demirbas et al., 2009). Using vegetable oils in diesel engines often requires significant engine modifications, such as changing the materials of pipes and injectors. Without these modifications, engine lifespan may be reduced, maintenance costs may increase due to higher wear, and the risk of engine failure rises.

2.3.2.3 Pyrolysis Method

Pyrolysis involves converting one organic material into another using heat, either alone or with the help of a catalyst (Uddin et al., 2018). The materials subjected to pyrolysis can include vegetable oils, animal fats, natural fatty acids, or methyl esters of fatty acids (Yusuf et al., 2011). Using thermal cracking reactions to convert vegetable oils and animal fats, which are primarily composed of triglycerides, shows great potential as a biodiesel production technology (Maher & Bressler, 2007). This method is especially promising in regions with established hydro processing industries, as it closely resembles conventional petroleum refining techniques (Maher & Bressler, 2007). The fuel properties of the liquid fractions obtained from the thermal decomposition of vegetable oil are expected to be like those of diesel fuels. Numerous studies have reported on the pyrolysis of triglycerides to produce products suitable for diesel engines (Lappi & Alén, 2009, 2011; Maher & Bressler, 2007). Research into triglyceride pyrolysis can be divided into catalytic and non-catalytic processes (Maher & Bressler, 2007).

Studies have investigated the pyrolysis of oils from sources like soybean, palm, and castor. Selecting appropriate distillation temperature (DT) ranges has allowed for the isolation of fuels with physical and chemical properties comparable to those of petroleum-based fuels (Lima et al., 2004). However, the equipment required for thermal cracking and pyrolysis can be costly for small-scale operations. Furthermore, while the resulting products are chemically like gasoline and diesel derived from petroleum, the removal of oxygen during thermal processing negates the environmental benefits associated with oxygenated fuels. Additionally, this process

can yield low-value byproducts and often produces more gasoline than diesel (F. Ma & Hanna, 1999b).

2.3.2.4 Transesterification Method

The most widely used method for biodiesel production is transesterification, where oils (triglycerides) react with alcohol to produce biodiesel, also known as fatty acid alkyl esters (FAAE), with glycerol as a byproduct. The process begins with the conversion of triglycerides into diglycerides, followed by the transformation of diglycerides into monoglycerides, and finally, monoglycerides into glycerol. At each stage, one methyl ester molecule is released from each glyceride (F. Ma & Hanna, 1999b). Transesterification, or alcoholysis, involves the exchange of one alcohol for another in a reaction like hydrolysis, but with alcohol replacing water (Barnwal & Sharma, 2005).

Methanol is mostly used as the alcohol feed material over ethanol due to is cost effectiveness, high reactivity, ease of availability, established reaction mechanism and industrial application, wide reaction temperature range, low boiling point making it require relatively less energy in product separation via distillation, resistance to azeotrope formation with water leading to easy product separation when homogeneous base catalysts are used, and relatively low required alcohol to oil ratio. However, in this work ethanol is used due to its sustainable and renewable nature (produced from renewable sources), low toxicity and low carbon footprint, less flammable, high solubility in triglyceride with better miscibility and potential to attain fully renewable biodiesel makes it a better option compared to methanol. This comes with the need to develop suitable catalyst for this transesterification to attain low activation energies. Typical methanol utilized transesterification processes have

activation energies ranging from 27.24kJ/mol to 180.8kJ/mol Click or tap here to enter text.(Komintarachat & Chuepeng, 2010; Mercy Nisha Pauline et al., 2021; Vitidsant et al., 2021).

Factors influencing the transesterification process include reaction temperature, time, pressure, the ratio of alcohol to oil, the concentration and type of catalyst, mixing intensity, and the type of feedstock used (Marchetti et al., 2007).

2.3.2.4.1 Non-Catalytic Transesterification

Non-catalytic transesterification reactions occur under supercritical conditions, requiring high temperatures and pressures, which make them harsh and often uneconomical. As a result, catalytic biodiesel production is more commonly used and preferred (Nasreen, 2018). In catalytic transesterification for biodiesel production, various steps are involved, such as ester purification, and the separation and recovery of unreacted reactants and catalysts. These steps complicate the conventional transesterification process, prompting interest in producing biodiesel from triglycerides via non-catalytic methods. In addition to catalytic methods, two non-catalytic transesterification processes exist: the supercritical alcohol process and the BIOX process.

2.3.2.4.2 Catalytic Transesterification

Catalysts play a crucial role in biodiesel production and are classified into biological and chemical catalysts (Figure 16). The efficiency of a catalyst for a specific application depends on factors such as surface area, pore size, volume, and the concentration of active sites on the catalyst surface(Nasreen, 2018).

Catalytic transesterification reactions have been carried out using enzymes, homogeneous, and heterogeneous catalysts (Li et al., 2021; Rezania et al., 2019b). These catalysts can either be derived from chemical/synthetic sources or biological/natural sources (Büyükoğlu et al., 2024).

Additionally, the catalytic process can either be a single-step process (transesterification using either acidic or basic catalysts) or a two-step process (acid esterification followed by base transesterification). This depends on the presence of high amounts of free fatty acids (FFAs) in the oil, which may require pretreatment before base transesterification (Talebian-Kiakalaieh et al., 2013).

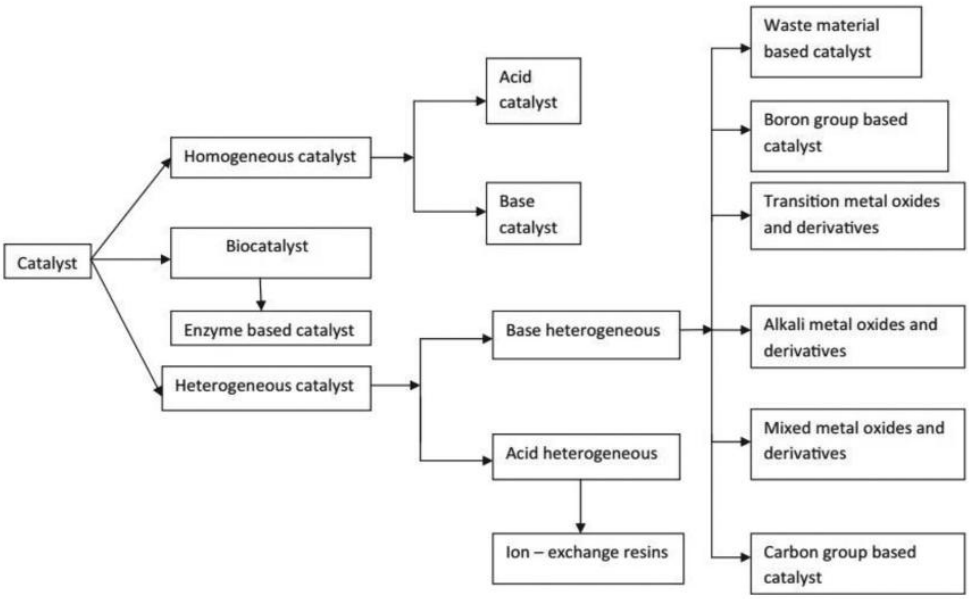

Figure 16: Catalyst classification (Bohlouli & Mahdavian, 2021)

2.3.2.4.2.1 Homogeneous catalysts

Homogeneous catalysts exist in the same phase as the reactants and products, making them soluble in alcohol during biodiesel production (De Boer, 2010). These catalysts are divided into two types: homogeneous alkaline catalysts and homogeneous acidic catalysts (Lotero E, 2006).

Transesterification using homogeneous catalysts typically occurs at moderate temperatures and atmospheric pressure. However, this method has several drawbacks. One major issue is that the catalyst is not typically recyclable (De Boer, 2010), requiring separation from the product streams (biodiesel and alcohol/glycerol) (Mittelbach, 2004) . Additionally, the catalyst can react with impurities in the oil, especially free fatty acids (FFAs), leading to soap formation as a side reaction (Lotero E, 2006)

2.3.2.4.2.1.1 Homogeneous Base catalysts

Homogeneous base catalysts used in the transesterification of edible oil include sodium hydroxide (NaOH), potassium hydroxide (KOH), sodium methoxide ($NaOCH_3$), potassium methoxide ($KOCH_3$), sodium ethoxide ($NaOC_2H_5$), sodium peroxide (Na_2O_2), and sodium butoxide (C_4H_9NaO) (Atadashi et al., 2013; Kulkarni & Dalai, 2006; Y. C. Sharma & Singh, 2009). These catalysts are effective, but their performance can vary. For instance, transesterification with potassium hydroxide and sodium hydroxide may reduce biodiesel performance due to the formation of water as a byproduct. In contrast, sodium methoxide and potassium methoxide often yield better results because they do not produce water during the reaction(Y. C. Sharma & Singh, 2009).

Homogeneous alkaline catalysts are best suited for clean oils with free fatty acid (FFA) levels below 0.5%, as higher FFA levels can lead to soap formation and complicate separation processes(Issariyakul & Dalai, 2014; Lotero et al., 2005). Although some studies suggest that alkaline catalysts can tolerate higher FFA levels, it is generally recommended to keep the FFA concentration between 0.5% and 2% for optimal performance.

The efficiency of biodiesel production is significantly influenced by the choice of catalyst, with the potential to achieve over 99% performance by adjusting the catalyst concentration.

The mechanism of base catalyzed transesterification is shown in Figure 17**.** In this base-catalyzed transesterification, the base generates an alkoxide ion that initiates the reaction by attacking the ester. Through the nucleophilic substitution process, the original ester (RCOOR) is converted into a new ester (RCOOR'), producing the biodiesel molecule, while glycerol or another alcohol byproduct is released. This involves a 4-step process

Nucleophilic attack of the alkoxide ion (RO^-): the reaction begins with the base (NaOH) reacting with the alcohol (R'OH) to form an alkoxide ion ($R'O^-$) and water (H_2O). This alkoxide ion ($R'O^-$) is a strong nucleophile, which can then attack the carbonyl carbon (C=O) of the ester (RCOOR).

Tetrahedral intermediate formation: the nucleophilic alkoxide ion ($R'O^-$) attacks the electrophilic carbonyl carbon of the ester (RCOOR). This results in the formation of a tetrahedral intermediate, where the double bond of the carbonyl (C=O) is temporarily broken, and an additional alkoxide group (OR') is attached.

Intermediate collapse and formation of new ester: the intermediate then collapses, reforming the carbonyl double bond and leading to the release of the original alcohol (ROH). This reaction yields a new ester (RCOOR') and the original alkoxide ion (RO^-).

Regeneration of alkoxide ion: the alkoxide ion (RO^-) produced can react with another molecule of the alcohol (R'OH) to regenerate the nucleophilic alkoxide ion ($R'O^-$) and continue the transesterification process.

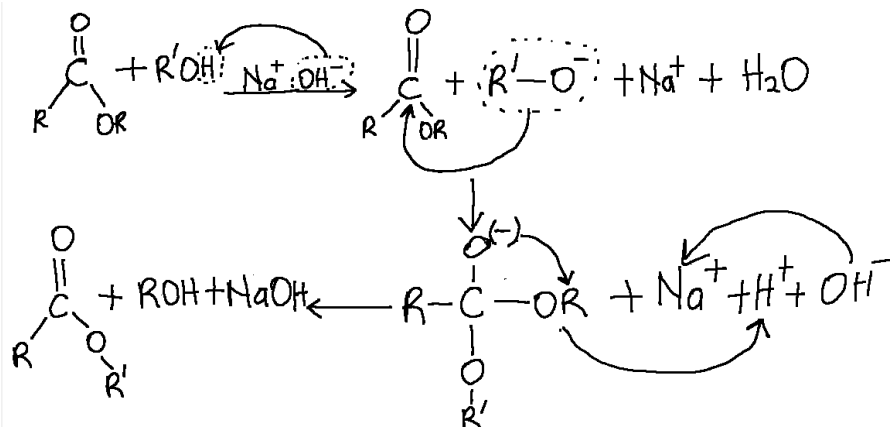

Figure 17: Base catalyzed transesterification reaction mechanism

2.3.2.4.2.1.2 Homogeneous Acid catalysts

Homogeneous acid catalysts are more tolerant of water or moisture during the reaction, making them suitable for reducing free fatty acids (FFAs) in used cooking oils and animal fats before full transesterification with alkaline catalysts. However, these catalysts require special, more expensive processing equipment due to their corrosive nature(Kulkarni & Dalai, 2006; Tariq et al., 2012).

The reaction rate of homogeneous acidic catalysts is significantly slower, about 4000 times lower compared to alkaline catalysts(Wang et al., 2006). They also necessitate higher reaction temperatures and a greater molar ratio of alcohol to oil, making them less commonly used in biodiesel production(De Boer, 2010; Najafpour et al., 2016). The most frequently used acidic catalysts include sulfuric acid (H_2SO_4), sulfonic acid (HSO_3R), and hydrochloric acid (HCl)(Atadashi et al., 2013).

Research has examined the effects of various parameters on the transesterification process, including the methanol-to-oil molar ratio (3.3:1–30:1), reaction temperature (25–60°C), H_2SO_4 concentration (1–5 wt.%), reaction time (48–96 hours), water content (1–5 wt.%), and FFA levels (0–33 wt.%). Even with FFAs of 5% or 0.5% and water content, oil conversion to ester can exceed 90% (Kulkarni & Dalai, 2006).

The reaction of FFAs with methanol helps limit the amount of water produced. Increasing the amount of alcohol can improve the conversion of oil to ester when the reaction is conducted at a temperature below the alcohol's boiling point (Kulkarni & Dalai, 2006).

2.3.2.4.2.2 Bio Catalysts (Enzymes)

The use of biocatalysts is a modern, effective method that has resolved various issues for both humans and the environment. Biocatalysts, such as enzymes, have several advantages over traditional catalysts. Unlike conventional catalysts, enzymes do not produce soap and can generate high-purity biodiesel from low-quality materials like used cooking oil(Maceiras et al., 2010). Free fatty acids (FFA) and water in raw materials often cause problems in traditional transesterification, but enzymes can effectively address these issues(Brask et al., 2011). Enzymatic transesterification works well with raw materials containing high FFA levels, such as waste oils and animal fats, by converting FFA into alkyl esters(Christopher et al., 2014).

There are two main types of enzymatic catalysts: extracellular and intracellular lipases. Biocatalysts are favored for their thermal stability, selectivity, high efficiency, minimal side reactions, and recyclability. However, their high production cost, slower reaction times, and challenges in use and recycling limit their efficiency(Fukuda et al., 2001c; Gog et al., 2012). Additionally, many lipases are inactivated by methanol, commonly used in alcoholysis, restricting the amount of methanol or ethanol that can be used during conversion(Magner, 2013). Solvent molecules can cause enzyme inactivation by binding to protein sites, leading to competitive inhibition or irreversible damage. Understanding these mechanisms is essential for overcoming the limitations of biocatalysts(Lotti et al., 2018).

2.3.2.4.2.3 Heterogeneous Catalysts

Heterogeneous catalysts operate in a different phase from the reactive materials, typically as solids interacting with a liquid reaction mixture at their surface (Dalvand & Mahdavian, 2018). Unlike homogeneous catalysts, which are in the same phase as the reactants, heterogeneous catalysts facilitate the reaction between different phases—solid and liquid (Mardhiah et al., 2017).

These catalysts are categorized into alkaline and acidic types, like their homogeneous counterparts. A key advantage of heterogeneous catalysts is their ease of separation from the final product, which allows them to be recycled and reused, making the process more cost-effective(Farooq et al., 2013; Y. Ma et al., 2017; Meher et al., 2013). Additionally, their use is considered environmentally friendly as it reduces the need for extensive filtration of biodiesel, leading to lower energy and water consumption(Meher et al., 2013; Tan et al., 2015a).

2.3.2.4.2.3.1 Acid Heterogeneous Catalysts (Ion Exchange Resin)

Acidic catalysts are primarily composed of materials such as zeolite, heteropoly acids, pure oxides, or modified transition metals like zirconium, molybdenum, silica, and alumina (Galadima & Muraza, 2014). Heterogeneous acidic catalysts are more stable and environmentally friendly compared to homogeneous ones(Galadima & Muraza, 2014). The ideal heterogeneous acidic catalysts should possess a high number of active sites, moderate acidity, water resistance, and good porosity to reduce diffusion issues(Avhad & Marchetti, 2015). Key benefits of these catalysts include their reusability, efficient conversion rates, and the ease of separating and filtering products(Guldhe et al., 2017). Replacing homogeneous with heterogeneous acidic

catalysts can also eliminate issues related to separation processes, hazardous wastewater, and corrosion(Arzamendi et al., 2007; Najafpour et al., 2016). However, heterogeneous acidic catalysts require higher temperatures and longer reaction times to achieve satisfactory conversion yields(Jacobson et al., 2008).

2.3.2.4.2.3.2 Base Heterogeneous Catalysts

Heterogeneous base catalysts are designed to address issues like saponification, which complicates the separation of glycerol from the methyl ester layer when using homogeneous base catalysts. These catalysts show superior catalytic activity even under mild conditions (Calero et al., 2014). They offer several advantages, including being non-corrosive, affordable, high transesterification selectivity, low temperature requirement, low activation energy requirement, environmentally friendly, and producing fewer disposal challenges. Additionally, they can be easily separated from the reaction mixture and engineered for enhanced activity, selectivity, and longevity (Liu et al., 2008).

Various metal-based oxides, such as alkali metals, alkaline earth metals, and transition metal oxides, have been used as catalysts in the transesterification of oils. These metal oxides consist of metal cations with Lewis acid properties and oxygen anions with Bronsted base properties (Serio et al., n.d.; Zabeti et al., 2009). Sometimes, multiple metal oxides are combined to create more effective catalysts. Other base heterogeneous catalysts include boron-based and waste-based catalysts (Semwal et al., 2011)

2.3.2.4.2.3.2.1 Alkali and Akali earth Metal Oxide Based Catalysts

Metal-based oxides are among the most widely used catalysts in heterogeneous transesterification. (Z. Zhang & Verykios, 1996) used temperature-programmed desorption (TPD) of adsorbed carbon dioxide to study the basic properties of alkaline earth metal oxides. They found that the number of basic sites per unit weight correlates with surface area, in the following order: CaO > MgO > SrO > BaO. Oxides with stronger basic sites tend to promote reactions more effectively. Calcium oxide (CaO) is the most extensively studied metal-based catalyst for biodiesel production due to its long catalyst life, high basic strength, activity, low solubility in methanol, and mild reaction conditions; (Latchubugata et al., 2018; Roschat, Siritanon, Kaewpuang, et al., 2016)

In a study by (Arun et al., 2017), biodiesel was produced from *Terminalia belerica* and *Garcinia gummi-gutta* using CaO calcined at 605°C for 5 hours. The transesterification was carried out at 60°C, with a 9:1 methanol-to-oil ratio, 2%w/v of catalyst, and a 3-hour reaction time. The resulting biodiesel met ASTM standards.

Similarly, (Roschat, Siritanon, Yoosuk, et al., 2016) used CaO for the transesterification of palm olein oil with a free fatty acid content of 0.29 mg KOH/g. The CaO was calcined at 700°C, 800°C, and 900°C for 3 hours, yielding 97.2% biodiesel. The catalyst maintained its activity for up to five cycles without significant degradation.

Additionally, (Du et al., 2019) synthesized three carbon-based MgO catalysts using sol-gel and calcination methods. These catalysts achieved a maximum conversion of 96.5% under transesterification conditions with a 12:1 methanol-to-oil ratio, 6 wt% catalyst concentration, and a temperature of 75°C.

2.3.2.4.2.3.2.2 Transition Metal Based Catalysts

Transition metal oxides like titanium oxide (TiO_2) and zinc oxide (ZnO) are commonly used as heterogeneous base catalysts for biodiesel production (Yoo et al., 2010). (Kaur et al., 2018) synthesized a tungsten (W)-supported TiO_2/SiO_2 catalyst using the sol-gel method and applied it to the transesterification of waste cottonseed oil for biodiesel production. The reaction, conducted with a methanol-to-oil ratio of 1:30M, at 65°C, and with 5 wt% catalyst, was completed in 4 hours. The catalyst was also reusable for up to four cycles without a notable decrease in activity.

(Lam et al., 2019) investigated the catalytic activity of a TiO_2-ZnO mixed oxide catalyst for palm oil transesterification. Under conditions of 5 hours, a 6:1 methanol-to-oil ratio, and 200 mg catalyst loading, they achieved a biodiesel yield of 92%. This yield was higher than the 83% yield obtained using only ZnO, indicating the mixed oxide catalyst was more effective.

2.3.2.4.2.3.2.3 Boron Group Based Catalysts

Various metal oxides, halides, nitrates, and alloys are supported by boron group-based compounds, especially alumina (Al_2O_3) (Choudhury, 2011). (Kesserwan et al., 2020) developed a novel hybrid CaO/Al_2O_3 aerogel catalyst using a rapid epoxide-initiated sol-gel process followed by calcination at 700°C. This catalyst was applied to the transesterification of waste cooking oil under optimized conditions: 1 wt% of 3:1 CaO/Al_2O_3 catalyst, an 11:1 methanol-to-oil ratio, a reaction time of 4 hours, and a temperature of 65°C, yielding 89.9% biodiesel.

Similarly, (Benjapornkulaphong et al., 2009) examined various alkali and alkaline earth metal nitrates supported on Al_2O_3, including $LiNO_3/Al_2O_3$, $NaNO_3/Al_2O_3$, Ca

$(NO_3)_2/Al_2O_3$, KNO_3/Al_2O_3, and $Mg(NO_3)_2/Al_2O_3$. These catalysts were synthesized via impregnation and calcined at 450–850°C, then used in the transesterification of palm kernel and coconut oils. They found that the biodiesel yield from all catalysts was below 90% when calcined at 450°C. Among them, Ca $(NO_3)_2/Al_2O_3$ was recommended as the most suitable catalyst, with a catalyst concentration of 10 wt%, a reaction temperature of 60°C, a methanol-to-oil ratio of 65:1, and a reaction time of 3 hours.

2.3.2.4.2.3.2.4 Mixed Metal Based Catalysts

Mixed metal-based oxides, commonly used as base catalysts, can have their basicity adjusted by altering their chemical composition and synthesis method (Teo et al., 2017). These oxides can also function as bifunctional acid-base catalysts. For instance, (Oliveira, 2022)investigated the catalytic activity of La_2O_3 in ZrO_2, synthesized via the sol-gel method, for biodiesel production from canola oil. Their study found that doping La_2O_3 into ZrO_2 enhances its basicity, with 3 wt% La_2O_3 yielding the highest catalytic activity in canola oil transesterification.
Similarly, (Limmanee et al., 2013) examined nanocrystalline CaMgZn mixed oxides as heterogeneous catalysts, synthesized by co-precipitation using Na_2CO_3. The study achieved a maximum biodiesel yield of 97.5% from palm kernel oil, using a CaMgZn catalyst with a 3:1:1 ratio.

2.3.2.4.2.3.2.5 Hydrotalcite Based Catalysts

Hydrotalcites, a class of anionic and basic clays, are used as heterogeneous catalysts due to their favorable morphology compared to alkaline earth metal oxides and their

high basic strength, which can be adjusted by modifying the Mg/Al ratio. However, they are sensitive to free fatty acids (FFAs) and water present in biodiesel feedstocks. In a study by (Rizwanul Fattah et al., 2020a) Zr-doped Mg-Al hydrotalcite with varying Zr/Mg molar ratios was tested for the transesterification of refined rapeseed oil, achieving an optimal oil conversion of 99.9%. This occurred under conditions of 373-393K temperature, 6 hours of reaction time, 4.8-5.0 atm pressure, and a Zr/Mg/Al ratio of 0.45:2.55:1. Similarly, (Navarro et al., 2018) evaluated the Mg-Al hydrotalcite catalyst, prepared via co-precipitation, in the transesterification of sunflower oil. The optimal conversion was 96%, obtained with a 48:1 methanol-to-oil ratio, 1 atm pressure, 60°C temperature, 24 hours reaction time, and 2 wt% catalyst. The catalyst's performance was linked to the presence of Bronsted-type basic sites at the catalyst edges

2.3.2.4.2.3.2.6 Carbon Group Based Catalysts

Carbon group-based catalysts, particularly those derived from carbon materials and carbon-based composites, have gained prominence in the field of transesterification for biodiesel production due to their unique properties and advantages. These catalysts include activated carbon, carbon nanotubes, graphene, and carbon-based composites. Their high surface area, tunable porosity, and chemical stability make them ideal candidates for efficient transesterification reactions.

Activated carbon, one of the most used carbon-based catalysts, has been shown to be effective in biodiesel production. According to (Buasri et al., 2012), activated carbon derived from coconut shells demonstrated significant catalytic activity and stability in the transesterification of waste cooking oil. The high surface area and mesoporous

structure of activated carbon facilitate the adsorption of reactants and promote reaction efficiency.

Carbon nanotubes and graphene are also notable for their catalytic properties. For example, (Dong et al., 2019) investigated the use of functionalized carbon nanotubes as catalysts for transesterification, achieving high biodiesel yields due to their large surface area and high thermal stability. Similarly, graphene oxide, when used as a catalyst support, enhances the catalytic performance of metal-based catalysts, as reported by (S. Zhang et al., 2020).

Carbon-based composites, which combine carbon materials with metal or metal oxide components, offer additional benefits. A study by (Li, 2023) demonstrated that a composite of activated carbon and metal oxides showed improved catalytic activity and stability in biodiesel production compared to single-component catalysts.

Overall, carbon group-based catalysts offer several advantages in transesterification processes, including high surface area, stability, and reusability. These properties make them valuable for sustainable biodiesel production. Ongoing research continues to explore and optimize these catalysts to enhance their performance and broaden their applications.

2.3.2.4.2.3.2.7 Waste Based Catalyst Materials

Household and industrial waste materials can be repurposed to create cost-effective and environmentally friendly catalysts, enhancing the sustainability of biodiesel production (Majhi & Ray, 2016; Pandit & Fulekar, 2019). Mussel, oyster and snail shells are naturally enriched with calcium and have become valuable in catalyst synthesis due to their low cost, availability, and support for recycling and waste minimization (Rizwanul Fattah et al., 2020b). Table 2 shows high biodiesel yields

obtained in the use of heterogeneous base (biobased) catalysts comparable to yields obtained in the use of homogeneous catalysts. The heterogeneous nature makes separation of products easier since there is no salt and water formed as by products. The primarily used biobased catalysts fall within two major categories based on their primary composition. Bones, shells and beaks of animals are mostly used as catalyst transesterification source due to their high calcium content. Calcium is in period 4, group 2 of the periodic table with 2 valence electrons giving its easy electron donating ability. The second group of catalysts are potassium rich sourced from peels of fruits, leaves of plants, shells and husks of nuts wood ash and bagasse. K is in period 4, group 1 of the periodic table, however, has only one valence electron making it relatively easy and faster to donate electrons in transesterification yielding high reaction rate.

2.3.2.4.2.3.2.7.1 Waste Eggshell Catalyst

Over the years, utilization of waste eggshells as a transesterification catalyst to produce biodiesel has become popular owing to their low cost, availability, and eco-friendliness. Egg shells, primarily composed of calcium carbonate, can be converted into calcium oxide (CaO) through thermal treatment, making them effective heterogeneous base catalysts for transesterification processes. This approach increases the biodiesel production process efficiency alongside serving as a waste disposal strategy for the eggshells. Studies have demonstrated that eggshell-derived CaO catalysts exhibit high catalytic activity, good stability, and reusability. For instance, (Rizwanul Fattah et al., 2020b) found that these catalysts offer advantages over conventional ones, including cost-effectiveness and reduced environmental impact.

Furthermore, (Majhi & Ray, 2016) highlighted the effectiveness of eggshell-based catalysts in lowering the free fatty acid content (FFAs) in the triglyceride raw material, which is vital for using waste oils to produce biodiesel. The ability to regenerate and reuse eggshell catalysts in several transesterification runs while maintaining its catalytic activity is another notable benefit, as reported by (Chouhan & Sarma, 2011). These findings underscore the potential of waste eggshell catalysts as a viable and sustainable option for biodiesel production, contributing to both waste reduction and green energy solutions.

2.3.2.4.2.3.2.7.2 Waste Cow bone Catalyst

Waste cow bones, rich in calcium, have emerged as effective transesterification catalyst due to its towering calcium content, which is converted to calcium oxide (CaO) through calcination. This conversion enhances the catalytic properties of the waste material, making it a viable option for transesterification reactions. Recent studies highlight the efficiency of cow bone-derived catalysts in producing biodiesel. For instance, (Majhi & Ray, 2016) demonstrated that calcined cow bones can produce biodiesel with a yield of up to 97% at an optimum 65°C reaction temperature and 9:1 methanol-to-oil ratio. Similarly, (Pandit & Fulekar, 2019) reported that cow bone catalysts possess good stability and activity for catalytic reactions, even amidst free fatty acids (FFAs), which typically is problematic for other types of catalysts. The use of waste cow bones not only provides an environmentally friendly alternative to conventional catalysts but also helps in waste management and reduces costs associated with biodiesel production (Hussain, Alshahrani, Abbas, Khan, Jamil, Yaqoob, Soudagar, et al., 2021). The reusability and low cost of cow bone-derived catalysts make them an attractive option for sustainable biodiesel production

(Rizwanul Fattah et al., 2020b). Overall, this underscores the potential of waste cow bones as a resourceful material in the biodiesel industry.

2.3.2.4.2.3.2.7.3 Waste Fish Scale Catalyst

Waste fish scales, abundant and often discarded, are a promising catalyst for production of biodiesel because they are made of large amounts of calcium. Recent research demonstrates their efficacy in transesterification processes, where they are converted into calcium oxide (CaO) through calcination, thus enhancing their catalytic activity. For instance, studies by (Jaiswal et al., 2024) show that calcined fish scale catalysts can achieve biodiesel yields of up to 94% under optimized conditions of 60°C reaction temperature and 12:1 methanol-to-oil ratio. Similarly, (Chakraborty et al., 2011a) found that fish scale-derived catalysts offer high reusability and stability, maintaining activity across several reaction cycles without significant deactivation. This makes them an attractive alternative to traditional catalysts, though faced with the drawback of water contamination and problems related to free fatty acids. Low cost as well as environmental benefits of using fish scales, which are otherwise a waste product, make this biodiesel production process more sustainable (Hussain, Alshahrani, et al., 2021). Additionally, fish scale catalysts facilitate better waste management and reduce the overall production costs of biodiesel, aligning with green chemistry principles (Lee et al., 2022). Thus, waste fish scales represent a valuable resource for enhancing the sustainability and cost-effectiveness of biodiesel production.

2.3.2.4.2.3.2.7.4 Waste Banana peel Catalyst

Waste banana peels, commonly discarded in the agricultural and food industries, have been repurposed as an effective catalyst to use in transesterification for production of biodiesel because of its high potassium composition. Recent studies highlight its potential for sustainable catalyst through a two-step process: the peels are first converted into potassium carbonate (K_2CO3) or potassium oxide (K_2O) via thermal activation, which then catalyzes transesterification reactions to convert vegetable oils. Khulbe et al. (2018) demonstrated that banana peel-derived potassium catalysts achieved biodiesel yields of up to 91% with optimized conditions of 65°C reaction temperature and 6:1 methanol-to-oil ratio. Similarly, Kumar et al. (2020) reported that the potassium-based catalysts derived from banana peels exhibit high catalytic activity and stability, with minimal loss of efficiency over multiple cycles. The use of banana peel catalysts not only reduces the environmental impact associated with waste disposal but lowers the cost of catalyst making it an economically viable process (Saha et al., 2019). This approach provides a waste to resource pathway, thus contributing to a circular economy and promoting green chemistry (Reddy et al., 2021). Consequently, waste banana peels offer a promising and eco-friendly alternative for biodiesel production.

2.3.2.4.2.3.2.7.5 Blending Waste Sourced Biobased Catalysts

Blending methods for biobased catalysts in biodiesel production offer innovative approaches to enhancing catalytic performance by combining various materials to exploit their synergistic effects. These methods involve integrating biobased materials

such as waste biomass or agricultural residues with conventional catalysts or supports to create composite catalysts with improved properties.

One prominent method involves blending biobased materials with metal oxides to produce effective catalysts. For instance, Zheng et al. (2018) explored the blending of rice husk ash with calcium oxide to create a composite catalyst for biodiesel production. The resulting catalyst demonstrated enhanced catalytic activity and stability compared to pure calcium oxide due to the improved surface properties imparted by the rice husk ash.

Another approach focuses on combining biobased polymers with active metal components. In a study by Ahammed et al. (2020), chitosan, derived from shrimp shells, was blended with metal nanoparticles to produce a biobased catalyst for transesterification. The chitosan-metal nanoparticle composites exhibited high biodiesel yields and stability, benefiting from the good catalytic properties of the metal nanoparticles, its large surface area and the structural support provided by chitosan.

Blending biobased materials with activated carbon is also common. Zhang et al. (2021) researched production of biodiesel using blended alumina and activated carbon derived from agricultural waste. The blend leveraged the alumina stability and activated carbon large surface area, resulting in a catalyst with superior performance and reusability.

Overall, blending methods for biobased catalysts provide a promising avenue for developing efficient and sustainable catalysts for biodiesel production. These methods not only enhance catalytic performance but also contribute to waste valorization and environmental sustainability.

2.3.2.4.2.3.7.6 Impregnating Promoters on Biobased Catalysts

Through impregnation of promoters on biobased catalysts, the stability and efficiency of the catalyst are enhanced. In this technique, metal or metal oxide promoters are loaded onto a biobased support material, such as agricultural residues or waste biomass, to improve its catalytic properties for transesterification reactions.

Pandit and Fulekar (2017) investigated the impregnation of potassium onto biobased calcium carbonate derived from eggshells. The potassium-promoted catalyst demonstrated enhanced activity for biodiesel production, increased surface area and improved basicity of the impregnated material. Similarly, Wang et al. (2019) explored manganese as a promoter on waste coconut shell-derived activated carbon. The manganese-impregnated catalyst exhibited superior performance and stability in biodiesel production due to the synergistic effects of manganese's catalytic properties and large activated carbon surface area.

Another significant contribution is by Uğuz et al. (2021), who examined the impregnation of copper onto waste fish scales. The copper-promoted fish scale catalyst showed notable improvements in catalytic activity and resistance to deactivation, which was linked to the role of copper in enhancing the catalyst's surface properties and interaction with the reactants.

The technique has also been applied to other biobased materials. For instance, a study by Zhang et al. (2020) reported on the impregnation of zinc onto rice husk-derived silica. The zinc-promoted catalyst exhibited high efficiency and selectivity in biodiesel production, benefiting from the combination of zinc's catalytic properties and the structural support provided by the rice husk-derived silica.

Overall, impregnating promoters onto biobased catalysts is promising in enhancing performance as well as sustainability of the transesterification process to produce

biodiesel by leveraging the benefits of both biobased supports and catalytic promoters.

2.3.2.4.2.4 Inorganic Based Catalyst

The robustness, high catalytic activity, and reusability of inorganic-based catalysts has gained attention in the production of biodiesel. These catalysts, often composed of metal oxides, salts, or mixed metal oxides, offers good sustainability relative to homogeneous catalysts. Metal oxides including magnesium oxide (MgO), and calcium oxide (CaO) have been extensively studied. Sari et al. (2019) demonstrates that CaO, derived from waste materials, provides high conversion rates for transesterification reactions, achieving up to 96% biodiesel yield under optimized conditions. Similarly, MgO catalysts have shown excellent performance due to their high basicity and stability, with studies by Reddy et al. (2020) highlighting a 95% yield with minimal catalyst deactivation over multiple cycles.

Mixed metal oxides, such as those combining transition metals, have also been explored for their enhanced catalytic properties. According to Patel et al. (2021), doping titanium dioxide (TiO2) with tungsten (W) significantly improves catalytic activity, achieving up to 98% biodiesel yield in transesterification processes. Wang et al. (2022) investigated zinc oxide (ZnO) and its mixed forms, which demonstrated superior performance compared to single-metal oxides, with yields reaching 97%.

Inorganic-based catalysts also offer advantages with regards to environmental impact and economics. They are generally more resistant to contamination and deactivation compared to their organic counterparts, making them suitable for use in continuous production systems (Singh et al., 2023). Furthermore, their synthesis often utilizes low-cost materials, contributing to a more sustainable biodiesel production process

(Gomez et al., 2024). Overall, inorganic-based catalysts represent a promising area of research, providing efficient and sustainable solutions for biodiesel production.

2.3.2.4.2.4.1 Co-impregnation Catalyst Preparation Method

The co-impregnation method is a widely used technique for preparing catalysts, particularly for applications involving complex catalytic reactions such as biodiesel production. This method involves the simultaneous impregnation of multiple metal precursors onto a support material, resulting in a catalyst with well-dispersed active metal phases and enhanced catalytic properties. According to Liu et al. (2021), co-impregnation allows for the precise control of metal loading and distribution, which is crucial for optimizing catalytic activity and stability.

In biodiesel production, co-impregnation has been effectively employed to develop catalysts with improved performance. Zhang et al. (2019) used co-impregnation to prepare a Ni-Cu catalyst supported on alumina with vegetable oil as feedstock for transesterification, achieving high yield of biodiesel alongside superior catalytic stability. Similarly, Kim et al. (2020) reported that co-impregnated Co-Mo catalysts demonstrated enhanced activity and selectivity in the hydrodeoxygenation of bio-oils, underscoring the versatility and effectiveness of this preparation method.

The advantages of co-impregnation include the ability to create catalysts with well-defined metal ratios and excellent metal dispersion, which are critical for high-performance catalytic applications. As noted by Chen et al. (2018), the method also facilitates the integration of different metal phases, allowing for the development of bifunctional catalysts with tailored properties. However, careful optimization of impregnation conditions, such as metal precursor concentration and support material, is essential to achieving desired catalyst performance (Smith et al., 2021).

Overall, the co-impregnation method remains a valuable approach in catalyst preparation, offering significant benefits in terms of metal distribution and catalytic efficiency.

2.3.2.4.2.4.2 Co-precipitation Catalyst Preparation Method

Co-precipitation is a widely utilized method for preparing catalysts due to its simplicity and effectiveness in achieving uniform catalyst compositions and high surface areas. This technique involves simultaneously precipitating two or more metal ions from a solution to form a solid precursor, which is then subjected to thermal treatment to produce the active catalyst. According to Lee et al. (2018), co-precipitation allows for precise control over the metal composition and distribution, leading to improved catalytic performance. The method is particularly useful for synthesizing mixed metal oxides and catalysts with complex compositions.
Co-precipitation has been utilized in the preparation heterogeneous catalysts exhibiting notable results in transesterification reactions. For example, Zhang et al. (2020) demonstrated the effectiveness of co-precipitated Ca-Mg-based catalysts for transesterification processes, achieving high biodiesel yields with robust performance. Similarly, Patel et al. (2021) prepared catalysts that were ZnO-based via co-precipitation, which showed improved stability and catalytic compared with traditional methods.
Advantages co-precipitation gives include the ability to produce catalysts with well-defined structures and high surface areas, as well as the versatility in catalyst design. As noted by Wang et al. (2019), the method can be easily scaled up for industrial applications and tailored to specific catalytic needs. However, the success of co-precipitation largely depends on factors such as the choice of precipitants, pH control,

and post-treatment conditions, which must be optimized to ensure high-quality catalyst preparation (Singh et al., 2022).

Overall, co-precipitation remains a key method in catalyst preparation, offering significant advantages in terms of material uniformity and performance. There are ongoing developments aimed at improving catalyst properties and expanding its applications in various chemical processes.

Table 2: Obtained biodiesel yields in the use of various base heterogeneous biobased catalysts

Catalyst	***Feedstock***	***Biodiesel yield (%)***	***References***
Eggshell derived CaO	Rapeseed oil	95.12	(Yaşar, 2019)
Chicken eggshell derived CaO	WCO	95	(Gollakota et al., 2019)
Na-K on calcined eggshell	Canola oil	97.6	(Khatibi et al., 2021)
KOH on calcined goat bone	WCO	84	(Ali, 2018)
K_2O and KCl from banana peel	Soybean oil	95.1	(Fan et al., 2019a)
Calcine banana peel	WCO	100	(Gohain et al., 2017a)
Orange peel ash	Soybean oil	98	(Changmai et al., 2020)
Calcined kola nut pod husk	Rubber seed oil	96.97	(Oladipo & Betiku, 2020)
Sugarcane leaf ash	Mastwood oil	97	(Arumugam & Sankaranarayanan, 2020)
Calcined quail beaks	Rapeseed oil	96.7	(Khan et al., 2020)
Calcined banana peduncle	Kapok tree oil	98.69	(Balajii & Niju, 2020)
Rice husk supported CaO	Palm oil	93.4	(Zhao et al., 2018)
Calcined walnut shell	Sunflower oil	98	(Miladinović et al., 2020)
Ram bone supported Cr	Mustard oil	96.85	(Pradhan & Chakraborty, 2018)
Oyster shell derived CaO	WCO	87.3	(Lin et al., 2020)

2.3.2.4.2.5 Characterization of Catalysts

Catalyst characterization is essential for assessing the effectiveness of a catalyst and understanding how its properties influence its performance. This process involves quantifying the catalysts chemical and physical properties that impact its reaction

capabilities. The primary goals in characterizing catalysts are (Annadurai et al., 1996); to explore the connections between chemical, catalytic and physical properties, and to identify the chemical and physical properties of the catalyst. Key characteristics examined during catalyst characterization include; chemical composition (surface and bulk composition), porosity and surface area (measurements of surface area and pore structure), bulk solid structure (the internal structure of the catalyst material), phase composition and crystallite size (analysis of the phases present and the size of crystalline particles), surface morphology (the shape and structure), chemical properties on the surface (includes the oxidation state and location of active metals, reducible-oxidizable characteristics and acid-base properties), aggregate size, resistance to attrition, density and mechanical strength, catalytic stability, activity, selectivity.

Nitrogen physisorption, x-ray diffraction (XRD), thermogravimetric analysis (TGA) and temperature-programmed desorption (TPD) are among the most used techniques

2.3.2.4.2.5.1 Temperature Programmed Desorption (TPD) Technique

Temperature-programmed desorption (TPD) assess quantity and strength in relation to acidic and basic sites on a catalyst. Ammonia is used to identify acidic sites, while carbon dioxide (CO_2) is used for basic sites. Prior to analysis, the catalyst is purged to get rid of surface contaminants with helium gas at elevated temperatures.

In evaluating basic site strength and activity, the temperature is reduced to 300-450 K and exposed to CO_2. After adsorption, the catalyst is flushed with helium to eliminate excess CO_2. The temperature-programmed desorption process is then initiated, and the amount of CO_2 released is measured and calibrated to create desorption profiles (Klepel, 2005)

Peaks appearing at lower temperatures in the desorption profile indicate physically adsorbed CO_2, whereas higher peaks suggest interactions with strong basic sites (Tan et al., 2015b). Analyzing the peak area determines density of basic sites. The desorption temperature of CO_2 indicates the strength of its binding to the catalyst surface (Bertarione et al., 2004).

2.3.2.4.2.5.2 N2 Physisorption

Catalyst physical properties such as specific pore size distribution, surface area, total pore volume, and average pore diameter are determined using this technique. This is done by analyzing nitrogen adsorption and desorption at -196℃, the temperature of liquid nitrogen (Feyzi et al., 2014). This method involves adsorbing nitrogen or another inert gas onto the catalyst surface to measure how the number of molecules required to completely create a monolayer. Nitrogen preference is due to its high purity, low cost, and effective interaction with most solids (Bardestani et al., 2019). Degassing is performed to get rid of adsorbates and moisture on the catalyst at elevated temperatures prior to the measurements in the flow of nitrogen (Istadi et al., 2015; Rashtizadeh et al., 2014)

The technique operates on the principle that nitrogen gas molecules are adsorbed onto the catalyst surface at -196°C through Van der Waals forces. Nitrogen quantity depends on relative pressure and surface characteristics of the catalyst (Bertier, 2016). For interpreting results from porous materials, it is usually assumed that the surface is uniform, so the amount of nitrogen adsorbed at specific pressures helps to determine the geometry and pore size. Pore area and volume are calculated using Barrett-Joyner-Halenda (BJH) method. Specific surface area in the isotherm data is estimated via Brunauer-Emmett-Teller (BET) equation.

2.3.2.4.2.5.3 X-Ray Diffraction (XRD)

Bulk structures and crystal characteristics of catalysts are analysed with x-ray diffraction (XRD) technique. It estimates the catalyst crystalline phases and particle size in terms of their arrangement and nature (Istadi et al., 2015). XRD works by measuring how electrons in atoms within a crystal scatter electromagnetic waves with wavelengths comparable to atomic dimensions. When X-rays interact with the crystal, they are diffracted by the electrons, creating a diffraction pattern. This pattern results from constructive interference of the waves scattered by the regularly spaced atoms in the crystal lattice.

The XRD diffraction pattern provides two key pieces of information: the positions and intensities of the peaks. The positions of the peaks reveal details about the crystal lattice geometry, unit cell dimensions, and atomic arrangements. The intensities of the peaks give insight into the types and positions of atoms within the unit cell, as well as their charges, thermal movements, and structural defects (Bertarione et al., 2004; Schlögl, 2009)

2.3.2.4.2.5.4 Thermogravimetric Analysis (TGA)

Thermogravimetric analysis (TGA) quantitatively measures 1g to several grams of catalyst sample, under either variable or stable flow of gas as it heats it to high temperatures like 1600°C. Originating from an early observation by Vitruvius in 27 BC, TGA is now commonly used in chemical engineering to analyze reaction conversions, kinetics, and mechanisms through various methods such as quasi-isothermal, non-isothermal and isothermal techniques.

Sample undergoes decomposition leading to changes in oxidation state, loss of volatile compounds and decrease in mass. In an oxygen rich environment (reactive), there maybe a notable increase in transition metal mass. Polymorphic transformations phase transitions, and reactions with no significant loss in mass are difficult to monitor with TGA. Physical from chemical changes can be distinguished when differential thermal analysis (DTA) and differential scanning calorimetry (DSC) methods are used alongside TGA. Gaseous products released during the TGA process can be analyzed using evolved gas analysis (Saadatkhah et al., 2019).

CHAPTER 3: EXPERIMENTAL SECTION

3.1 Laboratory Health and Safety

All experiments were carried out in a safe manner by adhering to health and safety measures. This was to ensure the safety of laboratory equipment, personnel and general safety. The measures taken include the following.

I. Required personal protective equipment (PPE) including a laboratory coat, goggles, hand gloves, nose masks and boots were worn in undertaking all laboratory related synthesis and experiments
II. The appropriate equipment, apparatus and glassware was used for the appropriate task to ensure safety
III. The transesterification reactions and solution preparation were performed in a fume hood, ensuring that the ventilation system was fully operational throughout the process.
IV. All laboratory waste was disposed of correctly in labeled containers placed in designated areas.
V. Following WHMIS guidelines, all chemicals were properly labeled and stored in a safe manner.
VI. Broken glassware was handled with caution and disposed off into designated, covered containers specifically intended for such materials.
VII. Used cooking oils were stored in sealed, labeled containers to prevent spills that could create slippery surfaces and pose a fall hazard. Additionally, any oil spills on worktables were cleaned with alcohol to ensure the surfaces remained clean and smooth.

VIII. A clean and organized workspace was consistently maintained to ensure good housekeeping, creating a safe environment for everyone using the laboratory.

IX. Chemical spills were promptly managed according to established safety procedures.

3.2 Materials, Chemicals and Equipment

The following chemicals and materials were utilized in the preparation of catalysts, transesterification of waste oil, and the determination of feedstock and product properties: ethanol (95%, Fisher Chemical), deionized water (ACS Reagent Grade, LabChem), phenolphthalein indicator (1% ethanol, Fisher Chemical), KNO_3, SiO_2, $Ca(NO_3)_2 \cdot 4H_2O$, $Mg(NO_3)_2.6H_2O$, H_3PO_4, $NaHCO_3$, $Al(NO_3)_3.9H_2O$, $Cu(NO_3)_2.H_2O$, $Zn(NO_3)_2.6H_2O$, Fe_2O_3 and MnO (reagent grade, Sigma-Aldrich), as well as waste cooking oil, waste cow bones, waste milkfish scales, waste eggshells, and waste banana peels all sourced from households.

The feedstock and product densities and viscosities were measured with the DMA 4500 M density meter and the Lovis 2000 M/ME micro viscometer from Anton Paar, providing an accuracy of 0.5% for viscosity and 0.02°C for temperature.

3.3 Overview

In line with the scope and objectives of this work, to improve calcined eggshell, fish scale and cow bone catalysts were mixed into a tri-blend heterogeneous catalyst. Various mixing methods were employed in the preparation of these tri-blend catalysts after which different blend ratios were also tested followed by impregnation with a metal promoter all in advance to improve the tri-blend catalyst. Due to the poor performance of the calcium based catalysts, banana peel which is potassium rich was

calcined and optimized as a heterogeneous catalyst to obtain high performance. Reaction conditions were varied to study their effect on performance until an optimum was obtained. Due to the good performance of the calcined banana peel catalyst, and its drawbacks in terms of availability for large scale production and calcination yield an inorganic replica (using inorganic precursors) of the optimized banana peel catalyst was synthesized using two different preparation methods and the results were compared to selecting the best performing. Kinetic data was obtained and the kinetic parameters (Activation energy, order of reaction with respect to reactants) were determined.

3.4 Waste Cooking Oil (WCO) Purification and Properties

It is salient to purify waste cooking oil prior to use in biodiesel production because during the use of the cooking oil, various small solid particles of food such as proteins and carbohydrates may find their way into the oil. These particles are contaminants in biodiesel and hence there is the need to get rid of them via simple filtration with the aid of a filter paper.

In the process of using vegetable oils, such as frying, triglycerides undergo oxidation and polymerization which increases their viscosity and density. Also, depending on the conditions surrounding the use of the oil (frying time, reusability, continuous use as well as use in foods containing sugars and proteins) can lead to polymers, free fatty acids and dimers forming. Water and other water-soluble salts could also be introduced into the oil during its use and the purification reduces the contamination level of the waste cooking oil for biodiesel production.

The waste cooking oil used in this work was purified by (Terza Anokye-Poku, 2022) by modifying steps employed by (Farooq & Ramli, 2015) as follows.

I. The waste cooking oil (WCO) was initially filtered through a sieve to remove food residues and larger suspended particles, preventing interference with the reactions and avoiding potential blockages or damage to the equipment used for analyzing the oil's properties.

II. The oil was subsequently heated to 50°C to lower its viscosity, making it easier to flow and separate during the following purification steps.

III. A second filtration step was performed using a vacuum pump, Büchner funnel, and Whatman filter papers to eliminate smaller suspended particles that had passed through the sieve and remained after the first filtration.

IV. The filtered oil was washed with deionized water at a 1:3 ratio to eliminate soluble impurities. The resulting water-oil mixture was transferred to a separating funnel, allowing the water to settle by gravity and enabling the separation from the oil.

V. The washed oil was weighed on a mass balance prior to heating to identify when all moisture had evaporated from the oil.

VI. The oil was heated in an oven at 110°C, with its mass monitored at regular intervals until a consistent mass was reached, which took about 24 hours.

The fatty acid composition of the feedstock used in this study was determined following a modified version of the EN 14103 method at the Petroleum Analytical Laboratories, part of the Saskatchewan Research Council on the University of Regina campus using gas chromatography.

The physicochemical properties (density, acid value and viscosity) of the oil and biodiesel samples were measured. Kinematic viscosities were measured at 40°C by configuring the desired measurement mode, filling vials, and placing them in the wells of the Lovis 2000 M/ME micro viscometer (ASTM D445). Similarly, densities

were determined by selecting a preferred measurement mode and using a syringe to inject samples into the DMA 4500 M density meter for density readings (ASTM D4053).

The acid value of the samples was determined using the following procedures:

I. Five grams of the oil sample were weighed into a 250 ml conical flask.

II. Fifty milliliters of 95% ethanol were added to the oil in the flask, which was then heated and stirred on a heater with a stirrer to ensure the oil dissolved completely in the ethanol.

III. Approximately 10 drops of phenolphthalein (1% in ethanol) indicator were added to the mixture in the conical flask and titrated against a 0.1 M standard KOH solution.

IV. The titration was continued until a noticeable pink color change persisted for at least 30 seconds.

V. The titre value (the volume of KOH titrant used) was recorded, and the acid value was calculated using Equation 1 according to ASTM D 664 (Hassani, 2013; Hsiao et al., 2021).

$$Acid\ value = \frac{Concentration\ of\ KOH * Molar\ mass\ of\ KOH * Titre\ value\ (ml)}{mass\ of\ oil\ (g)} \qquad Equation\ 1$$

3.5 Catalyst Preparation

3.5.1 Calcined Eggshell Catalyst (ES)

The catalysts derived from waste eggshells were prepared using the following modified procedures, based on the studies conducted by (F. Ma & Hanna, 1999c),Click or tap here to enter text. and (Niju et al., 2014a)

I. The collected eggshells were washed with deionized water to get rid of impurities like sands and shell membrane.

II. The washed eggshells were dried in an oven at 110 ℃ overnight to remove moisture content.

III. The dry eggshells were grinded with a mortar and pestle to reduce size

IV. The eggshell mass was weighed and recorded as W_i

V. The sample was calcined in a muffle furnace at 900℃ for 4hrs to remove carbon content.

VI. The calcined eggshell mass was weighed and recorded as W_f

VII. Th calcined catalyst was grinded with a mortar and pestle and sieved to obtain particles size of 250um and below.

VIII. The catalyst weight loss and catalyst yield were calculated using Equation 2 and 57.55% was the calcination yield.

$$Catalyst\ Yield = \frac{W_f - W_i}{W_i} x\ 100\% \qquad \textit{Equation 2}$$

3.5.2 Calcined Fish Scale Catalyst (FS)

The catalysts made from fish scales were developed using modified procedures inspired by the work of (Chakraborty et al., 2011a), (Uğuz et al., 2021), and (El yaakouby et al., 2023) as shown in Figure 18

I. The collected fish scales (Milk fish) were cleaned and washed with tap water to get rid of impurities like muscle tissues.

II. They were then washed with DI water.

III. The washed fish scales were dried in an oven at 110 ℃ overnight to remove moisture content

IV. The dry fish scales mass was weighed and recorded as W_i

V. The fish scales were calcined in a muffle furnace at 900 ℃ for 4hrs to remove carbon content.

VI. The calcined fish scales were grinded with a mortar and pestle and sieved to obtain particles sized 250um and below

VII. The calcined fish scales mass was weighed and recorded as W_f

VIII. The catalyst weight loss and catalyst yield were calculated using Equation 2 and 24.68% was the calcination yield

Washed fish scales

Dried fish scales

Calcined fish scales

Fish scale catalyst obtained after grinding and sieving to 250micron

Figure 18: Calcined fish scale catalyst preparation

3.5.3 Calcined Cow bone Catalyst (CB)

The catalysts derived from discarded cow bones were synthesized by adapting the methods described by (Hussain, et al., 2021), (Babatunde et al., 2022), and (Mitaphonna et al., 2019a), as shown in Figure 19.

I. The collected cow bones were cleaned and washed with tap water to get rid of impurities like muscle tissues, tendons and ligaments.
II. The cleaned cow bones were cooked in water at 100 ℃ for 5hrs while changing the water every 30mins to get rid of tissues and to make them tender.
III. They were then washed with DI water.
IV. The washed cow bones were dried in an oven at 110 ℃ overnight to remove moisture content
V. The dry cow bones were hammered to reduce size.
VI. The dry cow bone mass was weighed and recorded as W_i
VII. The hammered bones were calcined in a muffle furnace at 900 ℃ for 4hrs to remove carbon content.
VIII. The calcined cow bones were grinded first with a mortar and pestle followed by a coffee grinder and sieved to obtain particles sized 250um and below
IX. The calcined cow bone mass was weighed and recorded as W_f
X. The catalyst weight loss and catalyst yield were calculated using Equation 2 and 60.80% was the calcination yield

Clean and boiled Cow bones

Cow bones after calcination

Grinded calcined cow bones

Calcined cow bone catalyst after sieving to 250micron particles

Figure 19: Calcined cow bone catalyst preparation

3.5.4 Tri-blend Catalysts

These catalysts were synthesized by blending calcine eggshell (ES) catalyst, calcined fish scale catalyst (FS) and calcined cow bone catalyst (CB) to improve performance in use for transesterification reaction.

3.5.4. 1 Physically Mixed Tri-blend Catalysts (Phy)

The method used in the physical mixing was basically blending the different biobased catalysts physically without the addition of any extra chemicals

I. Individually synthesized calcined eggshell, fish scales and cow bone catalysts were physically mixed by blending in a grinder
II. Mix ratios (ES: FS: CB) were varied to obtain ES: FS: CB phy catalysts.

3.5.4.2 Room Temperature Water Mixed Tri-blend Catalyst (w)

The method used in room temperature water mixing was based on modifications from (Risso et al., 2018)

I. Eggshell, fish scale and cow bone catalysts were weighed in a 1:1:1 ratio respectively to obtain 15g
II. 60ml DI water at room temperature was added to the mix in a beaker
III. The water catalyst mixture was stirred for 2hrs with an electronic stirrer
IV. The obtained mixture was dried at 110˚C in an oven overnight
V. The dried sample was calcined at 600˚C in a muffled furnace for 3hrs
VI. The calcined sample was grinded with a mortar and pestle followed by sieving to obtain the room temperature water mixed tri-blend catalyst (1:1:1 w)

3.5.4.3 Hot Water Mixed Tri-blend Catalyst (Hw)

The method used in hot water mixing was based on modifications from (Niju et al., 2014b)

I. Eggshell, fish scale and cow bone catalysts were weighed in a 1:1:1 ratio respectively to obtain 15g

II. 60ml DI water at room temperature was added to the mix in a beaker
III. The water catalyst mixture was heated at 40 ℃ while being stirred for 3hrs with an electronic heater/stirrer.
IV. The obtained mixture was dried at 110˚C in an oven overnight
V. The dried sample was calcined at 600˚C in a muffled furnace for 3hrs
VI. The calcined sample was grinded with a mortar and pestle followed by sieving to obtain the hot water mixed tri-blend catalyst (1:1:1 hw)

3.5.4.4 Potassium Promoted Mixed Tri-blend Catalyst (%K)

The procedure used in impregnating the potassium on the tri-blend biobased catalyst is outlined below.

I. Eggshell, fish scale and cow bone catalysts were weighed in a 1:1:1 ratio respectively to obtain 15g
II. Weighed amount of KOH precursor (weight depending on the %K required) was added to the organic mix in a beaker
III. 60ml DI water at room temperature was added
IV. The water catalyst mixture was stirred for 3hrs with an electronic stirrer.
V. The obtained mixture was dried at 110˚C in an oven overnight
VI. The dried sample was calcined at 600˚C in a muffled furnace for 3hrs
VII. The calcined sample was grinded with a mortar and pestle followed by sieving to obtain the potassium promoted mixed tri-blend catalyst (1:1:1 xwt% K)

3.5.5 Calcined Organic Banana Peel Catalyst (BP)

The procedure used in preparing the calcined banana peel catalyst was based on improvements from (Fan et al., 2019a), (Meriatna et al., 2023a), and (Busca et al., 2024) as illustrated in Figure 20.

I. The collected banana peels were cleaned and washed with tap water to get rid of impurities like dirt, and banana pulp.
II. They were then washed with DI water.
III. The washed banana peels were cut into pieces to reduce size for easy handling
IV. They were then dried in an oven at 110 ℃ overnight to remove moisture content
V. The dry banana peels were grinded with a mortar and pestle to further reduce size.
VI. The dry banana peels mass was weighed and recorded as W_i
VII. The banana peels were calcined in a muffle furnace at 1000 ℃, 900 ℃, 800 ℃, 600 ℃ separately for 4hrs to remove carbon content.
VIII. The calcined banana peels were grinded further with a mortar and pestle and sieved to obtain particles sized 250um and below
IX. The calcined banana peel mass was weighed and recorded as W_f
X. The catalyst weight loss and catalyst yield were calculated using Equation 2 and 10.20% was the calcination yield (BP900)
XI. Catalysts were labelled BP900, BP800 and BP600 representing banana peel catalyst calcined at 900 ℃, 800 ℃ and 600 ℃ respectively.

Washed and cut banana peels

Dried banana peels

Grinded banana peels after drying

Final calcined catalysts obtained at 900 ℃, 800 ℃ and 600 ℃ from left to right order.

Figure 20: calcined banana peel catalyst preparation

3.5.6 Inorganic equivalent of banana peel Catalyst (BPIn)

The inorganic replica of the calcined organic banana peel catalyst was made from inorganic precursors. This was based on chemical composition in Table 3 reported by

(Pathak G, 2018). Three different inorganic replicas were prepared as seen in Figure 21.

Table 3: Composition of M. acuminata (banana peel) ash (Pathak G, 2018)

Name of component	**Mass fraction (%)**
K_2O	65.11
SiO	10.865
CaO	7.787
P_2O_5	6.068
SO_3	2.857
MgO	2.472
Cl	2.070
Fe_2O_3	1.152
Al_2O_3	0.737
MnO	0.227
CuO	0.192
Na_2O	0.145
SrO	0.134
Rb_2O	0.123
ZnO	0.114
TiO_2	0.086
Cr_2O_3	0.036

Figure 21: Inorganic replica of calcined banana peel catalyst (BP900)

3.5.6.1 Co-impregnated Inorganic equivalent of banana peel Catalyst

This procedure used to prepare two of the inorganic replica catalysts. BPIn 1 catalyst (Banana Peel Inorganic 1) was prepared using KNO_3, SiO_2, $Ca(NO_3)_2 \cdot 4H_2O$, $Mg(NO_3)_2.6H_2O$ and H_3PO_4 precursors while BPIn 3 was prepared using KNO_3,

SiO_2, $Ca(NO_3)_2 \cdot 4H_2O$, $Mg(NO_3)_2.6H_2O$, H_3PO_4, $Al(NO_3)_3.9H_2O$, $Cu(NO_3)_2.H_2O$, $Zn(NO_3)_2.6H_2O$, Fe_2O_3, MnO precursors.

I. Calculated amounts of precursors were weighed
II. 100ml DI water was added to form a precursor solution in a beaker
III. The solution mix was stirred at 600rpm while heating at 60˚C for 2hrs
IV. The resulting sample was dried overnight at 110˚C in an oven
V. The dried sample was calcine at 600˚C in a muffled furnace in the presence of air.

3.5.6.2 Co-precipitated Inorganic equivalent of banana peel Catalyst

The procedure used in synthesizing the inorganic equivalent of banana peel catalyst replica is outlined below.

I. A solution of KNO_3, SiO_2, $Ca(NO_3)_2 \cdot 4H_2O$, $Mg(NO_3)_2.6H_2O$ and H_3PO_4 precursors was prepared using 100ml DI water in a beaker based on calculated masses.
II. 10% excess precipitating agent ($NaHCO_3$) was used to prepare a solution with 100ml water in a separate beaker.
III. The precipitating agent solution ($NaHCO_3$) was added drop wise while stirring vigorously at 600rpm
IV. The stirring was continued for 2hrs
V. The obtained mixture was dried in oven at 110˚C overnight
VI. The dried sample was calcine at 600˚C in air to obtain BPIn 2 catalyst.

3.6 Catalyst Characterization

In this research, Temperature Programmed Desorption (TPD), BET evaluations were performed at the Clean Energy Technologies Research Institute (CETRI) at the University of Regina. Conversely, Powdered X-Ray Diffraction (P-XRD) analysis was conducted at the University of Manitoba, particularly within the Microscopy and Materials Characterization Department of the Faculty of Science.

3.6.1 BET

Using the Micrometrics 3Flex Surface Analyzer, nitrogen adsorption/desorption measurements were conducted to determine the average pore size, average pore volume, and surface area of the catalysts. Approximately 0.1 g of the sample was placed into the physisorption cells, followed by degassing at 200°C for 2 hours with nitrogen flow, facilitated by the Micromeritics VacPrep 061. The analysis of the degassed sample was then performed at -196°C in the Micrometrics 3Flex Analyzer. The BJH (Barrett, Joyner, and Halenda) method was employed to calculate the surface area, pore volume, and pore size based on the adsorption and desorption isotherms.

3.6.2 CO_2 TPD

The strength and quantity of basic sites were assessed using the CO_2-TPD method. These measurements were performed with the CHEMBET-3000 TPR/TPD instrument, which features a thermal conductivity detector (TCD) from Quantachrome Instruments. For each measurement, approximately 0.1 g of the catalyst sample was placed in a quartz U-type reactor. Helium gas was then introduced at a flow rate of 60

ml/min at 200°C for 1 hour. After this, the sample was cooled to 50°C, and a 3% v/v CO_2 in N2 mixture was introduced at a rate of 100 ml/min for 1 hour to facilitate CO_2 adsorption and identify basic sites. Following this, CO_2 desorption was conducted by flowing He gas at 60 ml/min while gradually increasing the temperature to 900°C at a rate of 10°C/min. The desorbed CO_2 was monitored using the thermal conductivity detector (TCD).

3.6.3 XRD

The XRD analysis was essential for identifying and examining the crystalline phase composition and structure of the catalyst. Powders were carefully packed into a shallow well within a zero-background sample holder, and XRD patterns for the four catalyst samples were recorded using a Bruker/Siemens D5000 diffractometer. The analysis employed Cu Kα radiation with a tube potential of 40 kV, a tube current of 25 mA, and a wavelength of 1.54178 Å (Cu K-alpha X-radiation; K-beta was removed using a graphite monochromator). The analysis parameters included 2θ scans ranging from 10 to 90° at a scanning rate of 1 step per minute, with intensities reported every 0.04° in 2θ.

3.7 Transesterification Reaction

The transesterification reaction was carried out in a batch process using a three necked round bottom flask submerged in a silicon oil bath to heat and maintain the required reaction temperature as shown in Figure 22. Thermometers were inserted to monitor temperature. The temperature was kept uniform with a magnetic stirrer stirring at 600rpm.

I. Weighed amount of ethanol depending on the required ethanol to oil ratio was stirred at 600rpm in catalyst in a 1000 ml three necked round bottom flask for 1hr at 60 ˚C to increase catalyst basicity

II. 200g of waste cooking oil (WCO)was stirred and heated to 60˚C in a separate beaker.

III. The heated WCO was added to the round bottom flask as stirring and heating continued.

IV. The reaction was allowed to proceed for required reaction time at 60˚C while stirring.

V. After the transesterification reaction, the products were transferred into a separating funnel and allowed to separate overnight into the catalyst, glycerol and biodiesel layers.

VI. The separated biodiesel layer kept in an oven at 110 ℃ overnight to remove unreacted ethanol before weighing to obtain the mass of biodiesel produced.

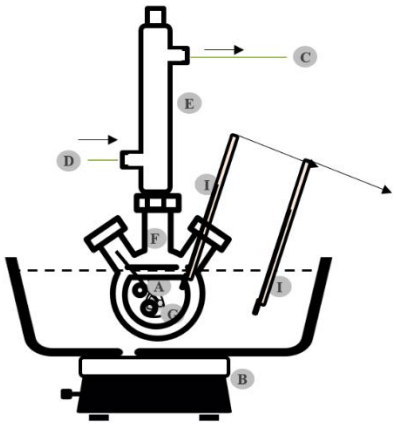

A – Catalyst E – Condenser

B – Dual heater/stirrer F – Round bottom flask (1000ml)

C – Cooling water out G – Ethanol + WCO

D – Cooling water in I – Thermometer

Figure 22: Transesterification reaction setup

The reaction conditions were selected based on reported optimum conditions from literature. These conditions were varied as seen in Table 4 to determine the optimum conditions in terms of the reaction time, catalyst wt%, reaction temperature, and ethanol to oil ratio.

Table 4: Transesterification reaction conditions

Condition	**Range**
Temperature	40˚C, 50˚C, 60˚C, 70˚C
Catalyst amount	1wt%, 2wt%, 3wt%, 4wt%
Stirring rate	600rpm
Reaction time	0.5hr, 1hr, 2hr, 4hr, 6hr
Ethanol: oil	6:1, 12:1 15:1, 21:1

CHAPTER 4: RESULT AND DISCUSSION

4.1 Characterization and properties of purified waste cooking oil (WCO)

Gas chromatography was used to determine the fatty acid composition of the waste cooking oil. This is a salient step because the degree of usage and original vegetable oil sources influence the properties of the waste cooking oil particularly its fatty acid composition, density, molar mass, viscosity and acid value as well as the quality of biodiesel produced from this feedstock. Figure 23 shows the GC-MS chromatograph of the fatty acid present in the waste cooking oil to be used for transesterification in this work.

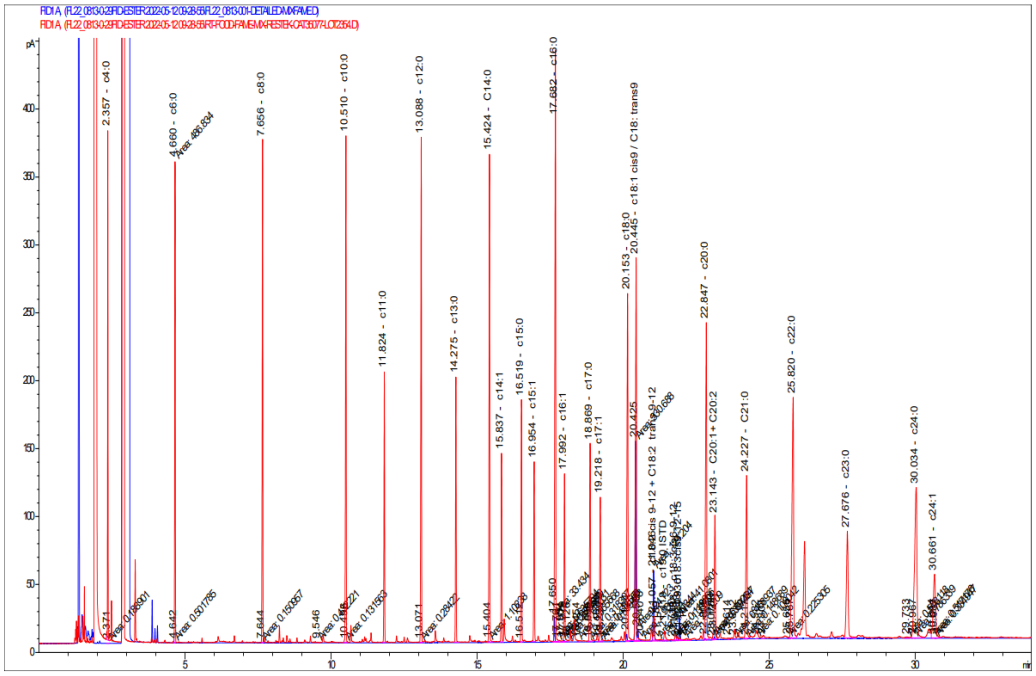

Figure 23: GC Chromatogram of purified waste cooking oil

(Moraes et al., 2021) stated that biodiesel feedstock with high monounsaturated fatty acid composition, low amount of polyunsaturated fatty acids with moderate saturated fatty acid content has the best potential of producing high quality biodiesel. As can be seen in Table 5, where the fatty acid components with their corresponding molar mass

and mass fractions are displayed, the waste cooking oil feedstock is comprised of 56.21% monounsaturated fatty acids, 28.31% polyunsaturated fatty acids and 9.51% saturated fatty acids. Biodiesel feedstocks with low polyunsaturated fatty acid composition and high saturated fatty acid composition produces biodiesel with good oxidation stability and low iodine number both of which are desirable. Increase in nitrogen oxide emission and reduction in biodiesel oxidation stability are associated with high levels of polyunsaturated fatty acids in feedstock whereas oxidative stability is favored by the presence of saturated fatty acids. The ideal targeted composition of biodiesel feed stock is monounsaturated fatty acids according to the US Energy department. This makes the obtained waste cooking oil a suitable feedstock in high quality biodiesel production. The properties of the feedstock are outlined in Table 6 as well as literature obtained properties (Anisah et al., 2019; Degfie et al., 2019; El Sherbiny et al., 2010b; Hamamci et al., 2011; Martínez et al., 2014). The WCO in this work has comparable properties to those used in literature. Although the acid value is low, the baseline in the use of base catalyst (Braga et al., 2015) is when the acid value is less than 2 mgKOH/g. Hence it is suitable for use in biodiesel production via base catalysis (4000 times faster than acid catalyzed transesterification).

Table 5: Composition of purified waste cooking oil (WCO)

Name of fatty acid	**Molar mass**	**Mass fraction (%)**
Butyric acid	102.13	0.03
Hexanoic acid	130.18	0.08
Caprylic acid	158.24	0.03
Capric acid	186.29	0.02
Lauric acid	214.34	0.05

Mystiric acid	242.4	0.18
Pentadecanoic acid	256.42	0.03
Palmitic acid	270.45	5.58
Palmitoleic acid	268.43	0.38
Margaric acid	284.48	0.05
Heptadecanoic acid	282.46	0.07
Stearic acid	296.49	2.05
Oleic & elaidic acid	296.49	55.21
Linoleic & linolaidic acid	294.47	20.74
Nonadecanoic acid	312.53	0.52
Cis-9,12-octadecatrinoic acid & Cis-9,12, 15-octadecatrinoic acid	292.46	7.08
Arachidic acid	326.56	0.49
Cis-11-eisosanoic acid & Cis-11, 14 -eicosadienoic acid	324.54, 322.53	0.98
Heneicosanoic acid	340.58	0.02
Behenic acid	354.61	0.25
Lignoceric acid	382.66	0.13
Nervonic acid	380.65	0.06

Table 6: Properties of purified waste cooking oil (WCO)

Property	Value (this work)	Values (literature)	Unit
Molar mass	848.6621	-	g/mol
Density	0.92150	0.91 to 0.98	g/cm^3
Specific gravity	0.92235	-	
Viscosity	36.61	28.3 to 60.96	mm^2 /s
Acid value	0.4975	0.82 to 3.3	mgKOH/g
Moisture content	325ppm	0.5% to 1.42%	

4.2 Characterization of Heterogeneous Catalysts Synthesized

It is salient to study catalyst properties and determine which properties contribute towards the performance in terms of producing biodiesel from waste cooking oil and optimize them. Through characterization it is possible to tell how the catalyst synthesis process and conditions such as calcination temperature influence the catalyst properties as well as its performance. Basicity is the main chemical activity determining property and is tested through CO_2 TPD test where peaks in 150℃ to 300℃ temperature range are considered weak basic sites, 300℃ to 500℃ temperature range are considered medium/intermediate basic sites and 530 ℃ to 720 ℃ are considered strong basic sites.

4.2.1 Calcined Eggshell Catalyst

The properties of the synthesized Eggshell catalyst calcined at 900 ℃ for 4hrs was determined from existing literature. The properties of eggshell catalysts synthesized using a similar procedure as used in this research was reported in (Wei et al., 2009). It

stated that beyond a calcination temperature of 800 ℃, particle sizes decreased significantly and led to irregularly shaped catalysts. This observation was attributed to the change in composition, being the change from $CaCO_3$ to CaO. According to TGA analysis, water and organics are removed at temperatures below 600 ℃ during calcination while CO_2 removal was between 700 ℃ and 800 ℃(Wei et al., 2009). (Buasri et al., 2013) reported that eggshell catalyst calcined at 900 ℃ for 4 hours contains 98.12% CaO, 1.16% MgO, . The surface area reported was 136.10m^2/g, a pore volume of 0.12cm^3/g (Buasri et al., 2013) and a mean pore diameter of 34.12Angstrom.

(Terza Anokye-Poku, 2022) reported that two peaks were observed at 402 ℃ and 609 ℃ respectively in a CO_2 TPD test to check the basic sites present. This represented medium and strong basic site strength respectively.

4.2.2 Calcined Fish scale Catalyst

4.2.2.1 CO_2 TPD

A CO_2 TPD test was undertaken to test the chemical properties of the fish scale catalyst calcined at 900 ℃ for 4hrs to determine the strength and number of basic sites. The profile obtained shows in Figure 24 that the catalyst has only one peak appearing at 662 ℃ representing strong basic sites. The number of basic sites was 0.56305mmol/g. Obtained peak was broad spanning from 400 ℃ to 900 ℃ which is a wide temperature range and indicates the presence of intermediate basic sites as well though in low quantities. In a work by (Terza Anokye-Poku Regina, 2022) a similar observation was made for calcined fish scale catalyst where only one peak was observed at a close temperature of 452 ℃.

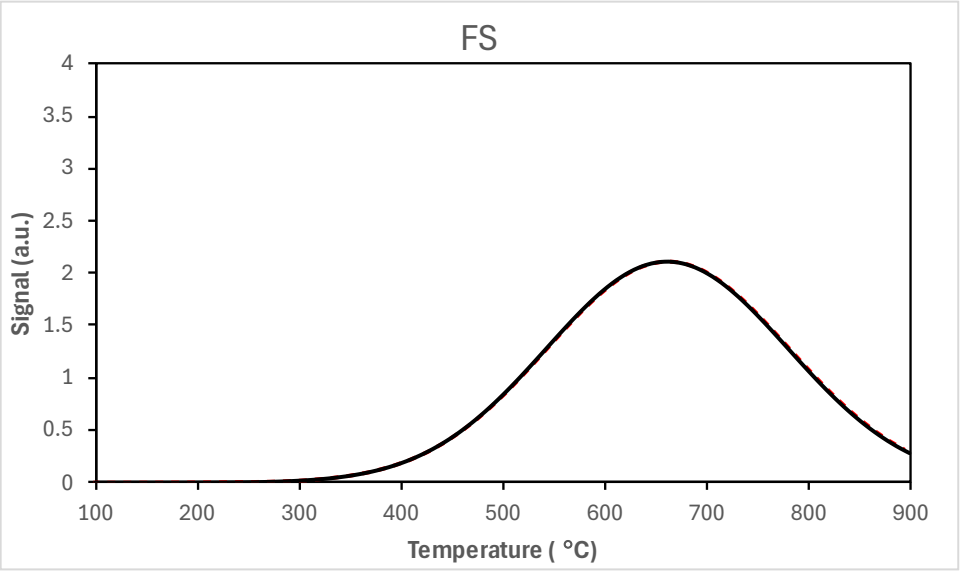

Figure 24: CO $_2$ TPD profile of calcined fish scale catalyst (basicity test)

4.2.2.2 XRD Analysis

The chemical composition of the calcined fish scale catalyst was determined. Figure 25 shows characteristic 2θ peaks at 25.9º and 28.9º which corresponds to hydroxyapatite (hexagonal rods or needle structure morphology) and at 22.9 º, 29.6 º, 30.5 º, and 35.6º which corresponds to calcium magnesium phosphate (platelike crystallites) according to International Center for Diffraction Data (ICDD). (Mustafa et al., 2015) reported that calcination of fish scales at a temperature of 900 ℃ for 5hrs at a heating rate of 5℃/min led to the formation of pure hydroxylapatite (HAp) (Venkatesan & Kim, 2010). Dry raw fish scale has a yellowish color to it but on calcination it changes to grayish white due to the HAp formation and had a 21.86wt% and 9.94wt% calcium and phosphorous content respectively. (Chakraborty et al., 2011b; Zaki et al., 2006) reported the high thermal stability of Fish scale catalyst but however, enhanced sintering occurs at temperatures above 1000 ℃ which lowers catalyst activity. At 900 ℃ some HAp transforms to beta tricalcium phosphates(Chakraborty et al., 2011b) which is used interchangeably with

Magnesium whitlockite(Scotchford, 1995), a base catalyst(Tada, 1975). (Goldberg et al., 2022) also confirmed the formation of Magnesium whitlockite when fish scales were calcined at 900 ℃

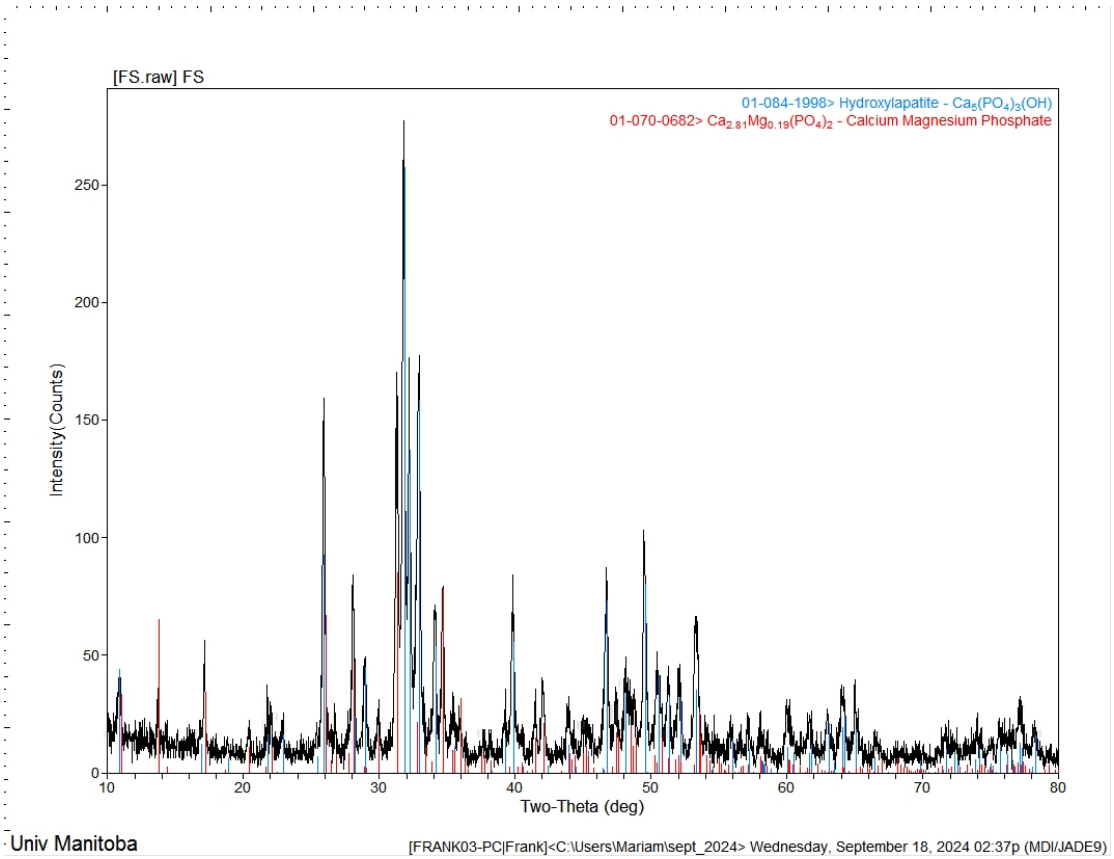

Figure 25: XRD of calcined fish scale catalyst (Catalyst composition)

4.2.3 Calcined Cow bone Catalyst

(Mitaphonna et al., 2019b) reported that fresh cow bone contains $CaCO_3$ and Hydroxyapatite however on calcination at 900 ℃ for 4hrs showed the formation of new compound; CaO and Ca(OH). The intensity of hydroxyapatite increased on calcination making it the main component in the calcined cow bone sample. The calcination temperature affects catalytic activity and active side density(Abdullah et al., 2017). At higher calcination temperatures, favor high catalyst activity resulting in

high biodiesel yield(Obadiah et al., 2012a). (Terza Anokye-Poku, 2022) also reported the presence of hydroxyapatite in calcined cow bone samples.

(Otori et al., 2021)observed that the particles were porous spherical shaped crystals with fine textures however in (Terza Anokye-Poku, 2022)agglomeration of particles also occurred, and this could be due to high temperature thermal sintering(Sobczak et al., 2009). Uncalcined cow bone catalyst also exhibits agglomeration however on calcination it yields high surface area catalyst(Obadiah et al., 2012b).

(Terza Anokye-Poku, 2022) reported that in CO_2 TPD of calcined cow bone catalysts, two peaks were observed at 381℃ and 528℃, indicating the presence of weak and strong basic sites respectively. The higher temperature had a broader peak (large area under the peak) than the former. (Prasetyo et al., 2024; Viriya-Empikul et al., 2012) reported the observation of broad desorption peak from 550 ℃ to 720 ℃ temperature range also indicating the presence of more strong basic sites. Table 7 gives a summary of BET and total basicity results.

Table 7: Summary of BET analysis on ES, FS and CB catalysts

Catalyst	BET Surface area (m2/g)	Total Basicity (mmol/g)	Avg. Pore size (nm)	Pore Volume (cm3/g)
ES	0.6658	0.805	2.0693	0.000344
CB	2.2152	0.046	2.0192	0.001118
FS	4.0362	0.56	105.9309	0.10689

4.2.4 Calcined Banana Peel Catalyst

4.2.4.1 CO_2 TPD

The result obtained for basicity (Puna et al., 2014) during CO_2 desorption of banana peel catalyst calcined in this work at 600 ℃ showed peaks at temperatures of 562℃, 752℃ and 848℃ (Figure 26) all of which are strong basic sites with a total basicity of 1.7347mmol/g of catalyst. The peak at 562℃ had the highest peak areas representing the most prominent type followed by obtained ta 752℃ and that at 848℃ had the least peak area. Similarly, (Fan et al., 2019b) also observed three peaks and the presence of strong basic sites present at 750 ℃ when banana peel was calcined at 600 ℃.

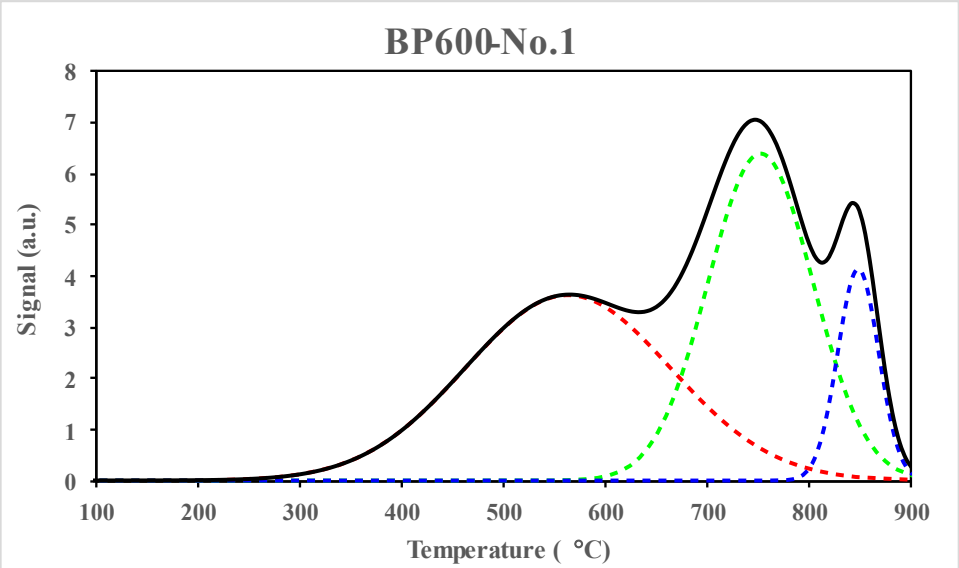

Figure 26: CO_2 TPD profile of banana peel catalyst calcined at 600 ℃ (basicity test)

The CO_2 TPD profile of banana peel calcined at 800 ℃ showed desorption peaks at 619℃, 732℃ and 810 ℃ as displayed in Figure 27. This represents the presence of strong basic sites with a total basicity of 0.8142mmol/g of catalyst. (Jitjamnong, 2021) reported that at temperatures as high as 700℃ sintering occurred. This sintering

leads to a reduction in surface area and exposed active sites which will be the contributing factor to the declined total basicity of banana peel calcined at 800℃ relative to that calcined at 600℃. The temperatures of the desorption peaks were alco comparably lower that that obtained in BP600.

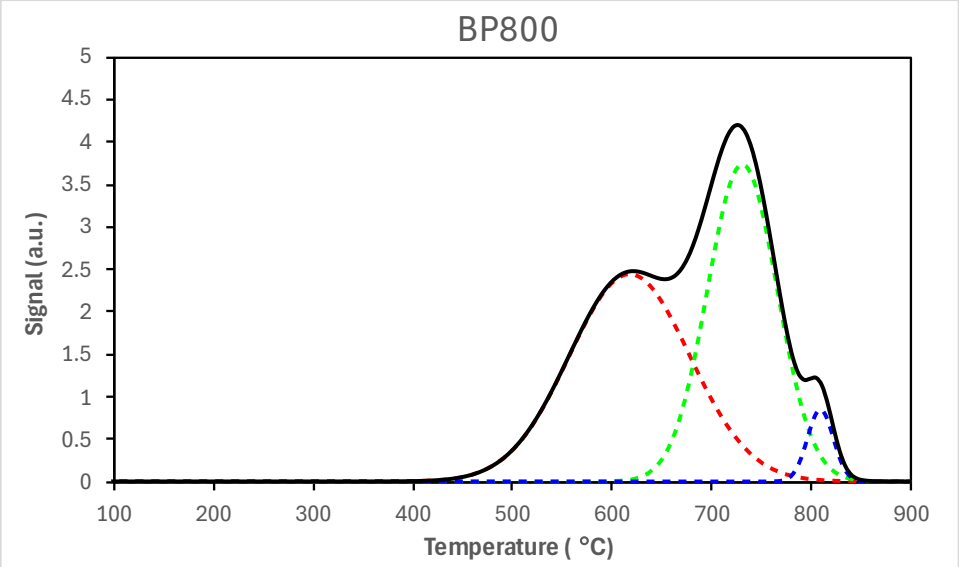

Figure 27: CO_2 TPD profile of banana peel catalyst calcined at 800 ℃ (basicity test)

As shown in Figure 28, the desorption profile of BP900 showed peaks at 564℃ and 742℃ which are relatively lower than that recorded for BP600 and BP800. The total basicity recorded was 0.7019 mmol/g. (Mouiya et al., 2019)reported sintering of banana peel catalyst at 900℃. This sintering is the reason for the recorded low basicity since the number active sites are reduced due to decrease in available surface area. 1t is observed that on increasing the calcination temperature, the total basicity and strength of basic site decreases due to the removal of carbon compounds.

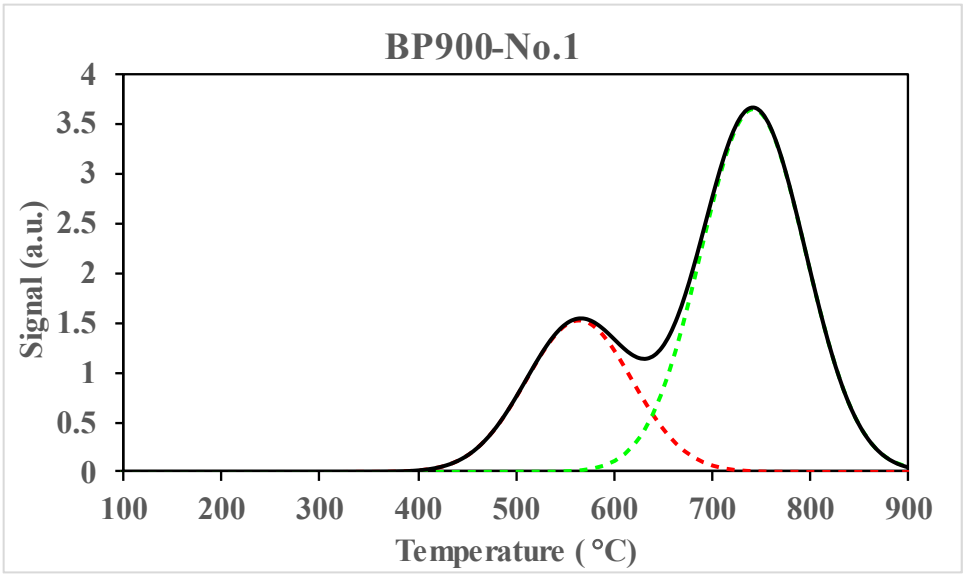

Figure 28: CO $_2$ TPD profile of banana peel catalyst calcined at 900 ℃ (basicity test)

4.2.4.2 XRD Analysis

The XRD results obtained in Figure 29 shows characteristic 2θ peaks at 28.4º, 40.6º, 50.3º, 66.2º, and 73.2º which corresponds to KCl (crystalizes in a face centered cubic structure) according to International Center for Diffraction Data (ICDD) and characteristic 2θ peaks at 16.5º, 27.2º, 32.8º, 37.6º, and 44.1º which corresponds to $KHCO_3$ (crystalizes in a monoclinic structure) in the banana peel catalyst calcined at 600 ℃. (Fan et al., 2019a) reported the KCl and K_2O in banana peel calcined at 600 ℃ similar the findings of this work. The volume of the sample in the crucible influences the removal of carbon compounds from the sample as it was observed that when a large volume was used even after 4hrs of calcination there was a color gradient in the sample from the top to the bottom in increase in darkness representing carbon presence. The presence of carbonates represents incomplete gasification. (Meriatna et al., 2023b) on carrying out calcination at 700 ℃ observed the presence of KCl, MgO, CaO, Na_2O Al_2O_3, K_2CO and K_2O. This proves the conversion of potassium carbonates to potassium oxide however a higher temperature is required to

complete the combustion to obtain banana peel ash. (Basumatary et al., 2021) calcined banana peel at 550 ℃ and observed the presence of KCO_3 in high amounts. (Gohain et al., 2017b; Nath et al., 2020), observed KCO_3 present in calcined banana peel catalyst indicating incomplete combustion at temperatures at and below 600 ℃ hence the presence of carbonates. (Gohain et al., 2017b) reported that on calcination at 700 ℃ it contained 41.37% potassium, 36.08% Calcium, 12.02% Magnesium, 10.41% calcium and traces of Zn.

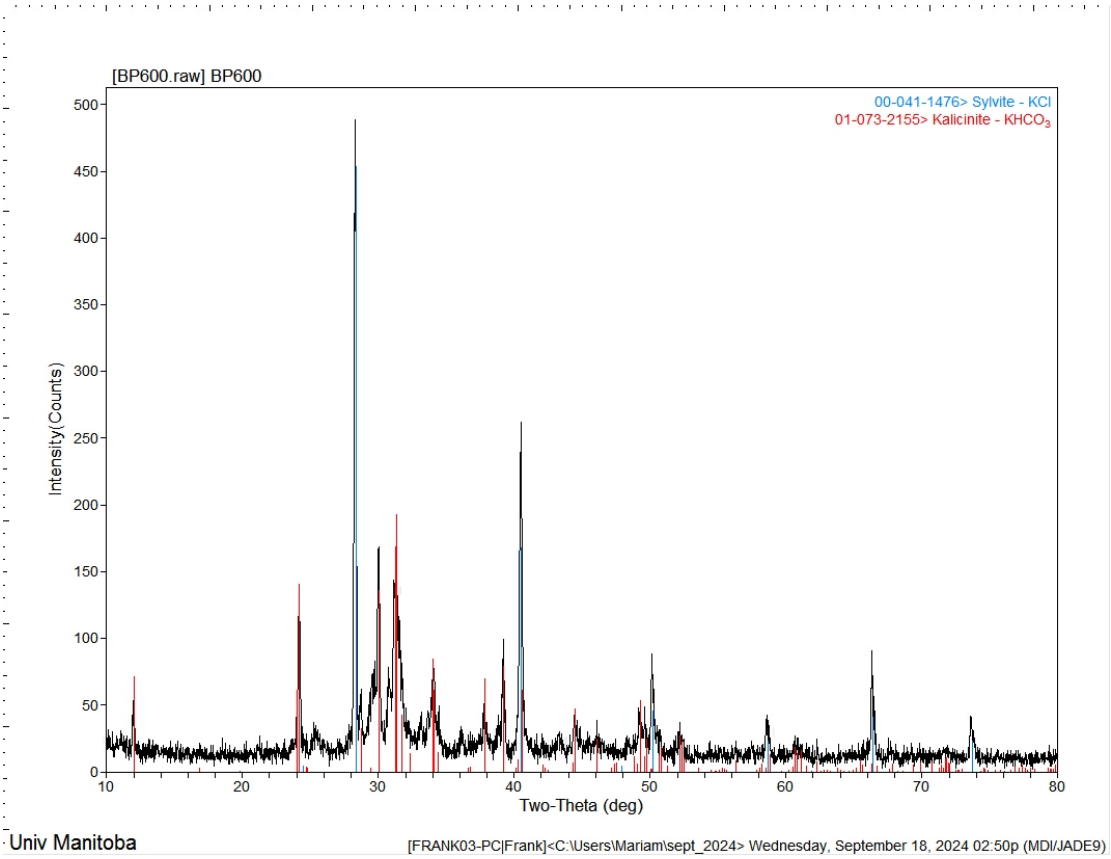

Figure 29: XRD of calcined banana peel catalyst calcined at 600 ℃ (Catalyst composition)

KCl was the main compound found in banana peel catalyst calcined at 800℃ and 900 ℃ as shown in Figure 30 characteristic 2θ peaks at 28.4º, 40.6º, 50.3º, 66.2º, and 73.2º which corresponds to KCl according to International Center for Diffraction Data (ICDD). This represents complete removal of carbonates. It is expected to find oxides

of metals especially K_2O on calcination beyond 600℃. An EDS of calcined banana peel by (Fan et al., 2019a) showed the presence of Potassium, Oxygen, Sodium, magnesium, and chlorine compounds, even though its XRD profile only showed KCl and K_2O as the main active content. The downside of calcining at high temperatures is the resulting low catalyst yield (Ozbay et al., 2019)which was about 10% for banana peel calcined at 900 ℃.(Fan et al., 2019a) reported that calcined banana peel yields a better K_2O-KCl dispersion relative to physically mixing K_2O and KCl. (Gohain et al., 2017c) stated its XRD depicted the complex of carbonates, oxides, silicates and sulfides of potassium and calcium in banana peel calcined at 700 ℃. not much literature is present on the calcination of banana peel at 800 ℃ and 900 ℃. The resulting samples had a blue green characteristic color of its crystalline structure. (Fan et al., 2019a) reported a change in color from brown (raw dry banana peel) through grey (banana peel calcined at 500 ℃) to a more whitish grey color (for both banana peel calcined at 600 ℃ and 700 ℃) however, their data did not include results at higher calcination temperatures.

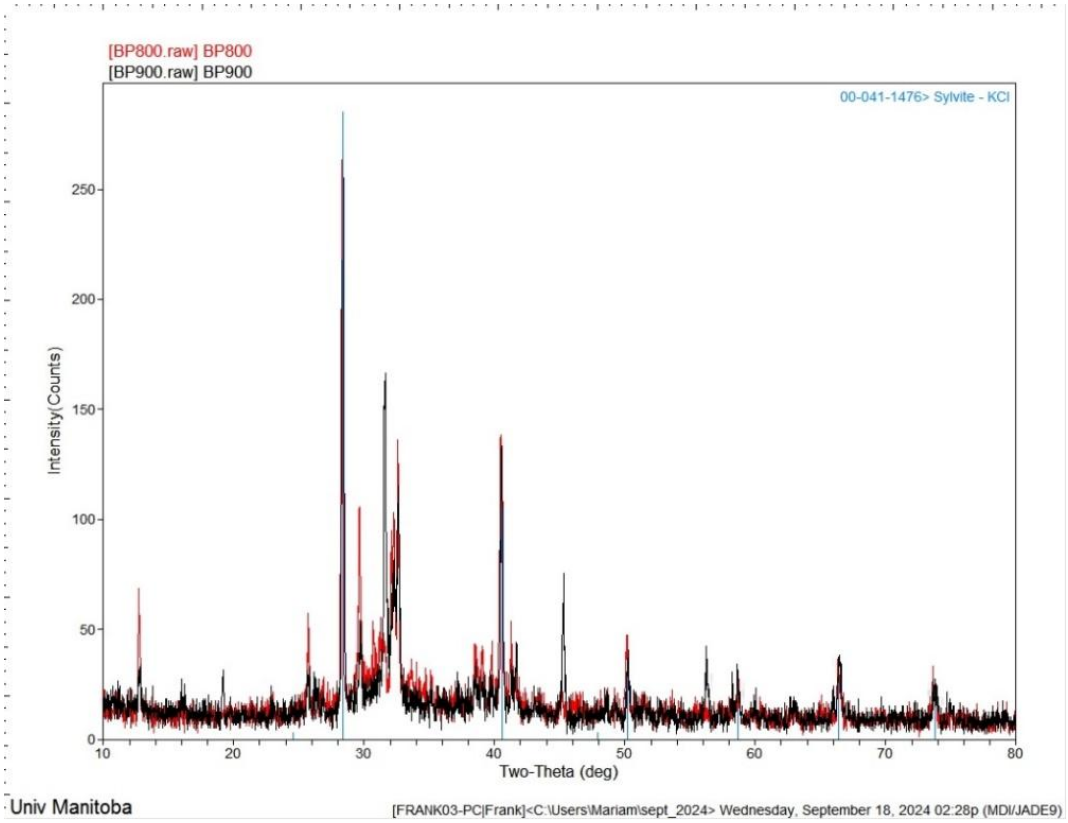

Figure 30: XRD of calcined banana peel catalyst calcined at 800 ℃ and 900 ℃ (Catalyst composition)

4.2.4.3 BET Analysis

From Figure 31, 32 and 33 the BET surface area, pore volume and particle size decreases with increasing calcination temperature. This was observed and explained by (Mouiya et al., 2019) to be because of sintering. Sintering occurs during high temperature calcination where there is collapse of the catalyst pore structure leading to a decrease in pore volume and surface area ultimately resulting in particle agglomeration as observed in Figure 31, 32 and 33 on calcining banana peels at 600℃ (BP600), 800℃ (BP800) and 900℃ (BP900)

This removal of carbon compounds leads to a decline in catalyst surface area as shown in graph 1 due to the loss of carbon particles surface area. (Singh AK, 2007)

also observed that the transesterification catalysts with the lowest surface areas had the highest biodiesel production yield.

The combination of lowering pore volume (Figure 32) and increasing particle size (Figure 33) with increasing calcination temperature of banana peel catalyst is due to compaction or agglomeration of the particles due to thermal sintering. Which further explains the decrease in catalyst surface area. (Mouiya et al., 2019) reported that at a temperature of 900℃ banana peel sinters and there is thermal decomposition of organic matter.

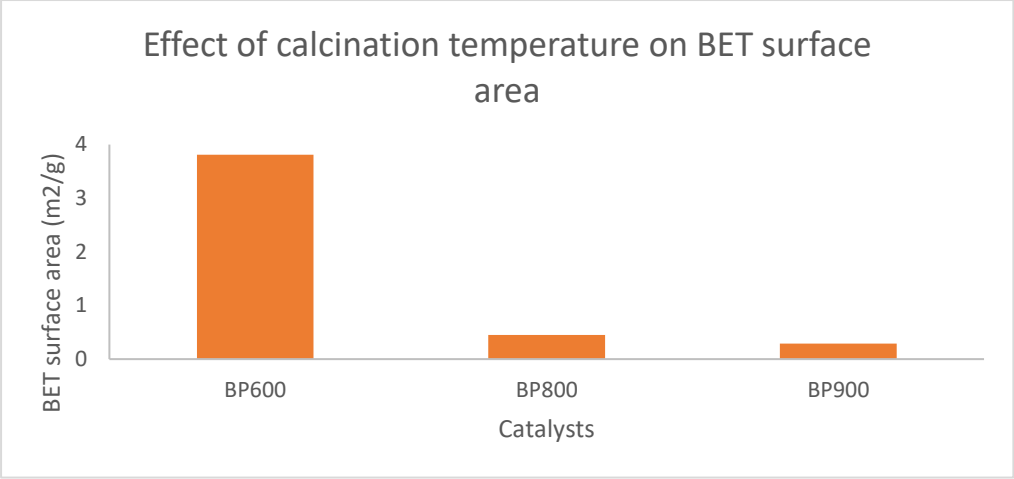

Figure 31: Effect of calcination temperature on BET surface area

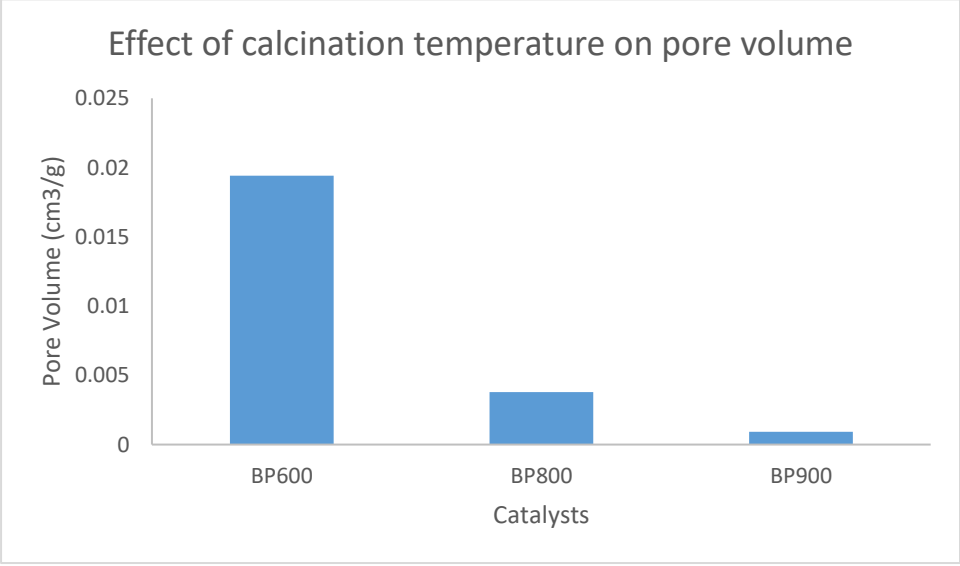

Figure 32: Effect of calcination temperature on catalyst pore volume

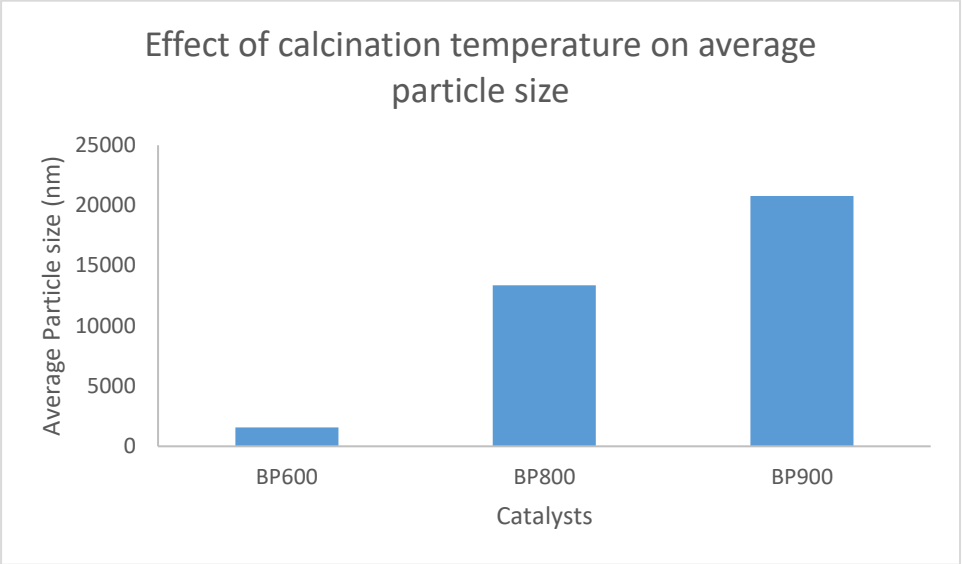

Figure 33: Effect of calcination temperature on average particle size

4.2.4.4 Thermogravimetric Analysis

The TGA analysis of BP600 and BP800 was performed to determine the thermal stability of the catalysts. In Figure 34, for BP600 catalyst TGA results, an initial loss of mass was observed till 107℃ which can be attributed to the desorption of volatile substances, free and bound water (A. Demirbas, 2007a). Most biomass studies report that moisture loss occurs up till 150℃. An intermediate weight loss stage occurs between 200℃ and 600℃ showing several DTG peaks. This weight loss is attributed to the decomposition of cellulose (occurring at 250℃ to 350℃), hemicellulose (occurring around 200℃ to 300℃) and lignin which is composed at roughly 60% carbon decomposing up till 600℃ (Sait et al., 2012; Yang et al., 2007). The final stage of the decomposition occurs around 950℃ indicated by the steep drop in mass implying the breakdown of any remaining char and inorganic residues(Mokhtar, 2017). Reported that at high temperatures, oxidation and mineral transformation occurs in carbonaceous materials (biomass) making it a good potential catalyst

material (mineral rich residues and biochar). This shows that banana peel catalysts have good thermal stability. Compared with the TGA results obtained for BP800 catalyst Figure 35, similar decomposition profiles were observed. The DTG graphs show similar rate of removal of adsorbed volatiles and moisture in the first mass drop indicating comparable hydration levels. In the intermediate region of mass drop, both samples showed multiple peaks indicating the decomposition of hemicellulose, cellulose and lignin (organic components). However, the intensity and positioning of these DTG peaks vary as well as the corresponding mass drops. On comparing the respective mass loss in Figure 36, the initial (25℃ to 107℃) percentage change in mass for BP600 and BP800 were comparable however that of BP800 was slightly higher and this is due to the ease of removal of adsorbed moisture at that temperature interval. BP800 which is composed primarily of KCl, a stable salt with high lattice energy hence low affinity for moisture easily, desorbs any absorbed moisture with less temperature requirement. BP600 on the other hand is composed primarily of both KCl and $KHCO_3$. $KHCO_3$ though hydrophobic, can decompose in highly humid environments to form K_2CO_3, CO_2 and water. K_2CO_3 is hygroscopic and requires high energy to desorb water from its lattice structure. Hence the low mass loss in BP600 at low temperature (107℃) relative to BP800. Between 107℃ and 600℃ much of the organic and any present moisture loss occurred. The loss in mass for BP600 was more than three times higher than BP800. This is because of the moisture weight loss as well as the decomposition of carbonates (carbonate loss). The mass losses in BP600 and BP800 were very similar at 800℃ and 900℃ (2.4% averagely). This implies similarity in properties.

At 950℃ the components of both BP600 and BP800 (any remaining carbonaceous materials and minerals) thermally degrade indicating their thermal stability up to

950°C. The slight mass loss difference at degradation is due to the difference in ratio of degradation products obtained in BP600 and BP800. Since BP600 is relatively high in carbonaceous products at the start of the analysis, it is expected to have high mass losses during degradation compared to BP800 which is composed of high inorganic mineral ratio.

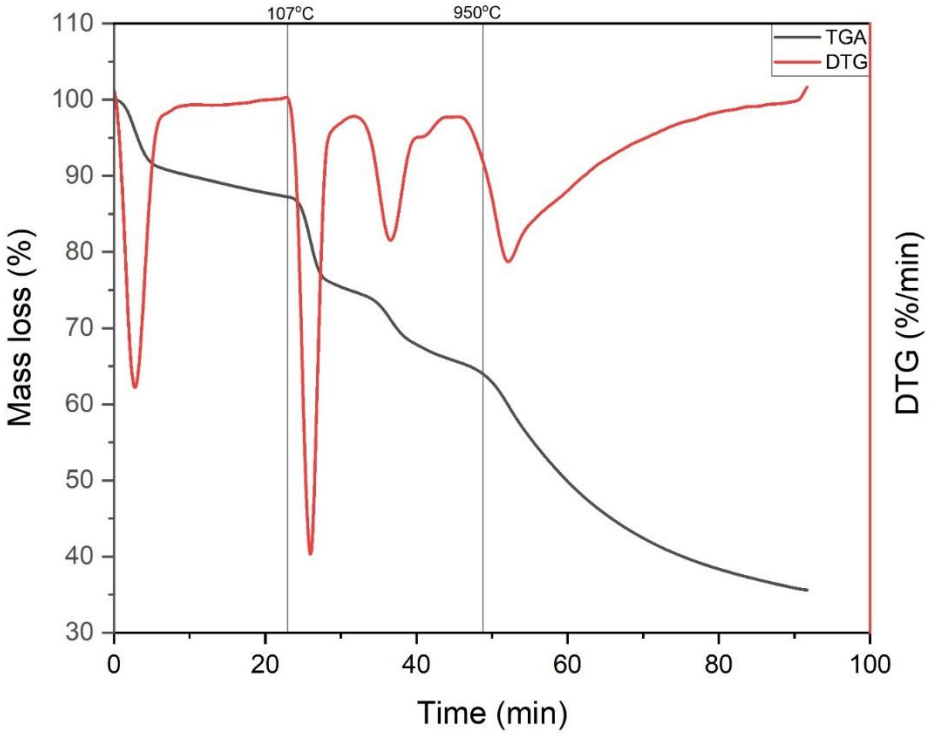

Figure 34: TGA results for BP600 catalyst

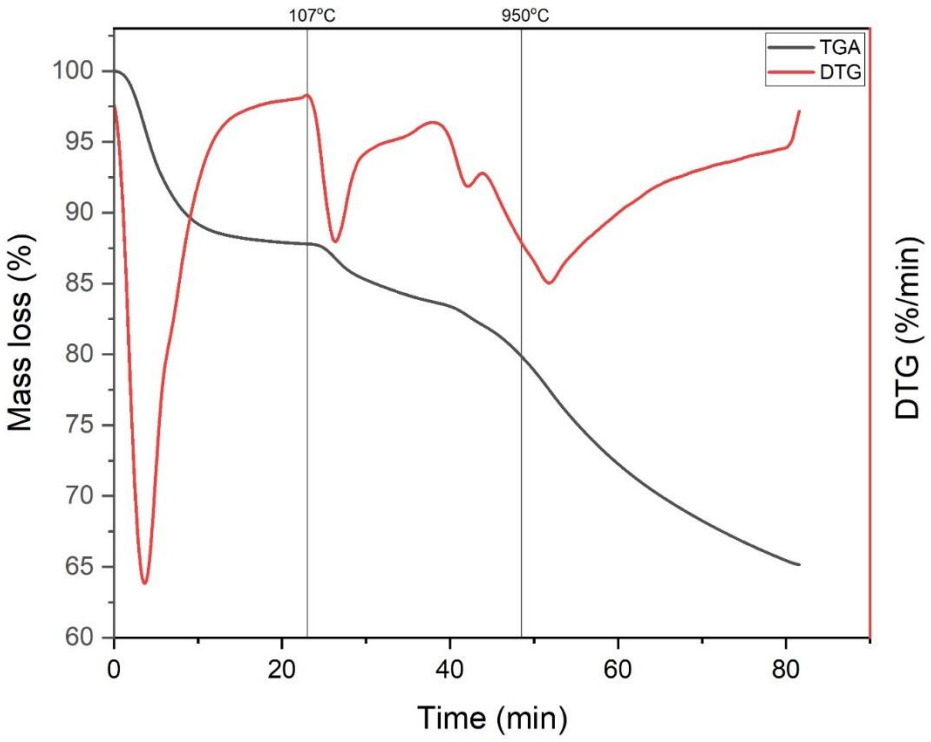

Figure 35: TGA results for BP800 catalyst

4.2.4.5 SEM/EDS Analysis

The EDS Figure 36 and elemental component (in line with literature) amounts Figure 37 show that on calcining banana peel catalyst at 600℃ much of its carbon content is lost and potassium remains the most abundant component representing 43.3% of the total catalyst mass. The presence of large amounts of oxygen suggests the presence of oxides (formed during calcination) or residual organic compounds of the metals present (Mg, Ca, K). The presence of a substantial carbon peak indicates the presence of residual carbon which is expected since banana peel is an organic material. Si, S, and P are present in trace amounts. The presence of a quite significant amount of Cl indicates the presence of residual salt compounds which maintain stability at high temperatures. Calcium contributes to the structural stability of the catalyst.

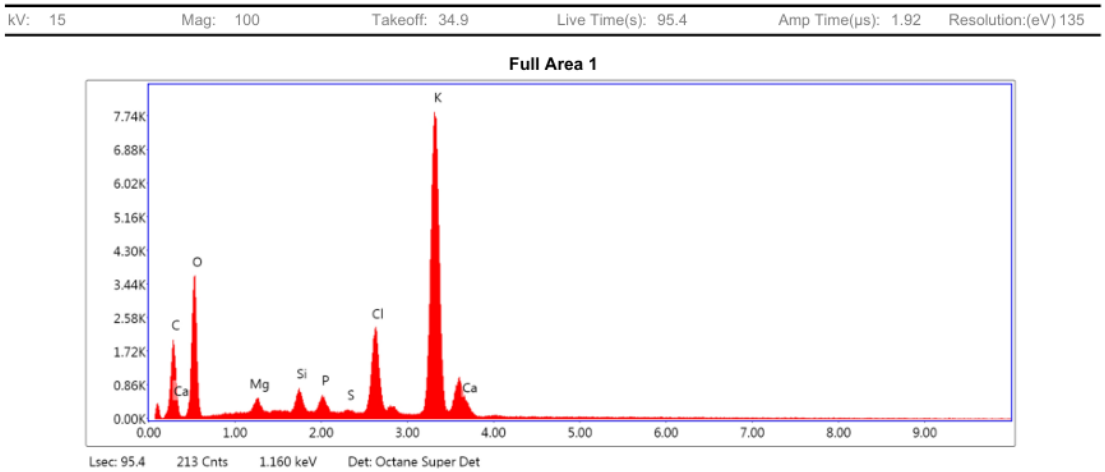

Figure 36: EDS results of BP600 catalyst

Element	Weight %	Atomic %	Error %
O K	42.4	63.4	10.1
MgK	0.9	0.9	9.4
SiK	1.4	1.2	6.2
P K	1.4	1.1	7.1
S K	0.3	0.2	17.9
ClK	8.3	5.6	3.0
K K	43.3	26.5	2.2
CaK	2.1	1.3	8.9

Figure 37: Elemental composition of BP600 catalyst

In the SEM image of BP600 Figure 38, the dark area in the middle image shows porosity of the catalyst. The pores appear to be quite uniformly distributed and more dispersed with some clustering. The particles appear to be finer and more fragmented possessing angular and irregular shapes suggesting a rough surface texture.

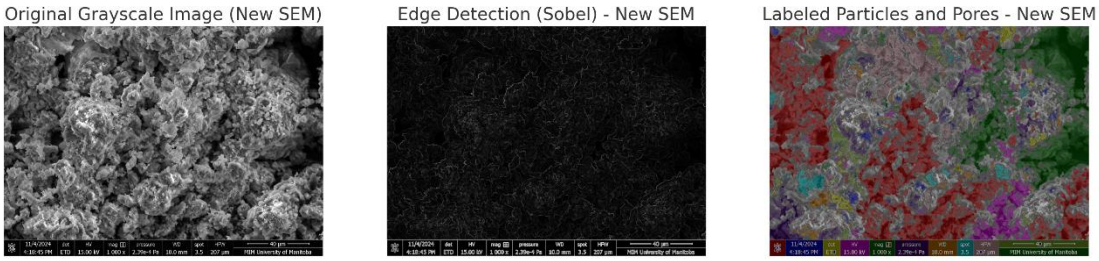

Figure 38: SEM results of BP600 catalyst

The EDS Figure 39 and elemental component amounts Figure 40 show that on calcining banana peel catalyst at 800℃ the potassium, magnesium and silicon content increase in concentration due to the removal of excess carbon compounds between 600℃ and 800℃ during calcination. This is associated with a decrease in oxygen content since the carbon is removed in the form of CO_2. There was a detectable amount of aluminum on calcining at elevated temperatures as well. Though Aluminum is not a naturally occurring plant mineral, its presence may be due to environmental contamination.

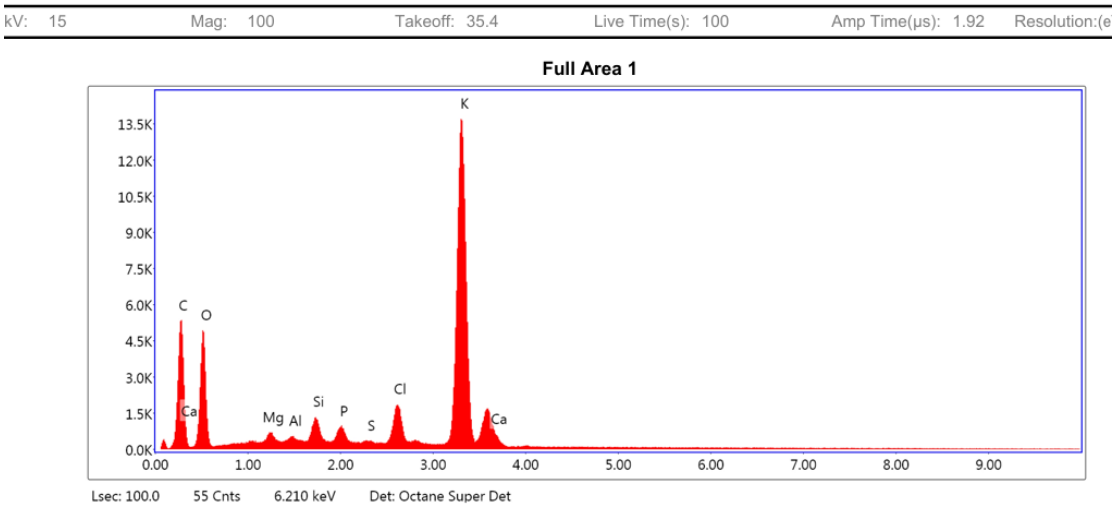

Figure 39: EDS results of BP800 catalyst

Element	Weight %	Atomic %	Error %
O K	39.7	60.8	10.1
MgK	0.7	0.7	9.1
AlK	0.4	0.4	10.6
SiK	1.8	1.6	5.1
P K	1.6	1.3	5.4
S K	0.3	0.2	16.7
ClK	4.2	2.9	3.2
K K	49.4	31.0	2.0
CaK	1.9	1.1	10.3

Figure 40: Elemental composition of BP800 catalyst

The EDS Figure 41 and elemental component amounts Figure 42 show that on calcining banana peel catalyst at 900℃ the potassium content increases in concentration due to the removal of carbon compounds between 600℃ and 900℃ during calcination. The associated drop in oxygen composition is due to the decomposition of metal carbonates including $CaCO_3$ (825℃), $MgCO_3$ (650℃) to form metal oxides releasing CO_2. The presence of aluminum in small is also observed and this is due to the removal of carbon leading to an increase in Al concentration in the catalyst. Though Aluminum is not a naturally occurring plant mineral its presence may be due to environmental contamination. There was a 72% increase in the silicon content on increasing the calcination temperature from 800℃ to 900℃.

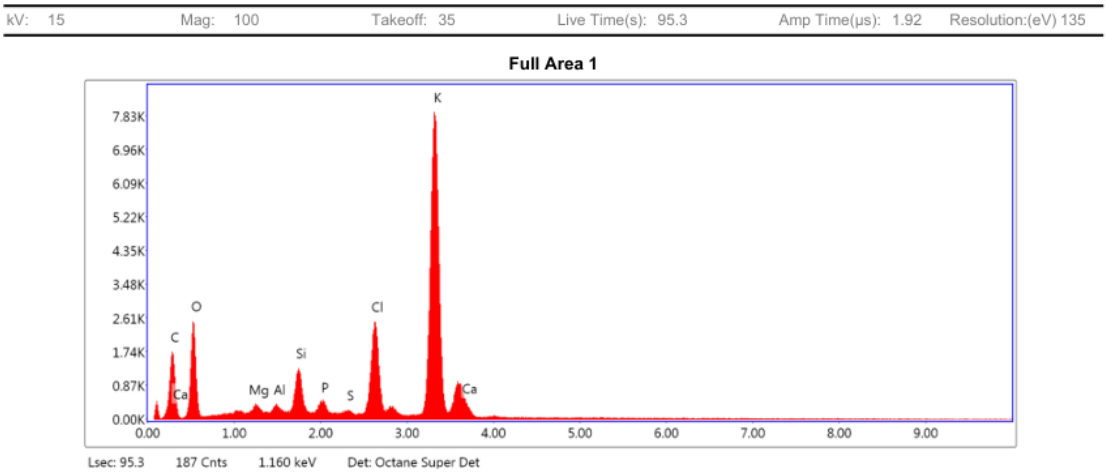

Figure 41: EDS results of BP900 catalyst

Element	Weight %	Atomic %	Error %
O K	34.9	55.5	10.4
MgK	0.6	0.6	11.6
AlK	0.5	0.5	11.8
SiK	3.1	2.8	4.8
P K	1.2	1.0	8.4
S K	0.4	0.3	15.7
ClK	9.9	7.1	2.9
K K	47.2	30.8	2.3
CaK	2.2	1.4	9.5

Figure 42: Elemental composition of BP900 catalyst

In the SEM image of BP900 Figure 43, interconnected porous networks are observed. Relative to BP600, they appear to be more irregularly shaped particles with a mix of angular and elongated shapes. Sharp boundaries observed suggest rough and fragmented morphology. BP900 appears to have relatively high porosity and larger interconnected voids suggesting a high degree of material decomposition which is expected as the calcination temperature was high (900°C). The particles appear to be

more dispersed possibly leading to increased surface area to moderation despite possible decomposition.

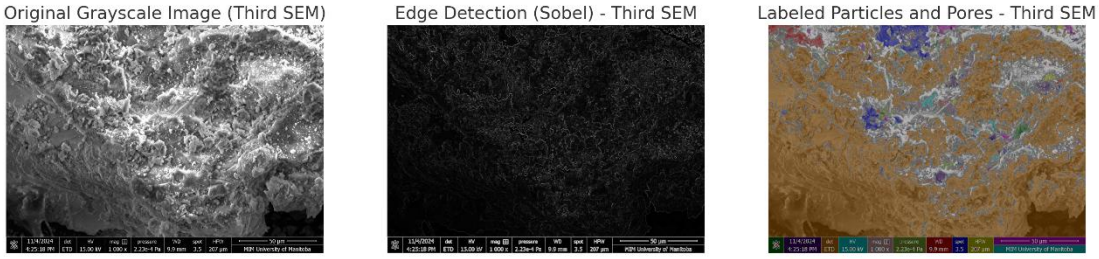

Figure 363: SEM results of BP900 catalyst

4.2.5 Inorganic Equivalent of Banana Peel Catalyst

4.2.5.1 CO_2 TPD

BPIn 1, prepared via co-impregnation of precursors of potassium oxide, silicon oxide, calcium oxide, magnesium oxide and phosphorous pentoxide, had three desorption peaks appearing at 726℃, 823℃ and 862℃ as shown in Figure 44 with a total basicity of 2.9537mmol/g of catalyst.

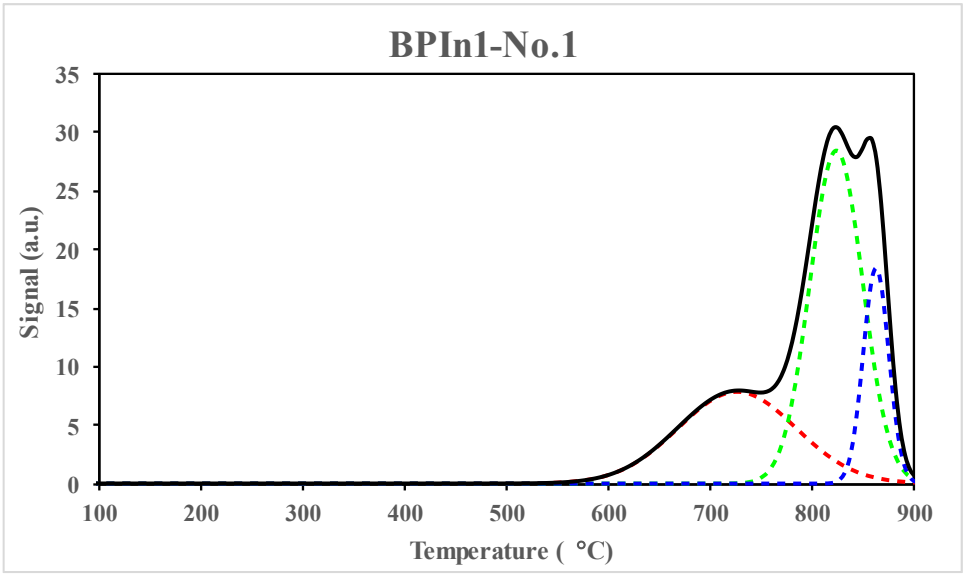

Figure 374: CO_2 TPD profile of BPIn 1 catalyst

As shown in Figure 45, BPIn 2 catalyst which was prepared by co-precipitation showed only one desorption peak at 743℃ with a total basicity of 2.5665mmol/g

catalyst. This amount is lower relative to the other two catalysts prepared via co-impregnation and this could be due to the presence of some precipitating agent diluting the targeted amounts of respective metals per gram of catalyst in the calcined sample.

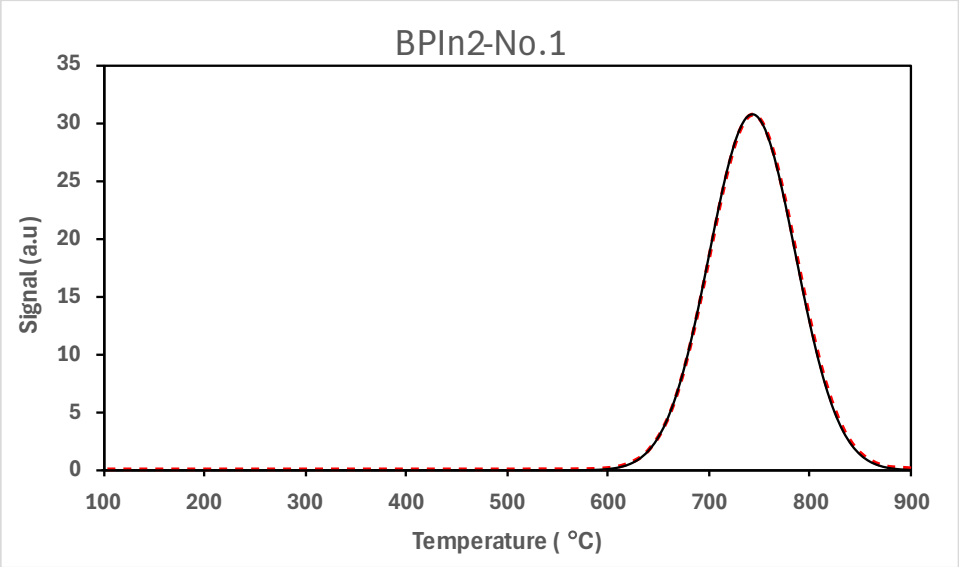

Figure 385: CO_2 TPD profile of BPIn 2 catalyst

BPIn 3 which was prepared via co-impregnation of the constituents of BPIn 1 with an additional precursor for oxides of iron, aluminum, manganese, copper and zinc recorded the highest basicity of 3.2038mmol/g of catalyst. It is evident that the addition of the extra precursors enhanced the basicity. The desorption peaks were observed at 659℃, 725℃ and 772℃ temperatures as shown in Figure 46.

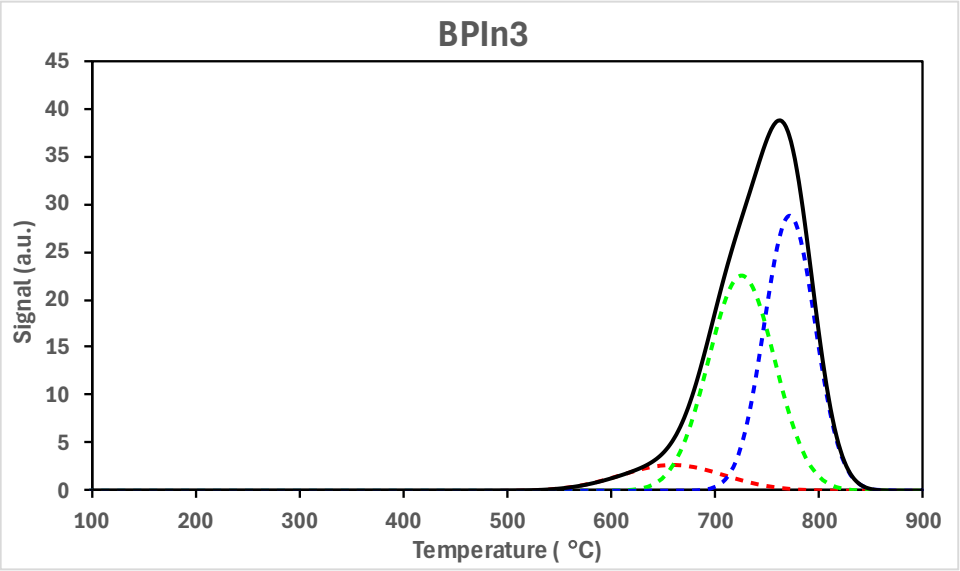

Figure 396: CO_2 TPD profile of BPIn 3 catalyst

4.2.5.2 XRD Analysis

The XRD profile of all three inorganic replicas, BPIn 1, BPIn 2 and BPIn 3 showed the presence of KNO_3 as the main active component in Figure 47. This is no surprise because it comprised roughly 70% of the catalysts. Although it was expected that on calcination, the thermal degradation would cause its breakdown to produce K_2O that was not the observed case. This could be due to insufficient heat (low calcination temperature), insufficient calcination time or the presence of a degradation inhibitor component. (Soares et al., 2010) reported that catalyst activity decreased with increasing calcination temperature due to agglomeration. Table 8 shows the nitrogen physisorption results indicating the physical properties of the catalysts.

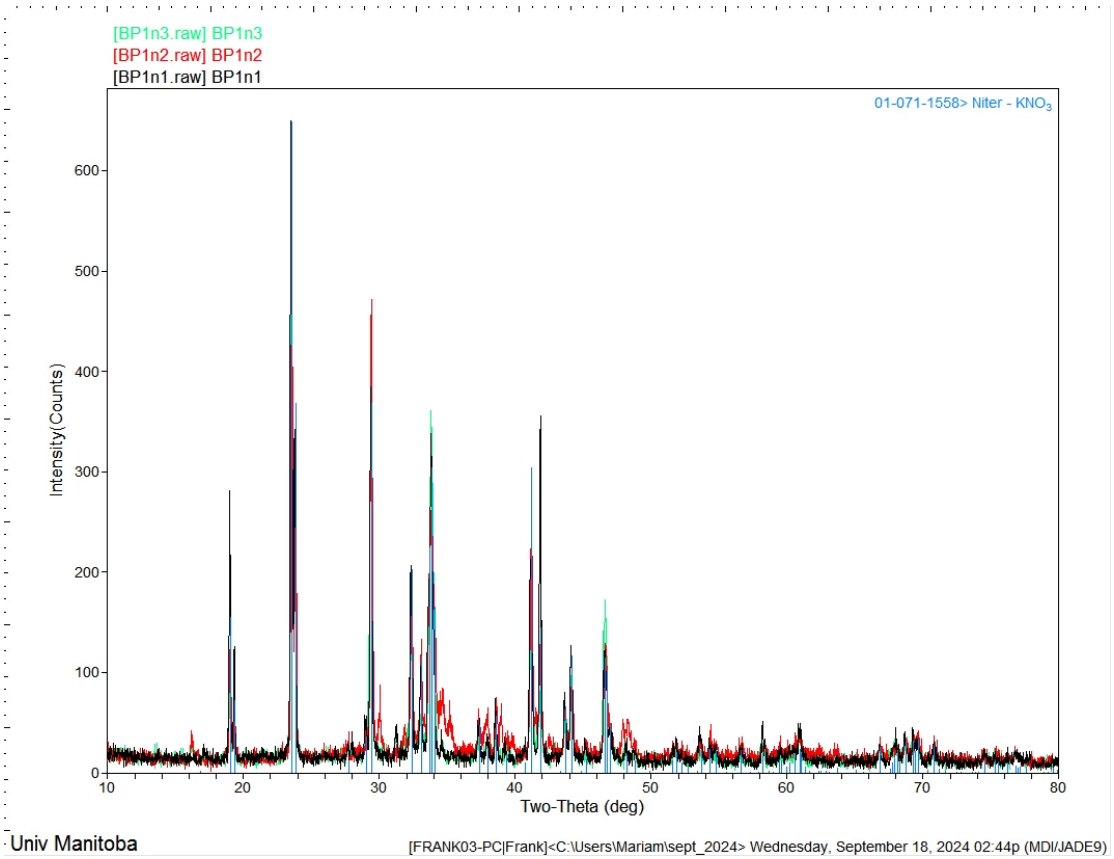

Figure 407: XRD profile of BPIn 1, BPIn 2 and BPIn 3 catalyst

Table 8: N2 physisorption results for BPIn 1, BPIn 2 and BPIn 3 catalyst

Catalyst	BET Surface area (m^2/g)	Total Basicity (mmol/g)	Avg. Pore size (nm)	Avg. Particle size (nm)	Pore Volume (cm^3/g)
BPIn3	0.1955	3.2	861.689	30695.1312	0.042109
BPIn2	0.0835	2.57	54.0816	71862.4558	0.001129
BPIn1	1.7638	2.95	14.3003	3401.8285	0.006306

4.2.5.3 EDS of BPIn 2

The EDS Figure 48 and elemental component amounts Figure 49 show the presence of K, Ca, Mg, P, and Si which were used as precursors in the preparation. However, their targeted amounts were not met, and this is due to the presence of components of the precipitation agent (Na) which should have removed via through washing during the catalyst preparation. However, the high Lewis basic nature of the $NaCO_3$ which is possibly present (oxygen and carbon amounts in EDS results) will potentially boost catalytic performance. The detected amounts of Al (0.8 mass% with 8.8% in error) and Cl (0.2 mass % with 22.1% error) which were not included in any stage of the preparation are explained due to the high error values associated with their composition inferring possible minute amounts in precursors as contaminants (traces of NaCl in commercial grade $NaHCO_3$ is quite common) .

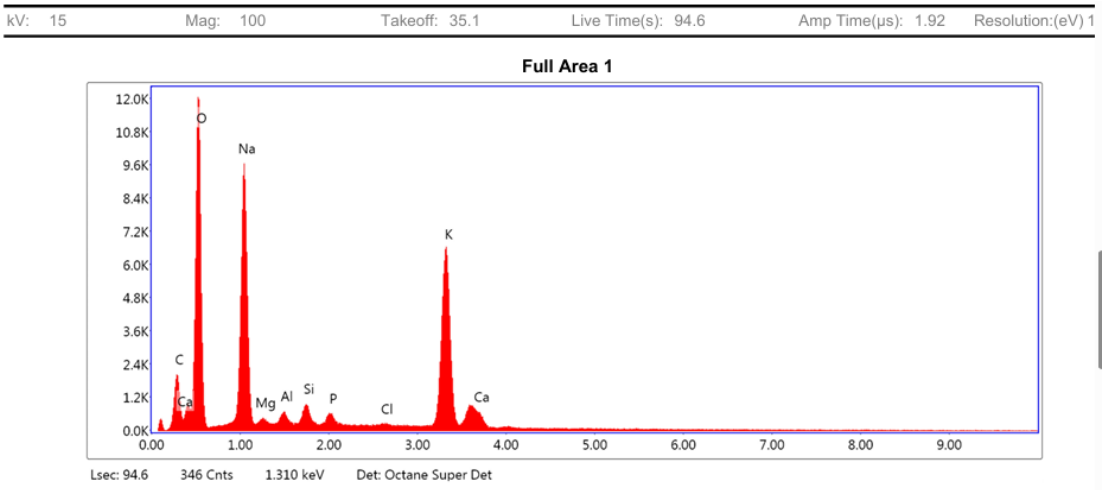

Figure 41: EDS results of BPIn 2 catalyst

Element	Weight %	Atomic %	Error %
O K	47.9	62.4	8.3
NaK	24.7	22.4	6.6
MgK	0.5	0.4	12.4
AlK	0.8	0.6	8.8
SiK	1.2	0.9	6.6
P K	0.9	0.6	8.7
ClK	0.2	0.1	22.1
K K	21.4	11.4	2.2
CaK	2.3	1.2	5.7

Figure 42: Elemental composition of BPIn 2 catalyst

In the SEM images of BPIn2 Figure 50, the pores appear to have varying degrees of density and dispersed. This suggests the presence of a mix of small, isolated pores and large voids. The variability in pore distribution suggests heterogeneous structure. The particles appear to be irregular angular shaped with well-defined edges implying a rough fragmented texture. Compared to the BP600 and BP900 SEM images, this image shows clusters of particles and pores. This kind of distribution indicates that the synthesis conditions allowed partial consolidation, leading to some interconnected and isolated pore structures.

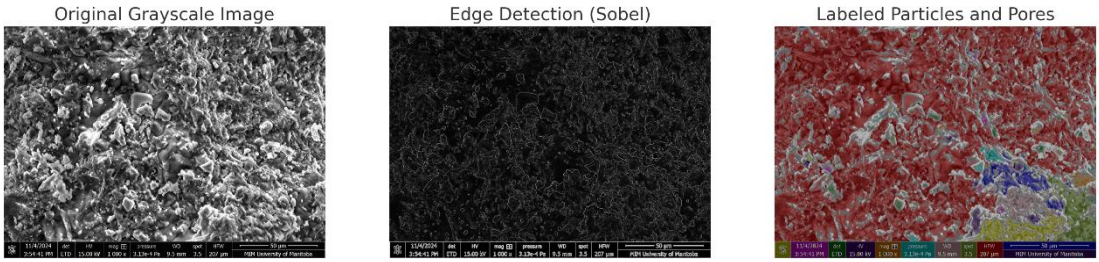

Figure 43: SEM results of BPIn 2 catalyst

4.3 Heterogeneous transesterification reactions

A more accurate biodiesel yield calculation is based on the use of gas chromatography as used by (Zabeti et al., 2010; Chakraborty et al., 2011b) where a GC equipped with a flame ionizing detector (FID) was used with a capillary column DB23 to determine the total weight percentage of FAME in the biodiesel sample. In this work, the biodiesel yield was calculated using Equation 3 as also used in (Mercy Nisha Pauline et al., 2021; Takase, 2022)

$$Biodiesel\ yield = \frac{Mass\ of\ biodiesel\ produced * 100\%}{Mass\ of\ oil\ used} \quad Equation\ 3$$

In comparing the performance of the various catalysts, the reaction conditions used was 60°C reaction temperature, 15:1 ethanol to oil ratio, 600rpm stirring rate, 2wt% catalyst dosage and a 6-hour reaction time. Table 9 shows some literature obtained biodiesel properties. High kinematic viscosity will cause incomplete fuel combustion in the combustion chamber hindering engine operation and fuel flow(Alias et al., 2018). Prior to the heterogeneous runs, an uncatalyzed run was conducted. The resulting product was separated into layers and the biodiesel layer had an acid value of 0.3318 mgKOH/g which is comparable to that of the purified WCO (0.4976 mgKOH/g) and shows a low degree of FFA conversion.

Table 9: Literature values of biodiesel properties

Feedstock	**Viscosity (mm^2 /s)**	**Density (g/cm^3)**	**Acid value (mgKOH/g)**	**Moisture content**	**Reference**
Canola oil	4.38	0.883	-	-	(Knothe & Steidley, 2009)
Coconut oil	2.75	0.874	-	-	(ASTMD, 2012)

Sunflower oil	4.42	0.878	-	-	(Brennan & Owende, 2010)
-	1.9- 6.0	-	0.80 max	0.05% max	ASTM D 6751

4.3.1 Individual ES, FS and CB catalyzed transesterification reactions

On using individually synthesized biobased catalysts, thus eggshell catalyst (ES), fish scale catalyst (FS) and cow bone catalyst (CB), fish scale catalyst and cow bone catalyst had relatively high biodiesel yield of 68.44% and 68.15% respectively as shown in Figure 51 while eggshell catalyst had a low biodiesel yield of 64.42% although higher than that obtained in an uncatalyzed reaction (33.34% with a 0.3318 mgKOH/g acid value) These low recorded values spring the need to combine them to obtain a synergistic effect on catalyst properties and possibly improved biodiesel yield. Table 10 shows the characteristics of the obtained biodiesel which are within ASTM D 6751 standard properties for 100% biodiesel.

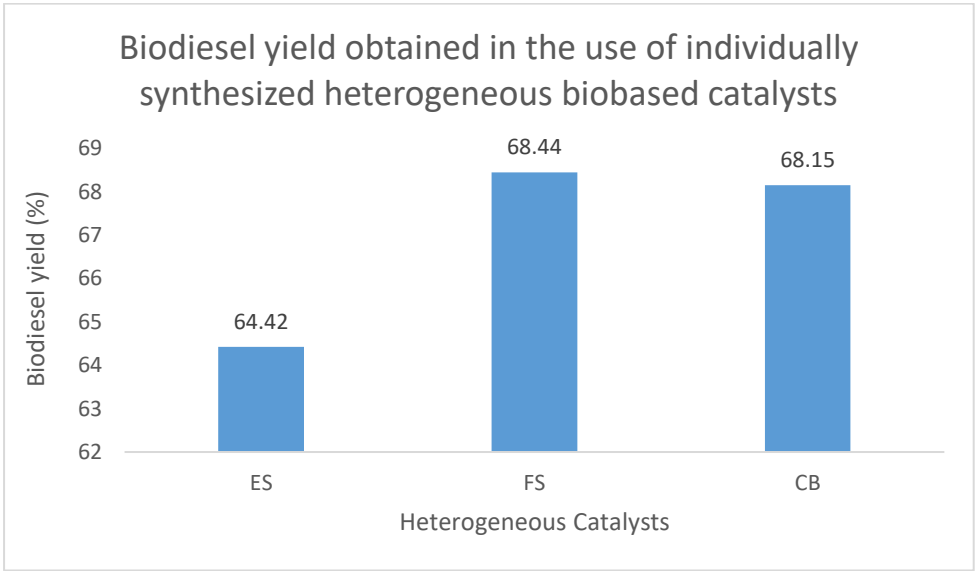

Figure 44: Biodiesel yield obtained in the use of individually synthesized heterogeneous biobased catalysts

Catalyst	Viscosity (mm^2 /s)	Density (g/cm^3)	Acid Value (mgKOH/g)
ES	1.803	0.8138	0
FS	2.195	0.7985	0.2044
CB	2.076	0.7983	0.3324

Table 10: Biodiesel characteristics in the use of ES, FS and CB catalysts

4.3.2 Comparing various ES:FS: CB mix procedures on catalyzed transesterification reaction performance

Three mix procedure types were explored to enhance catalyst performance in biodiesel production using a 1:1:1 mix ratio of eggshell, fish scale and cow bone catalysts as shown in Figure 52. Although all the mix procedures used increased the biodiesel yield that obtained through mixing in room temperature water (1:1:1 w) had a 65% biodiesel yield which was not much different from the poorest performing individual biobased catalyst (eggshell catalyst). The low temperature in this case could be the influencing factor. On the other hand, physically mixed (1:1:1 phy) and hot water mixed (1:1:1 hw) biobased blend catalyst showed a slight improvement in the biodiesel yield of 70.79% and 71.04% respectively. Since physical mixing requires less steps and energy in its synthesis relative to the hot mixing and has a comparably similar performance in terms of biodiesel yield, it was used in further optimizations. Table 11 shows the characteristics of the obtained biodiesel which are within ASTM D 6751 standard properties for 100% biodiesel.

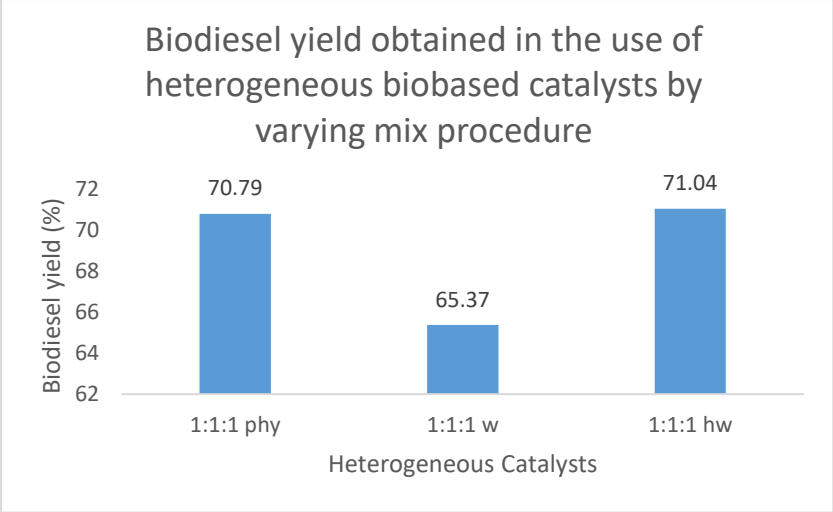

Figure 45: Biodiesel yield obtained in the use of heterogeneous biobased catalysts by varying mix procedure

Catalyst	Viscosity (mm^2 /s)	Density (g/cm^3)	Acid Value (mgKOH/g)
1:1:1phy	2.457	0.8264	0.2215
1:1:1w	2.627	0.8297	0.2235
1:1:1hw	2.454	0.8249	0.1680

Table 11: Biodiesel characteristics in varying mix procedures of catalysts

4.3.3 Comparing ES:FS: CB mix ratios on catalyzed transesterification reaction performance

On varying the mix ratios of eggshell, fish scale and cow bone catalysts via physical mixing it was observed in Figure 53 that catalysts with low eggshell ratios (0.1) as in 1:6:3phy and 1:3:6phy catalysts had the best performance in terms of biodiesel yield producing up to 73.66% and 71.3% respectively. It was previously observed in the use of individual biobased catalyst that eggshell catalyst had the least biodiesel yield and this ratio variation results also emphasizes it.

The other catalysts, which had eggshell ratio of 0.3 and 0.6 had low biodiesel yield performances as follows; 70.23% and 70.26% for 3:1:6phy and 3:6:1phy respectively for the 0.3 mass basis ratio of eggshell catalyst and 67.84% and 70.55% for 6:3:1phy and 6:1:3phy catalysts respectively.

Therefore 1:6:3phy and 1:3:6phy catalysts were selected for further optimization and enhancing. Table 12 shows the characteristics of the obtained biodiesel which are within ASTM D 6751 standard properties for 100% biodiesel.

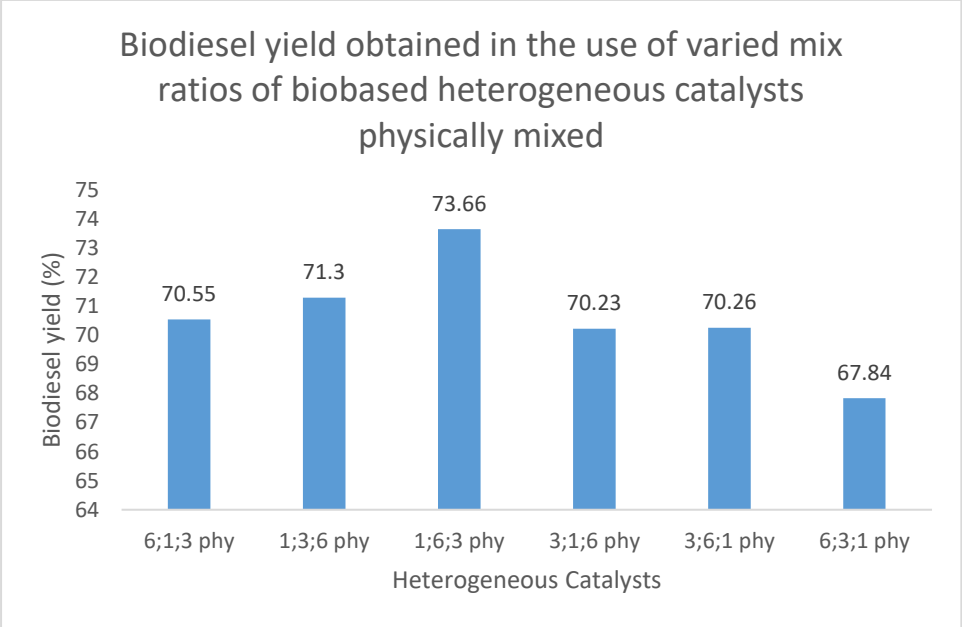

Figure 46: Biodiesel yield obtained in the use of varied mix ratios of biobased heterogeneous catalysts physically mixed

Catalyst	Viscosity (mm^2 /s)	Density (g/cm^3)	Acid Value (mgKOH/g)
6:1:3 phy	1.904	0.8044	0.1676
1:3:6 phy	1.971	0.7994	0.1673
1:6:3 phy	2.062	0.8006	0.1667
3:1:6 phy	1.988	0.8028	0.1657
3:6:1 phy	2.700	0.8293	0.2229
6:3:1 phy	3.512	0.8451	0.2802

Table 12: Biodiesel characteristics in the use of varied mix ratios of biobased catalysts physically mixed

4.3.4 Comparing amount of potassium promoter (wt%) on ES:FS: CB catalyst in transesterification reaction performance

1%, 5% and 10% (on mass basis) of potassium (K) as impregnated on 1:1:1 eggshell, fish scale and cow bone tri-blend catalyst and their performance are shown in Figure 54. The 1wt% K impregnated catalyst had the highest performance in terms of biodiesel yield of 75.83% and an acid value of 0.1944 mgKOH/g biodiesel followed

by 10wt% K impregnated catalyst with a 73.73% biodiesel yield and 0.1387 mgKOH/g biodiesel acid value. The 5-wt% K impregnated catalyst had the lowest performance among the three with a 71.82% biodiesel yield and 0.1382 mgKOH/g biodiesel acid value. From the above results, 10wt% potassium impregnation was selected as optimum since it had a good biodiesel yield and low acid value balance. Table 13 shows the characteristics of the obtained biodiesel which are within ASTM D 6751 standard properties for 100% biodiesel.

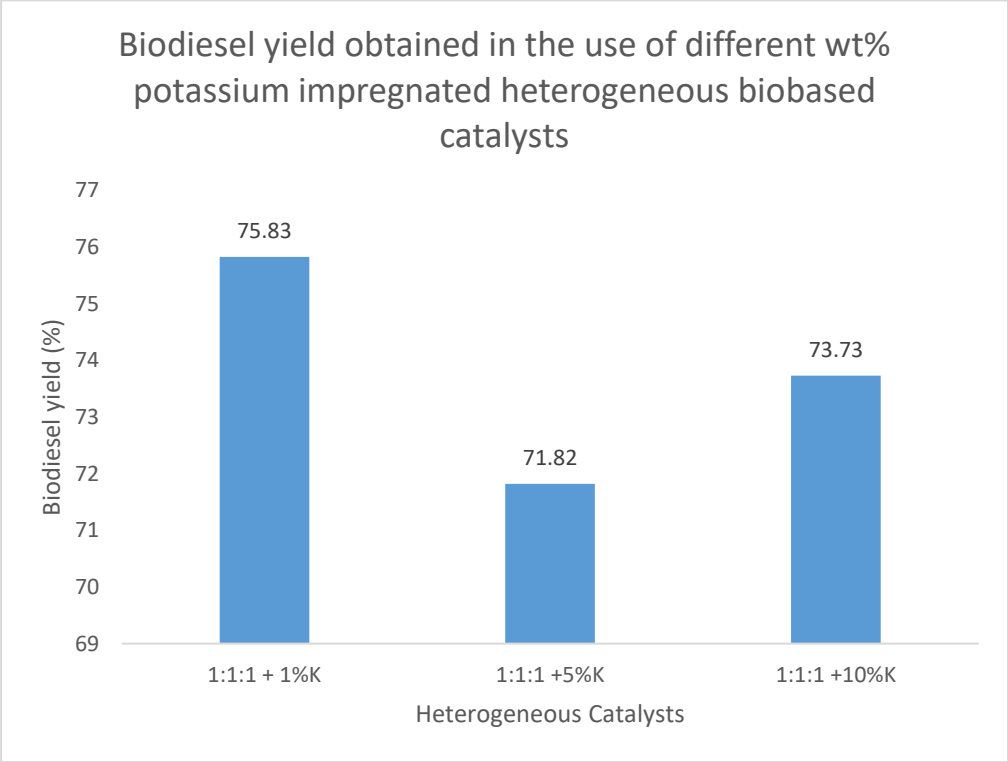

Figure 47: Biodiesel yield obtained in the use of different wt% potassium impregnated heterogeneous biobased catalysts

Catalyst	Viscosity (mm^2 /s)	Density (g/cm^3)	Acid Value (mgKOH/g)
1:1:1 +1%K	2.559	0.8250	0.1944
1:1:1 +5%K	2.437	0.8247	0.1382
1:1:1 +10%K	2.485	0.8257	0.1387

Table 13: Biodiesel characteristics in the use of different wt% potassium impregnated catalysts

4.3.5 Optimum ES:FS:CB tri-blend catalysts for transesterification

The best performing tri-blend catalyst mix ratios i.e. 1:3:6 and 1:6:3 catalysts and the worst tri-blend mix ratio catalyst i.e. 3:1:6 catalyst was selected for the impregnation of 10wt% potassium. It was notable that all the catalysts showed an improved yield of biodiesel. The biodiesel yield of 1:3:6phy catalyst increased from 71.3% to 71.5% which was not that significant; from 73.66% to a significant 75.34% from 1:6:3phy catalyst to 1:6:3 +10wt%K and 69.47 for 3:1:6 +10wt%K respectively as shown in Figure 55.

In conclusion the best biodiesel yield in the use of eggshell, fish scale and cow bone catalyst were obtained when a catalyst mix ratio of 1:6:3 (ES:FS:CB) was impregnated with 10wt% potassium. The optimum biodiesel yield was 75.34% which still is not high enough. Hence there is a need to seek alternative biobased sources. Table 14 shows the characteristics of the obtained biodiesel which are within ASTM D 6751 standard properties for 100% biodiesel except for viscosity values which are about 4% lower than the standard.

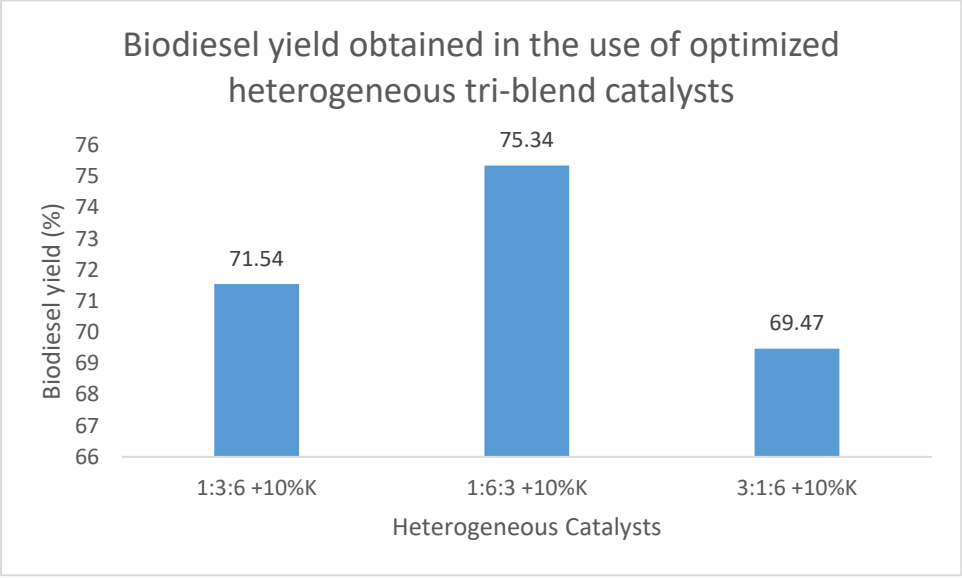

Figure 48: Biodiesel yield obtained in the use of optimized heterogeneous tri-blend catalysts

Catalyst	Viscosity (mm^2 /s)	Density (g/cm^3)	Acid Value (mgKOH/g)
1:3:6 +10%K	1.852	0.8046	0.0884
1:6:3 +10%K	1.823	0.8016	0.0655
3:1:6 +10%K	1.907	0.8049	0.0440

Table 14: Biodiesel characteristics in the use of optimized heterogeneous tri-blend catalysts

4.3.6 Effect of Banana peel catalyst calcination temperature on transesterification performance

Banana peels, which are known to have a high potassium content were explored as a potential biobased catalyst source. Potassium based biobased catalysts (banana peel) are expected to be a relatively more active Lewis base compared to the calcium based biobased catalysts (eggshell, fish scales and cow bones) due to high electro positivity and ease of electron donation.

Freshly dried and grinded banana peels were calcined at 600℃, 800℃ and 900℃ to obtain BP600, BP800 and BP900. It was observed that the color of the catalyst changed from a dark brown (freshly dried and grinded sample) through grey (BP600) to a turquoise (BP900) color this was due to thermal decomposition at high temperatures releasing the carbon constituents to obtain inorganic compounds.

In Figure 56 is observed that as the calcination temperature was increased the performance of the catalyst for transesterification also increased from 61.14% through 76.18% to 96.16% for BP600, BP800 and BP900 respectively.

BP900 gave the highest biodiesel yield of 96.16%, making it the best performing biobased catalyst in this work. Table 15 shows the characteristics of the obtained biodiesel which are within ASTM D 6751 standard properties for 100% biodiesel.

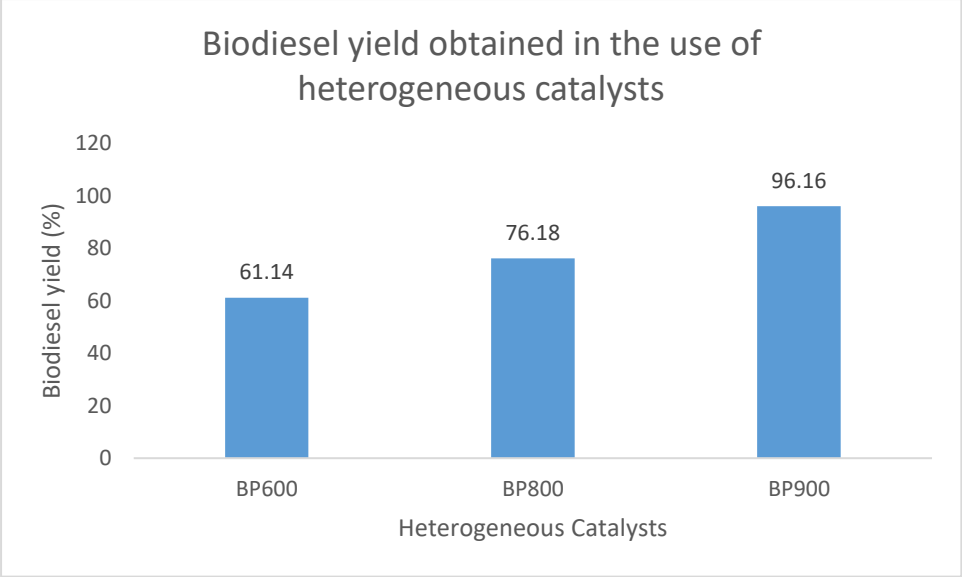

Figure 49: Biodiesel yield obtained in the use of banana peel catalysts

Catalyst	Viscosity (mm^2 /s)	Density (g/cm^3)	Acid Value (mgKOH/g)
BP600	2.541	0.8293	0.1119
BP800	2.835	0.8327	0.1008
BP900	4.125	0.8574	0.0547

Table 15: Biodiesel characteristics in the use of banana peel catalysts

4.3.6.1 Effect of Banana peel catalyst characteristics on transesterification performance

The CO_2 TPD characterization shows that the catalysts with high basic site strength influenced the performance where the catalyst with the strongest basic sites had the lowest performance (BP600). Strong basic sites make it difficult for adsorbed products to desorb form the catalyst surface hence hindering the catalysis process and causing low catalyst performance as observed in Figure 57

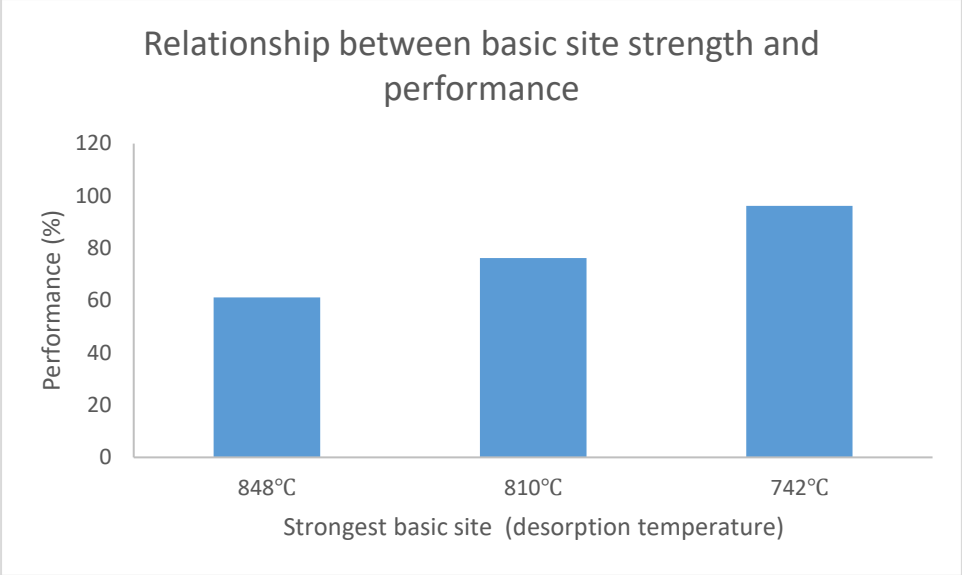

Figure 50: Catalyst characteristics that influence performance

It was observed in the SEM/EDS results that, as the banana peel calcination temperature increased, the carbon content was reduced and the potassium content increased. The increasing catalyst calcination temperature also saw an increase in biodiesel yield. This shows a positive direct correlation between the banana peel catalyst potassium content and the biodiesel yield as shown in Figure 58. Carbon is known to reduce catalyst selectivity though it has good basic properties and hence it was observed that as its quantity reduced the basicity also reduced but led to high potassium content with high selectivity for biodiesel production.

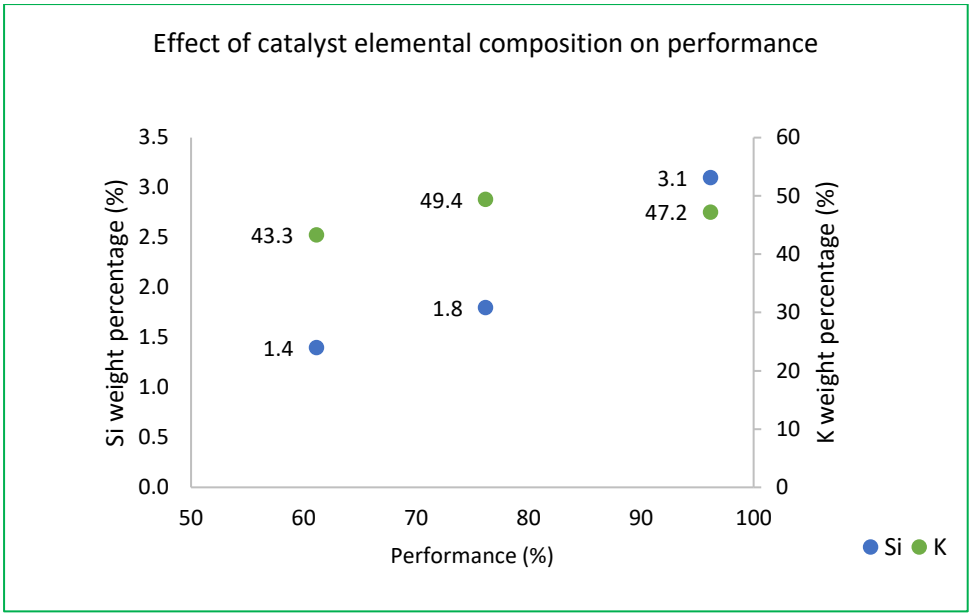

Figure 51: Relationship between potassium and silicon content on banana peel catalyst performance

4.3.7 Comparing Inorganic equivalent of banana peel catalysts based on transesterification performance

The inorganic replica of the best performing biobased catalyst (Banana peel catalyst) prepared using coprecipitation method (BPIn 2) and that prepared via co impregnation (BPIn 1) of precursors had a similar performance as shown in Figure 59 with a biodiesel yield of 84.58% and 84.47% respectively. The respective acid values were 0.0709 mgKOH/g biodiesel and 0.0955 mgKOH/g biodiesel.

BPIn 3 which entailed the addition of extra precursors (iron, zinc, aluminum, and manganese) yielded a slightly lower biodiesel amount 83.26% and an acid value of 0.1368 mgKOH/g biodiesel. Since all the produced inorganic replicas had comparable results, the coprecipitated catalyst, BPIn 2 was selected for further studies due to its calcination yield and the low acid value of its produced biodiesel which signifies high purity. Table 16 shows the characteristics of the obtained biodiesel which are within ASTM D 6751 standard properties for 100% biodiesel.

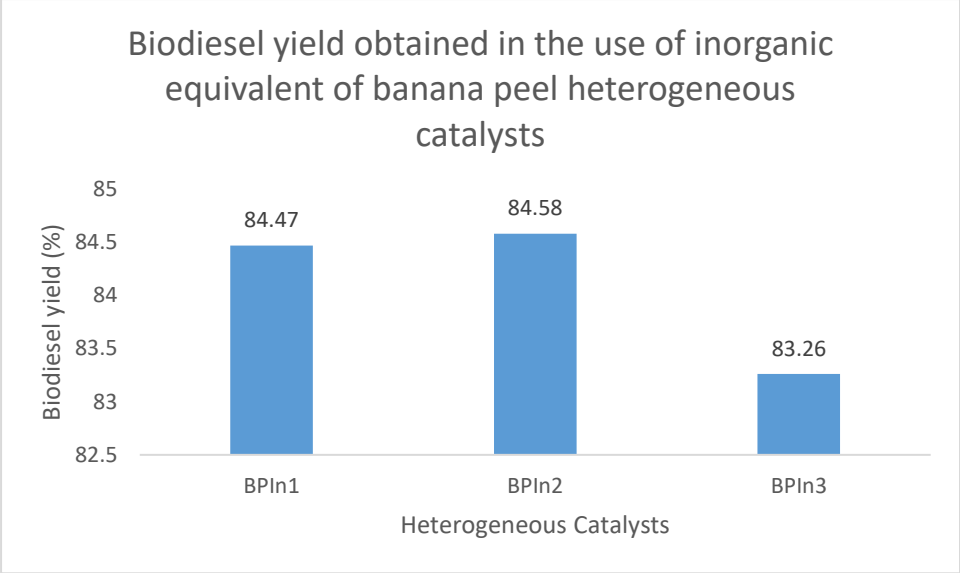

Figure 52: Biodiesel yield obtained in the use of inorganic equivalent of banana peel heterogeneous catalysts

Catalyst	Acid Value (mgKOH/g)
BPIn1	0.0955
BPIn2	0.0709
BPIn3	0.1368

Table 16: Biodiesel characteristics in the use of inorganic equivalent of banana peel catalysts

4.4 Catalyst (BPIn 2) stability

The stability of BPIn2 in was determined by subjecting the catalyst to five transesterification runs at 60℃ reaction temperature, 2wt% catalyst dosage, four-hour reaction time and 21:1 ethanol to oil ratio. The performance in terms of biodiesel yield remained constant with a 1.3 difference in biodiesel yield between the first and fifth run indicating a stable catalyst as shown in Figure 60. After each transesterification run, the next run followed without washing and drying the catalyst (no regeneration). Its stable nature based on preliminary analysis makes its suitable for continuous biodiesel production (preferrable due to ease of operation and automation) requiring less frequent catalyst replacement over time. This reduces

operational costs as opposed to low stability catalysts requiring frequent regeneration or replacement.

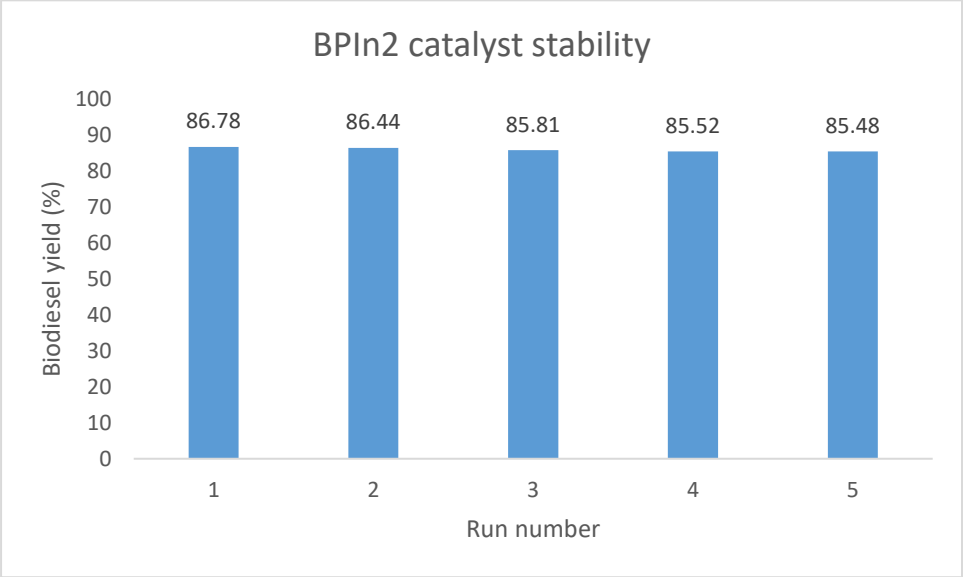

Figure 53: Stability of BPIn 2 catalyst

Run	Acid Value (mgKOH/g)
1	0.0717
2	0.0724
3	0.1113
4	0.1118
5	0.0553

Table 17: Acid value of biodiesels obtained in stability studies

4.5 Effect of reaction conditions on performance

(F. Ma & Hanna, 1999c) reported that the effect of rection conditions on biodiesel yield was also dependent on the catalyst used. Therefore, different catalysts have different responses to biodiesel yield with varying reaction conditions. This section analyses the effect of reaction temperature, time, catalyst dose and ethanol to oil ratio on the biodiesel yield in the use of BPIn 2 catalyst.

4.5.1 Effect of catalyst amount (wt%) on performance

Reactions in this comparison were carried out at 60℃ reaction temperature, 6hour reaction time and 15:1 ethanol to oil ratio while varying the catalyst dosage. (F. Ma & Hanna, 1999c) reported that at high catalyst dosage of 10wt% the reaction mixture becomes too viscous leading to mixing limitations and ineffective reaction. It was observed in Figure 61 that the biodiesel yield increased significantly from 77.75% to 84.58% when the catalyst dosage increased from 1wt% to 2wt% respectively. The dip observed at 3wt% catalyst dosage could be attributed to experimental error. However, it was not worth increasing the catalyst dosage to 4wt% from 2wt% since doubling the mass of catalyst did not affect any significant increment in biodiesel yield (less than 1% yield increment). Table 18 shows the acid values of the biodiesels obtained.

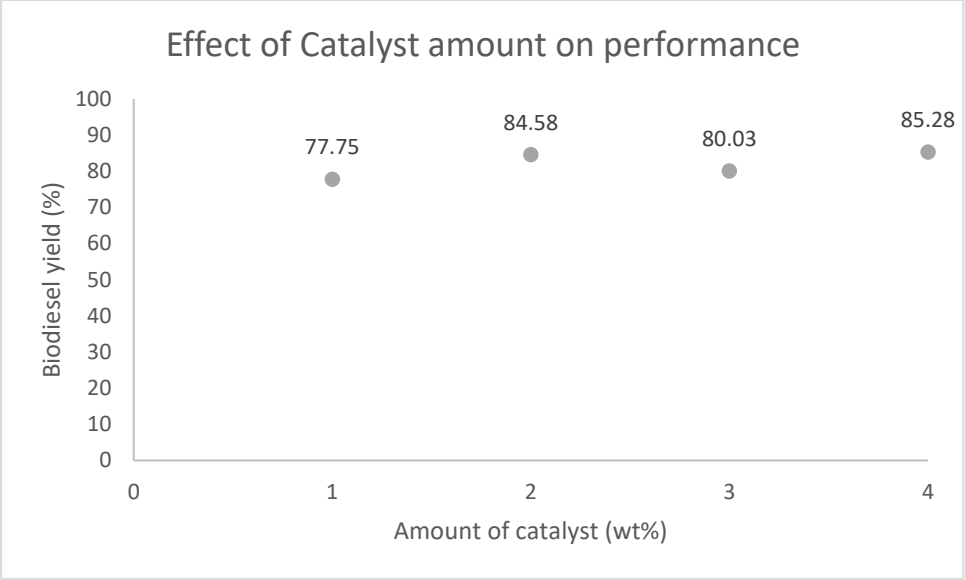

Figure 54: Effect of Catalyst amount on performance

Catalyst dosage (wt%)	Acid Value (mgKOH/g)
1	0.0656
2	0.0709
3	0.0667
4	0.1082

Table 18: Acid value of biodiesels obtained in using BPIn 2 and varying catalyst dosage

4.5.2 Effect of Ethanol to oil ratio on performance

Reactions in this comparison were carried out at 60℃ reaction temperature, 6-hour reaction time and 2wt% catalyst dosage while varying ethanol to oil ratio. According to literature (F. Ma & Hanna, 1999c) biodiesel yield increases with increasing ethanol to oil ratio. Significant difference in biodiesel yield was observed when the ethanol ratio was increased recording a 29% biodiesel yield at a 6:1 ethanol to oil ratio, 65.82% biodiesel yield at a 12:1 ethanol to oil ratio, an 84.58% biodiesel yield at a 15:1 ethanol to oil ratio and ultimately a 94.37% biodiesel yield at a 21:1 ethanol to oil ratio as shown in Figure 62. Table 19 shows the acid values of the biodiesels obtained.

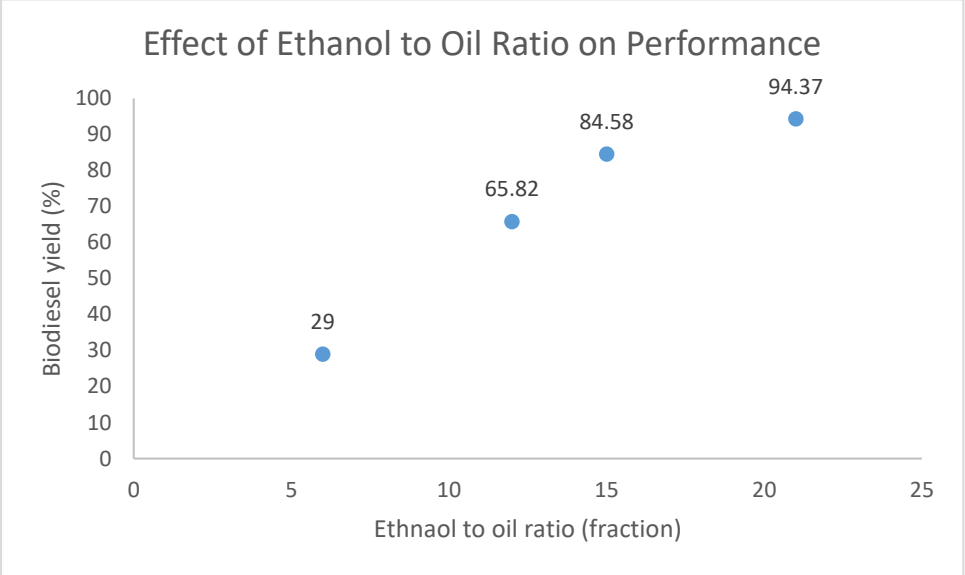

Figure 55: Effect of Ethanol to Oil Ratio on Performance

Ethanol: oil	Acid Value (mgKOH/g)
6:1	0.1111
12:1	0.0878
15:1	0.0709
21:1	0.0540

Table 19: Acid value of biodiesels obtained in using BPIn 2 and varying ethanol to oil ratio

4.5.3 Effect of reaction Time on performance

Reactions in this comparison were carried out at 60℃ reaction temperature, 2wt% catalyst dosage and a 21:1 ethanol to oil ratio while varying the reaction time for BPIn 2 catalyst. The effect of reaction time on biodiesel yield was checked for both BPIn 2 catalyst and BP900 catalysts. In Figure 63 it is observed that the biodiesel yield obtained in the use of BPIn 2 catalyst increases as the reaction time increases from an 82.2% biodiesel yield at half an hour to 94.05% after a six-hour reaction time. It is worth nothing that there was a significant increase in biodiesel yield between the 4-hour run (86.2%) and the 6-hour run (94.05%). Table 20 shows the acid values of the biodiesels obtained.

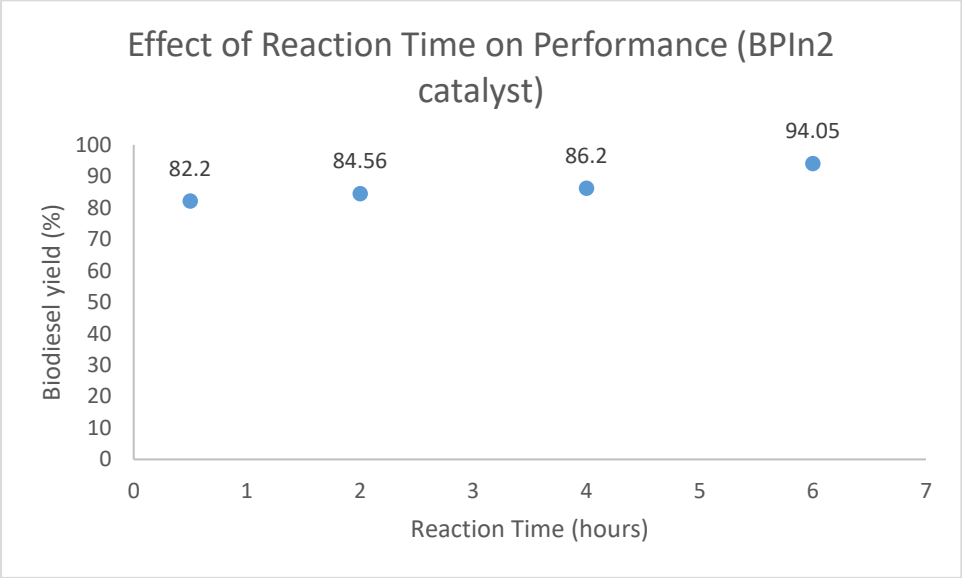

Figure 56: Effect of Reaction Time on Performance (BPIn2 catalyst)

Reaction time (hours)	Acid Value (mgKOH/g)
0.5	0.1665
1	0.0992
4	0.0612
6	0.0552

Table 20: Acid value of biodiesels obtained in using BPIn 2 and varying reaction time

For BP900 the same reaction conditions were used except for the ethanol to oil ratio which was 15:1. In the use of BP900 catalyst, the biodiesel yield was also observed to

increase with increasing reaction time as shown in Figure 64. However, the highest increase in yield was from the second hour (81.09%) to the fourth hour (91.05%) unlike in BPIn 2 where the most significant increment was between the fourth and sixth hour. The highest biodiesel yield for BP900 was recorded to be 96.16% after a six-hour reaction time. Table 21 shows the acid values of the biodiesels obtained.

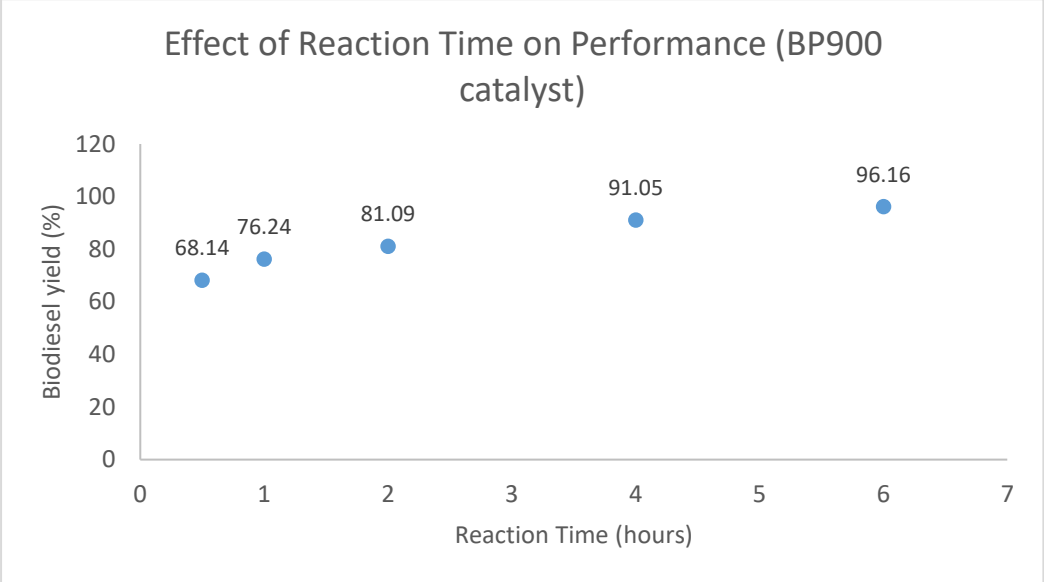

Figure 57: Effect of Reaction Time on Performance (BP900 catalyst)

Rection time (hours)	Acid Value (mgKOH/g)
0.5	0.0882
1	0.0655
2	0.0445
4	0.0496
6	0.0492

Table 21: Acid value of biodiesels obtained in using BP900 and varying reaction time

4.5.4 Effect of reaction Temperature on performance

Reactions in this comparison were carried out at 4-hour reaction time, 2wt% catalyst dosage and a 21:1 ethanol to oil ratio while varying the reaction temperature. It was observed in Figure 65 that the biodiesel yield increased significantly with increasing temperature from 40°C to 70°C with 80.58% and 94.11% respectively. (Buasri et al., 2013) reported an increase in biodiesel yield with increasing reaction temperature.

Because transesterification reaction is endothermic and is facilitated by high reaction temperatures, this observation is in line with literature reported trends. Table 22 shows the acid values of the biodiesels obtained.

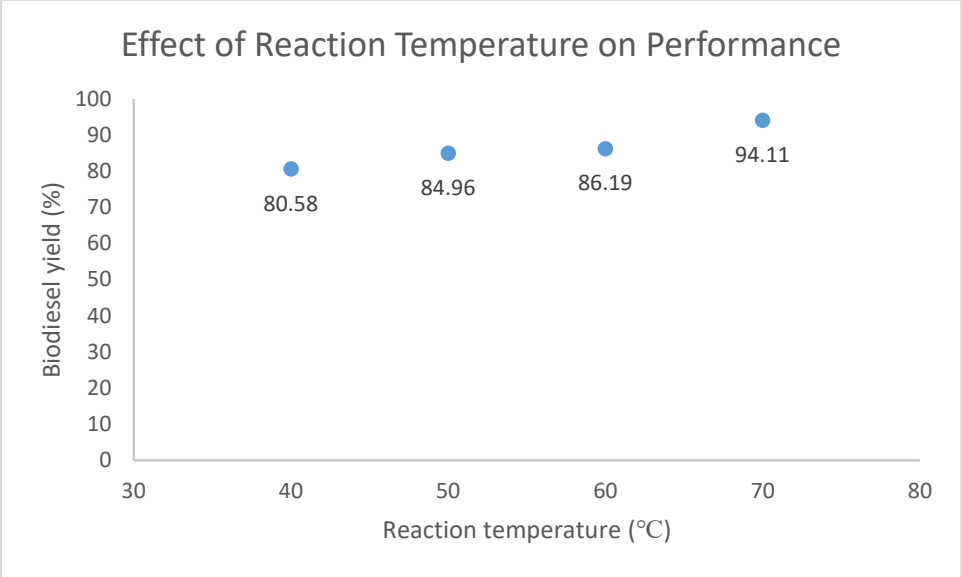

Figure 58: Effect of Reaction Temperature on Performance

Reaction temperature (℃)	Acid Value (mgKOH/g)
40	0.0983
50	0.0713
60	0.0612
70	0.0554

Table 22: Acid value of biodiesels obtained in using BPIn 2 and varying reaction temperature

4.6 BPIn2 catalyst reaction kinetics

The kinetic model in the use of BPIn 2 was developed for easy determination of required reactor volume for upscale production. There is need to ensure the kinetic rates obtained are solely due to chemical reaction and hence eliminate mass transfer-controlled reaction. Kinetic studies conducted by (Bambase et al., 2007; Kumar et al., 2010; Okullo et al, 2015; Noureddini, 1997) concluded that during transesterification, at stirring rates from 400rpm to 600rpm and above, the mass transfer-controlled reaction is eliminated, and only chemical reaction controls the reaction kinetics.

Hence, since a 600rpm stirring rate was used in this work, the reaction kinetics is said to be solely dependent on the rate of chemical reaction.

Three power law models are developed for prediction of reaction rate for a given the reaction conditions. The overall transesterification reaction equation is given in Equation 4 where three moles of ethanol are required for each mole of oil which is used synonymously as triglyceride.

$$\boldsymbol{Oil + 3Ethanol \rightarrow 3Biodiesel + Glycerol} \qquad \textit{Equation 4}$$

This implies that the rate of consumption of products and generation of products in an uncatalyzed rection is given in Equation 5

$$\frac{-dN_O}{dt} = \left(\frac{1}{3}\right)\frac{dN_B}{dt} = \left(-\frac{1}{3}\right)\frac{dN_E}{dt} = \frac{dN_G}{dt} \qquad \textit{Equation 5}$$

Table 23 shows the experimental data obtained for the kinetic studies of BPIn 2 catalyst transesterification. Various biodiesel yields were obtained in varying reaction temperature, reaction time and the ethanol to oil ratios.

Table 23: Experimental data obtained for the kinetic studies of BPIn 2 catalyst

No	Reaction Temperature (K)	Catalyst mass (g)	Reaction Time (hr)	Ethanol: oil ratio	Biodiesel yield (%)
1	343	4	0.5	21;1	83.73
2	343	4	1	21;1	90.70
3	343	4	4	21;1	94.11
4	333	4	0.5	21;1	82.20
5	333	4	1	21;1	84.56
6	333	4	4	21;1	86.20

7	323	4	1	21;1	80.20
8	323	4	4	21;1	85.66
9	313	4	1	21;1	75.82
10	313	4	4	21;1	80.58
11	333	4	1	15;1	78.92
12	333	4	2	15;1	79.65
13	333	4	4	15;1	84.58
14	313	4	1	15;1	73.37
15	313	4	2	15;1	78.56
16	313	4	4	15;1	80.13
17	333	4	1	6;1	23.93
18	333	4	2	6;1	27.84
19	333	4	4	6;1	29.00
20	313	4	1	6;1	20.38
21	313	4	2	6;1	25.26
22	313	4	4	6;1	26.76

The following steps were taken to obtain the parameters required to calculate the rate of reaction.

1. The mass of biodiesel at time t ($\boldsymbol{m_{Biodiesel,t}}$), in the reaction was calculated using Equation 6

$$\boldsymbol{m_{Biodiesel,t}} = \frac{\boldsymbol{Biodiesel\ yield} * \boldsymbol{m_{oil,0}}}{\boldsymbol{100}} \qquad \textit{Equation 6}$$

2. The moles of biodiesel at any time t ($\boldsymbol{N_{Biodiesel,t}}$), was calculated using Equation 7

$$\boldsymbol{N_{Biodiesel,t}} = \frac{\boldsymbol{m_{Biodiesel,t}}}{\boldsymbol{M_{Biodiesel}}} \qquad \textit{Equation 7}$$

3. The moles of ethanol reacted at any point in the reaction ($\boldsymbol{N_{Ethanol,reacted}}$ is equal to the moles of biodiesel produced ($\boldsymbol{N_{Biodiesel,t}}$) since they have the same stoichiometric coefficients in the reaction Equation 8

$$\boldsymbol{N_{Ethanol,reacted} = N_{Biodiesel,t}} \qquad \textit{Equation 8}$$

4. The initial moles of oil, $\boldsymbol{N_{oil,0}}$ (at time = 0) was calculated by dividing the mass of oil used by the molar mass of the waste cooking oil as shown in Equation 9

$$\boldsymbol{N_{oil,0} = \frac{m_{oil,0}}{M_{Oil}}} \qquad \textit{Equation 9}$$

5. The initial moles of ethanol, $\boldsymbol{N_{Ethanol,0}}$ (at time = 0) was calculated by dividing the mass of ethanol used by the molar mass of the ethanol as shown in Equation 10

$$\boldsymbol{N_{Ethanol,0} = \frac{m_{Ethanol,0}}{M_{Ethanol}}} \qquad \textit{Equation 10}$$

6. The moles of oil reacted ($\boldsymbol{N_{Oil,reacted}}$) is given by Equation 11 and is based on the reaction stoichiometry with respect to biodiesel

$$\boldsymbol{N_{Oil,reacted} = \frac{N_{Biodiesel,t}}{3}} \qquad \textit{Equation 11}$$

7. The moles of ethanol remaining unreacted at any time t ($\boldsymbol{N_{Ethanol,t}}$), is calculated using Equation 12

$$\boldsymbol{N_{Ethanol,t} = N_{Ethanol,0} - N_{Ethanol,reacted}} \qquad \textit{Equation 12}$$

8. Finally, the rate of reaction with respect to biodiesel production ($\boldsymbol{r_{Biodiesel}}$) which is the same as that with respect to ethanol consumed ($\boldsymbol{-r_{Ethanol}}$) due to the reaction stoichiometry is calculated using Equation 13. *W* represents the catalyst amount in grams and *t* is the reaction time in hours.

$$r_{Biodiesel} = -r_{Ethanol} = \frac{\Delta N_{Biodiesel}}{W * \Delta t} \qquad \textit{Equation 13}$$

Table 24: Moles and mass of the reactants before and after transesterification.

Ethanol				oil			
moles reacted (mol)	Initial Mass (g)	Initial moles (mol)	Final moles (mol)	Initial mass (mol)	Initial moles (mol)	moles reacted (mol)	moles unreacted (mol)
0.541076215	240	5.20969	4.668614	200	0.23568	0.180358738	0.05531773
0.586076367	240	5.20969	4.623614	200	0.23568	0.195358789	0.040317679
0.608124938	240	5.20969	4.601565	200	0.23568	0.202708313	0.032968155
0.53113579	240	5.20969	4.678554	200	0.23568	0.177045263	0.058631205
0.546393337	240	5.20969	4.663297	200	0.23568	0.182131112	0.053545356
0.55696481	240	5.20969	4.652725	200	0.23568	0.185654937	0.050021531
0.518198701	240	5.20969	4.691491	200	0.23568	0.1727329	0.062943568
0.553548131	240	5.20969	4.656142	200	0.23568	0.184516044	0.051160424
0.48993816	240	5.20969	4.719752	200	0.23568	0.16331272	0.072363748
0.520701306	240	5.20969	4.688989	200	0.23568	0.173567102	0.062109366
0.509992181	172	3.733611	3.223619	200	0.23568	0.169997394	0.065679074
0.514688981	172	3.733611	3.218922	200	0.23568	0.171562994	0.064113474
0.546568171	172	3.733611	3.187043	200	0.23568	0.18218939	0.053487078
0.474136021	172	3.733611	3.259475	200	0.23568	0.15804534	0.077631128
0.507609612	172	3.733611	3.226002	200	0.23568	0.169203204	0.066473264
0.517798872	172	3.733611	3.215812	200	0.23568	0.172599624	0.063076844
0.154641458	68.57	1.488452	1.33381	200	0.23568	0.051547153	0.184129315
0.179908356	68.57	1.488452	1.308543	200	0.23568	0.059969452	0.175707016

0.187404181	68.57	1.488452	1.301048	200	0.23568	0.06246806	0.173208408
0.131723822	68.57	1.488452	1.356728	200	0.23568	0.043907941	0.191768528
0.163257997	68.57	1.488452	1.325194	200	0.23568	0.054419332	0.181257136
0.17290966	68.57	1.488452	1.315542	200	0.23568	0.057636553	0.178039915

The kinetic equation is given by.

$$r_{biodiesel} = \frac{\Delta N_{biodiesel}}{W * \Delta t} = k_0 e^{-E_a/RT}.\ N_{oil,t}{}^{o}.N_{ethanol,\ t}{}^{e}$$

Where.

- $r_{biodiesel}$ is the rate of reaction in terms of biodiesel production
- $N_{biodiesel}$ are the moles of biodiesel
- W is the weight of catalyst in grams
- t is the reaction time in hours
- k_0 is the pre-exponential factor
- E_a is the activation energy in J/mol
- T is the reaction temperature in K
- o is the order of reaction with respect to WCO
- e is the order of reaction with respect to ethanol

NLReg software was used to regress the kinetic data in Table 24 to obtain the activation energy and order of reaction with respect to ethanol and oil reactants (Model 1).

Table 25: Data for NLReg regression as well as the predicted rates and absolute deviations

No	Experimental rate	Reaction Temperature (K)	Moles of ethanol (mol)	Moles of oil (mol)	Predicted rate	Absolute deviation

1	0.270538108	343	4.668613808	0.05531773	0.283602083	0.048288856
2	0.146519092	343	4.623613656	0.040317679	0.104821494	0.28458815
3	0.038007809	343	4.601565085	0.032968155	0.055939872	0.471799465
4	0.265567895	333	4.678554233	0.058631205	0.198613846	0.252116505
5	0.136598334	333	4.663296687	0.053545356	0.149003642	0.090815953
6	0.034810301	333	4.652725214	0.050021531	0.120187122	2.452630985
7	0.129549675	323	4.691491322	0.062943568	0.140173191	0.082003418
8	0.034596758	323	4.656141893	0.051160424	0.072675371	1.100641075
9	0.12248454	313	4.719751863	0.072363748	0.118822946	0.029894339
10	0.032543832	313	4.688988718	0.062109366	0.072942956	1.241375779
11	0.127498045	333	3.223619002	0.065679074	0.067413552	0.471258155
12	0.064336123	333	3.218922202	0.064113474	0.06231353	0.0314379
13	0.034160511	333	3.187043012	0.053487078	0.034643455	0.0141375
14	0.118534005	313	3.259475162	0.077631128	0.035689661	0.698907829
15	0.063451202	313	3.226001571	0.066473264	0.021440596	0.66209314
16	0.03236243	313	3.215812311	0.063076844	0.018070806	0.441611562
17	0.038660365	333	1.333810395	0.184129315	0.052421012	0.355936812
18	0.022488545	333	1.308543498	0.175707016	0.042280411	0.880086589
19	0.011712761	333	1.301047673	0.173208408	0.039605336	2.381383368
20	0.032930955	313	1.356728032	0.191768528	0.019352307	0.412336919
21	0.02040725	313	1.325193857	0.181257136	0.014910915	0.269332454
22	0.010806854	313	1.315542194	0.178039915	0.013734116	0.270870938

The NLReg results are displayed in Figure 66

Parameter	Initial guess	Final estimate	Standard error	t	Prob(t)
	---- Calculated Parameter Values ----				
k0	1	331327570	0	1.0E+030	0.00001
Ea	1	51334.9848	0	1.0E+030	0.00001
e	1	3.8240973	0	1.0E+030	0.00001
o	1	3.02960545	0	1.0E+030	0.00001

Figure 59: Results from NLReg software regression.

The absolute standard deviation obtained was 0.2869 with an R square of 69.37%

The overall kinetic equation obtained is Equation 14.

$$r_{biodiesel} = \frac{\Delta N_{biodiesel}}{W * \Delta t} = 3.3 * 10^8 \, e^{-51.33kJ/mol/RT} . \; N_{oil,t}{}^{3.03} . N_{ethanol,\,t}{}^{3.82}$$

Equation 14

The parity plot was drawn to check the correlation between experimentally determined rates and the rates predicted by the obtained kinetic equation as shown in Figure 67. The R square obtained was 0.7398. The reduction in predictability accuracy could be because of fixing the drying time for excess ethanol removal from biodiesel prior to weighing.

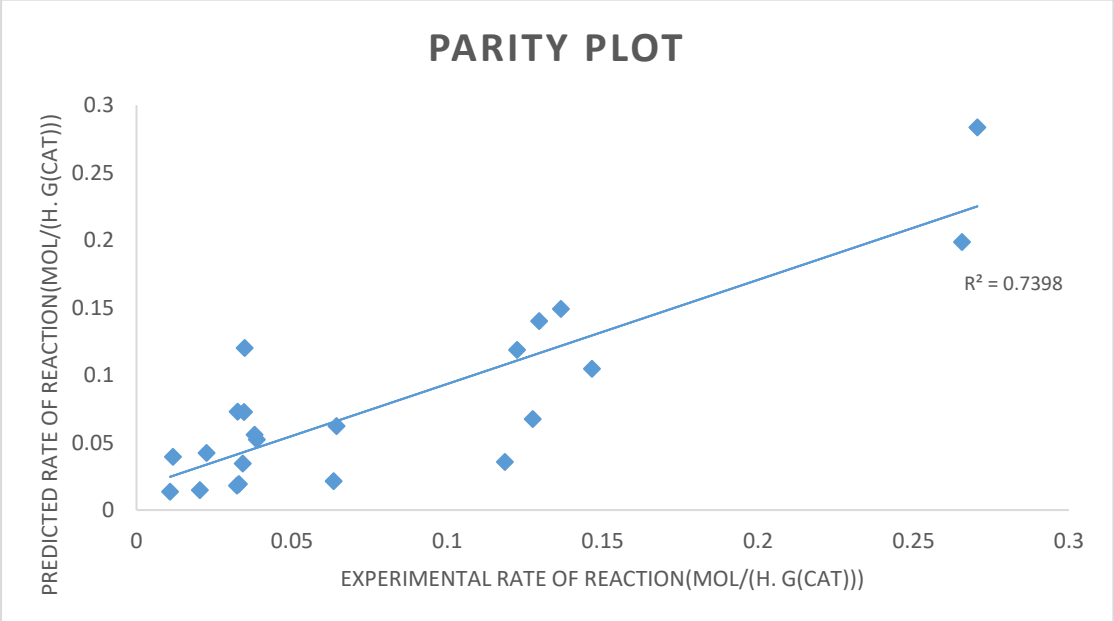

Figure 60: Parity plot of predicted and experimentally acquired rate of reaction

In a second analysis (Model 2), data points with absolute deviations greater than 10% in the previous analysis were discarded prior to this nonlinear regression.

The obtained NLReg result is displayed in Figure 68

	---- Calculated Parameter Values ----				
Parameter	Initial guess	Final estimate	Standard error	t	Prob(t)
k0	1	1476953.11	0	1.0E+030	0.00001
Ea	1	39071.1935	0	1.0E+030	0.00001
e	1	3.2124057	0	1.0E+030	0.00001
o	1	2.32917143	0	1.0E+030	0.00001

Figure 61: NLReg results in using Model 2 data

The absolute standard deviation obtained was 0.2243 with an R square of 84.65%

The overall kinetic equation obtained is Equation 15.

$$r_{biodiesel} = \frac{\Delta N_{biodiesel}}{W * \Delta t} = 1.5 * 10^6 \, e^{-39.071 kJ/mol / RT} . \; {N_{oil,t}}^{2.33} . {N_{ethanol,\, t}}^{3.21}$$

Equation 15

Parity plot was drawn to check the correlation between experimentally determined rates and the rates predicted by the obtained kinetic equation as shown in Figure 69. the R square obtained was 0.8468.

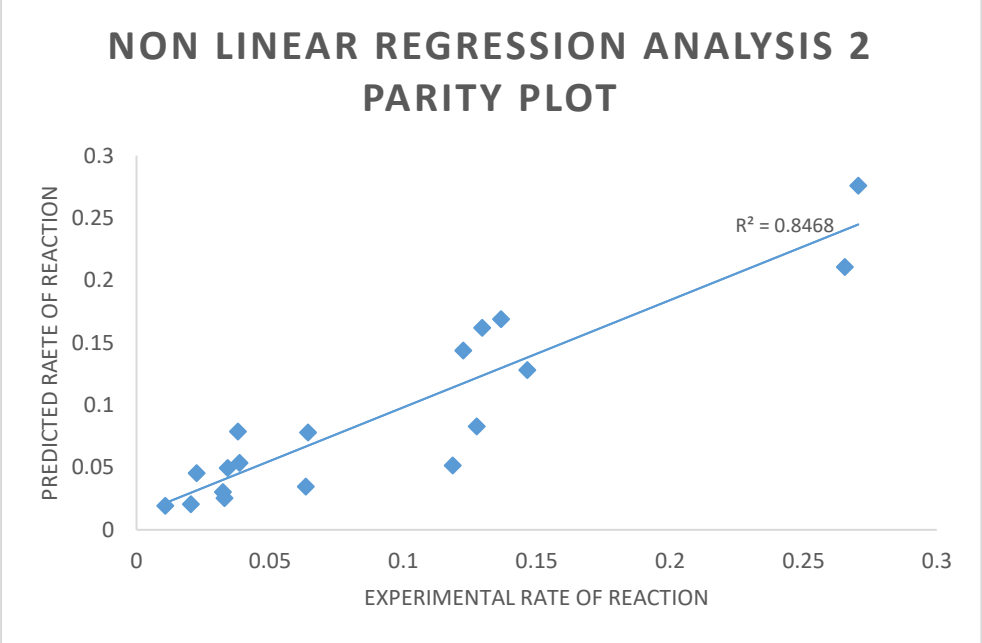

Figure 62: NLReg Model 2 Parity plot of predicted and experimentally acquired rate of reaction

In a third kinetic analysis (Model 3), the rate equation was linearized as shown in Equation 16 and MS excel was used to regress the data to obtain the kinetic parameters.

$$ln\, r_{biodiesel} = \frac{\Delta N_{biodiesel}}{W*\Delta t} = lnk_0 - \frac{E_a}{RT} + o\ ln\, N_{oil,t} + e\ ln\, N_{ethanol,\ t} \quad \textit{Equation 156}$$

Table 27 shows the data used in this regression analysis and Table 28 shows the absolute deviation of the predicted reaction rate from the experimentally determined rate.

Table 26: Regression data used in linear regression

ln r	1/RT	ln $N_{ethanol,\ t}$	ln $N_{oil,t}$
-1.30734	0.000351	1.540862	-2.89466
-1.9206	0.000351	1.531177	-3.21097
-3.26996	0.000351	1.526396	-3.41221
-1.32588	0.000361	1.542989	-2.83649
-1.99071	0.000361	1.539723	-2.92723
-3.35784	0.000361	1.537453	-2.9953
-2.04369	0.000372	1.545751	-2.76552
-3.364	0.000372	1.538187	-2.97279
-2.09977	0.000384	1.551756	-2.62605
-3.42517	0.000384	1.545217	-2.77886
-2.05965	0.000361	1.170505	-2.72297
-2.74363	0.000361	1.169047	-2.7471
-3.37668	0.000361	1.159094	-2.92832
-2.13256	0.000384	1.181566	-2.55579
-2.75748	0.000384	1.171243	-2.71096
-3.43076	0.000384	1.16808	-2.7634
-3.25294	0.000361	0.28804	-1.69212
-3.79475	0.000361	0.268915	-1.73894
-4.44708	0.000361	0.26317	-1.75326
-3.41334	0.000384	0.305076	-1.65147
-3.89187	0.000384	0.281559	-1.70784
-4.52757	0.000384	0.274249	-1.72575

The obtained kinetic parameters using Ms. Excel regression analysis is as follows:

$$r_{biodiesel} = \frac{\Delta N_{biodiesel}}{W*\Delta t} = 3.25^3\ e^{-24.93kJ/mol/RT}.\ \ N_{oil,t}{}^{2.00}.N_{ethanol,\ t}{}^{3.02} \quad \textit{Equation 17}$$

Table 27: Absolute deviation of predicted reaction rate from experimental rates

Predicted rate	Experimental rate	Absolute deviation
0.167317	0.270538	0.381541
0.086395	0.146519	0.410352
0.056972	0.038008	0.498953
0.145469	0.265568	0.452234
0.120167	0.136598	0.12029
0.104175	0.03481	1.99264
0.127901	0.12955	0.012725
0.082637	0.034597	1.388589
0.12791	0.122485	0.044298
0.092425	0.032544	1.84003
0.059324	0.127498	0.534704
0.056285	0.064336	0.125136
0.038034	0.034161	0.113385
0.048179	0.118534	0.593542
0.034256	0.063451	0.460116
0.030557	0.032362	0.055803
0.032454	0.03866	0.160537
0.0279	0.022489	0.240617
0.026647	0.011713	1.275046
0.020843	0.032931	0.367068
0.017348	0.020407	0.149902
0.016374	0.010807	0.515106

The obtained absolute average deviation was 29.37% comparable to that obtained in using non-linear regression analysis. Figure 70 shows a parity plot between the predicted rate and the experimental rate, and the R square obtained was 0.6357.

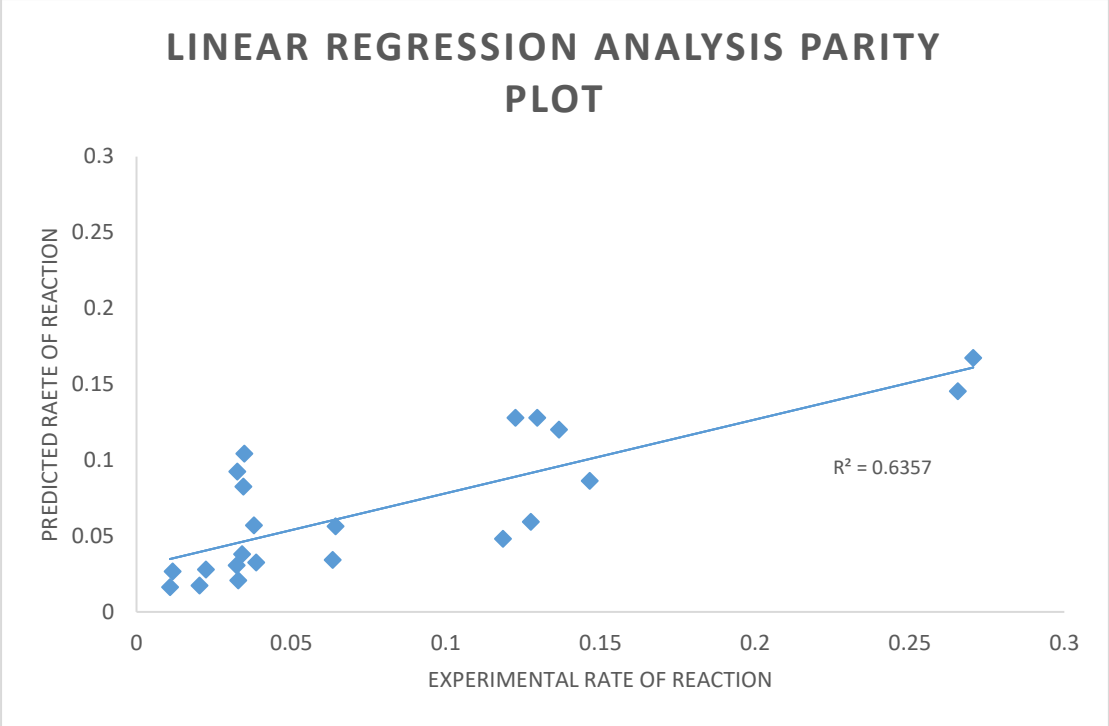

Figure 63: Linear regression results parity plot of predicted and experimentally acquired rate of reaction

On comparing the three kinetic models obtained, model two and model three showed similarity in the values of the orders of reaction and activation energy. Since the R square of Model 2 is high (0.8468) with a lower AAD (22.42%), It is the concluded model for the use of BPIn 2 catalyst. A low activation energy is desired so that the energy barrier to be overcome by reactants to form products is less leading to the ease of product formation. From literature a low 27.24kJ/mol activation energy was obtained (Mercy Nisha Pauline et al., 2021) in the use of waste cooking oil, methanol and sodium hydroxide catalyst which is comparable to the 39.07kJ/mol obtained in this work with the use of WCO, ethanol, and a heterogeneous base catalyst. Xiao Yang et al, 2010 recorded a 111.6kJ/mol transesterification activation energy in the use of a heterogeneous base catalyst. This indicates that the catalyst developed in this work falls within the low activation energy spectrum implying a low energy intensive process.

CHAPTER 5: CONCLUSION AND RECOMMENDATION

5.1 Conclusions

The production of biodiesel using waste cooking oil and ethanol as feedstock via transesterification reaction was optimized by using heterogeneous catalysts to obtain high biodiesel yield.

Initially, calcined eggshell(ES), fish scale (FS) and cow bone (CB) catalysts were used in biodiesel production and the obtained yields were low recording 64.42%, 68.44% and 68.15% respectively. Mixing the individual catalysts in a1:1:1 mix ratio via physical mixing and hot water mixing significantly increased the biodiesel yield to 70.79% and 71.04% respectively. On varying the ES:FS:CB mix ratio, the mix ratios with low amount of eggshell reflecting high fish scale and cow bone ratios had better biodiesel yields though the percentage increase was not significantly higher than the 1:1:1phy catalyst (approximately 3% increment). Impregnating 1wt% potassium as a promoter had the best biodiesel yield of relative to impregnating 5wt% and 10wt%. however, the 10wt% impregnated catalyst yielded a low acid value biodiesel which is desirable. On impregnating 10wt% potassium on the best performing tri-blend catalyst, 75.34% biodiesel yield was achieved.

Unsatisfied with the biodiesel yields obtained in the use of the tri-bled catalysts, banana peel which is potassium rich was explored and optimized in terms of calcination temperature. It was observed that on increasing the calcination temperature from 600℃ through 800℃ to 900℃ sintering occurred and the carbon content reduced which was evident in the color change from brown through grey to turquoise. However, this led to the production of BP900 which yielded the highest biodiesel yield of 96.16% because the carbon content reduced and potassium content

increased, leading to high selectivity for the biodiesel. Also, strength of the basic sites decreased as the calcination temperature increased causing ease in product desorption and hence good catalyst performance under reaction conditions of 60℃ reaction temperature, 6 hour reaction time and 15:1 ethanol to oil ratio and 2wt% catalyst dosage (same as conditions were used with the other bio-based catalysts) making it the best performing bio-based catalyst. Potassium chloride was the active sites found on BP800 and BP900 catalysts which had the highest performances. BP600 however had a low biodiesel performance, and its active site was made of potassium bicarbonate (presence of carbon).

Due to the low calcination yield of BP900 (10%), and low availability to feed a large-scale production plant, inorganic precursors were used to synthesize three replicas using co-precipitation and co-impregnation methods based on a literature reported composition of banana peel calcined at 700℃. All three replicas produced comparable biodiesel yields under the same conditions as used in BP900 transesterification and the highest obtained biodiesel yield was 84.58%.

The effect of reaction conditions on the biodiesel yield was checked in the use of BPIn 2 catalyst and the performance increased with increasing reaction temperature, time, ethanol to oil ratio and catalyst dosage. The optimum condition was 70℃ reaction temperature, 6hour reaction time and 21:1 ethanol to oil ratio and 2wt% catalyst dosage.

On performing kinetic analysis in the use of BPIn 2 catalyst for transesterification of waste cooking oil and ethanol, three kinetic models were developed out of which the one with the highest R square was selected the obtained activation energy is $39.07kJ/mol$, a collision factor of $1.5 * 10^6 /[g(cat).h.mol^{5.6}]$ an order of reaction

with respect to oil of 2 and an order of reaction with respect to ethanol of 3 with an AAD of 22%.

5.1 Recommendations

Although much research has been done with regards to optimizing waste sourced biobased catalysts and synthesizing and in organic replica of the best performing biobased catalyst for high yield biodiesel production using waste cooking oil and ethanol as feedstock. Future research can improve this work with the following recommendations.

1. Pelletizing catalysts with the use of appropriate binder to ensure easy separation of catalyst and product mixture.
2. Explore alternative thermal degradation methods (such as pyrolysis) aside calcination which have the potential of increasing BP900's catalyst yield.
3. Use a more analytical approach to determine the biodiesel yield by performing GC MS analysis on product samples to ascertain fatty acid ethyl ester (FAEE) composition of the produced biodiesel samples for a more accurate kinetic model.
4. Drying biodiesel fractions of products to get rid of excess ethanol should be carried out till the mass of biodiesel remains constant on further drying and not on an overnight limited time basis.
5. Optimize the production of the inorganic equivalent of banana peel catalyst by including a chloride (Cl) precursor and basing composition on BP900 EDS results.

6. Carry out qualitative tests to determine the cloud point, calorific value, pour point and flash point of the biodiesel samples to determine their impact on diesel engine performance.
7. Perform a detailed cost benefit analysis on the economic feasibility of a large-scale biodiesel production plant in the use of BP900 catalyst.

REFERENCES

Abbaszaadeh, A., Ghobadian, B., Omidkhah, M. R., & Najafi, G. (2012). Current biodiesel production technologies: A comparative review. *Energy Conversion and Management*, *63*, 138–148. https://doi.org/10.1016/j.enconman.2012.02.027

Abdullah, S. H. Y. S., Hanapi, N. H. M., Azid, A., Umar, R., Juahir, H., Khatoon, H., & Endut, A. (2017). A review of biomass-derived heterogeneous catalyst for a sustainable biodiesel production. *Renewable and Sustainable Energy Reviews*, *70*, 1040–1051. https://doi.org/10.1016/J.RSER.2016.12.008

Adewale, P., Dumont, M. J., & Ngadi, M. (2015). Recent trends of biodiesel production from animal fat wastes and associated production techniques. *Renewable and Sustainable Energy Reviews*, *45*, 574–588. https://doi.org/10.1016/J.RSER.2015.02.039

Agarwal, A. K., Bijwe, J., & Das, L. M. (2003). Effect of biodiesel utilization of wear of vital parts in compression ignition engine. *Journal of Engineering for Gas Turbines and Power*, *125*(2), 604–611. https://doi.org/10.1115/1.1454114

Alias, N. I., A/L JayaKumar, J. K., & Md Zain, S. (2018). Characterization of Waste Cooking Oil for Biodiesel Production. *Jurnal Kejuruteraan*, *si1*(2), 79–83. https://doi.org/10.17576/jkukm-2018-si1(2)-10

Anisah, P. M., Suwandi, & Agustian, E. (2019). Effect of transesterification on the result of waste cooking oil conversion to biodiesel. *Journal of Physics: Conference Series*, *1170*(1). https://doi.org/10.1088/1742-6596/1170/1/012067

Arumugam, A., & Sankaranarayanan, P. (2020). Biodiesel production and parameter optimization: An approach to utilize residual ash from sugarcane leaf, a novel heterogeneous catalyst, from Calophyllum inophyllum oil. *Renewable Energy*, *153*, 1272–1282. https://doi.org/10.1016/J.RENENE.2020.02.101

Arun, S. B., Suresh, R., Yatish, K. V., Omkaresh, B. R., & Channa Keshava Naik, N. (2017). Use of CaO and Na3PO4 Catalysts in the Synthesis of Biodiesel and Investigation of Fuel Properties. *Materials Today: Proceedings*, *4*(10), 11111–11117. https://doi.org/10.1016/J.MATPR.2017.08.074

Arzamendi, G., Campo, I., Arguiñarena, E., Sánchez, M., Montes, M., & Gandía, L. M. (2007). Synthesis of biodiesel with heterogeneous NaOH/alumina catalysts: Comparison with homogeneous NaOH. *Chemical Engineering Journal*, *134*(1–3), 123–130. https://doi.org/10.1016/J.CEJ.2007.03.049

Atadashi, I. M., Aroua, M. K., Abdul Aziz, A. R., & Sulaiman, N. M. N. (2013). The effects of catalysts in biodiesel production: A review. *Journal of Industrial and Engineering Chemistry*, *19*(1), 14–26. https://doi.org/10.1016/J.JIEC.2012.07.009

Avhad, M. R., & Marchetti, J. M. (2015). A review on recent advancement in catalytic materials for biodiesel production. *Renewable and Sustainable Energy Reviews*, *50*, 696–718. https://doi.org/10.1016/J.RSER.2015.05.038

Babatunde, E. O., Bamidele, S. H., Aderibigbe, F. A., Yusuff, A. S., Karmakar, B., Rokhum, S. L., & Halder, G. (2022). Valorization of restaurant waste oil and cow-bone doped siliceous termite hills towards biodiesel production: Kinetics and thermodynamics. *Sustainable Chemistry and Pharmacy*, *30*, 100895. https://doi.org/10.1016/J.SCP.2022.100895

Balajii, M., & Niju, S. (2020). Banana peduncle – A green and renewable heterogeneous base catalyst for biodiesel production from Ceiba pentandra oil. *Renewable Energy*, *146*, 2255–2269. https://doi.org/10.1016/J.RENENE.2019.08.062

Balat, M., & Balat, H. (2010). Progress in biodiesel processing. *Applied Energy*, *87*(6), 1815–1835. https://doi.org/10.1016/J.APENERGY.2010.01.012

Bambase, M. E., Nakamura, N., Tanaka, J., & Matsumura, M. (2007). Kinetics of hydroxide-catalyzed methanolysis of crude sunflower oil for the production of fuel-grade methyl esters. *Journal of Chemical Technology and Biotechnology*, *82*(3), 273–280. https://doi.org/10.1002/jctb.1666

Bardestani, R., Roy, C., & Kaliaguine, S. (2019). The effect of biochar mild air oxidation on the optimization of lead(II) adsorption from wastewater. *Journal of Environmental Management*, *240*, 404–420. https://doi.org/10.1016/J.JENVMAN.2019.03.110

Barnwal, B. K., & Sharma, M. P. (2005). Prospects of biodiesel production from vegetable oils in India. *Renewable and Sustainable Energy Reviews*, *9*(4), 363–378. https://doi.org/10.1016/J.RSER.2004.05.007

Basu, P., Rao, S., & Dhungana, A. (2012a). *An Investigation into the Effect of Biomass Particle Size on its Torrefaction*. https://doi.org/10.1002/cjce.21710

Basu, P., Rao, S., & Dhungana, A. (2012b). *An Investigation into the Effect of Biomass Particle Size on its Torrefaction*. https://doi.org/10.1002/cjce.21710

Basumatary, B., Basumatary, S., Das, B., Nath, B., & Kalita, P. (2021). Waste Musa paradisiaca plant: An efficient heterogeneous base catalyst for fast production of biodiesel. *Journal of Cleaner Production*, *305*, 127089. https://doi.org/10.1016/J.JCLEPRO.2021.127089

Benjapornkulaphong, S., Ngamcharussrivichai, C., & Bunyakiat, K. (2009). Al2O3-supported alkali and alkali earth metal oxides for transesterification of palm kernel oil and coconut oil. *Chemical Engineering Journal*, *145*(3), 468–474. https://doi.org/10.1016/J.CEJ.2008.04.036

Berglund, M., & Börjesson, P. (2006). Assessment of energy performance in the life-cycle of biogas production. *Biomass and Bioenergy*, *30*(3), 254–266. https://doi.org/10.1016/J.BIOMBIOE.2005.11.011

Bertarione, S., Scarano, D., Zecchina, A., Johánek, V., Hoffmann, J., Schauermann, S., Frank, M. M., Libuda, J., Rupprechter, G., & Freund, H. J. (2004). Surface reactivity of Pd nanoparticles supported on polycrystalline substrates as compared to thin film model catalysts: Infrared study of CO adsorption. *Journal of Physical Chemistry B*, *108*(11), 3603–3613. https://doi.org/10.1021/jp036718t

Bertassoli, D. J., Sawakuchi, H. O., De Araújo, K. R., De Camargo, M. G. P., Alem, V. A. T., Pereira, T. S., Krusche, A. V, Bastviken, D., Richey, J. E., & Sawakuchi, A. O. (2021). How green can Amazon hydropower be? Net carbon emission from the largest hydropower plant in Amazonia. In *Sci. Adv* (Vol. 7). https://www.science.org

Bhatia, S. K., Jagtap, S. S., Bedekar, A. A., Bhatia, R. K., Rajendran, K., Pugazhendhi, A., Rao, C. V., Atabani, A. E., Kumar, G., & Yang, Y. H. (2021). Renewable biohydrogen production from lignocellulosic biomass using fermentation and integration of systems with other energy generation technologies. *Science of The Total Environment*, *765*, 144429. https://doi.org/10.1016/J.SCITOTENV.2020.144429

Bohlouli, A., & Mahdavian, L. (2021). Catalysts used in biodiesel production: a review. *Biofuels*, *12*(8), 885–898. https://doi.org/10.1080/17597269.2018.1558836

Borges, M. E., & Díaz, L. (2012). Recent developments on heterogeneous catalysts for biodiesel production by oil esterification and transesterification reactions: A

review. In *Renewable and Sustainable Energy Reviews* (Vol. 16, Issue 5, pp. 2839–2849). https://doi.org/10.1016/j.rser.2012.01.071

Braga, E. D. A. S., Malveira, J. D. Q., Milhome, M. A. L., De Aquino, M. D., & Nascimento, R. F. D. (2015). Characterization of the fatty acids present in wastewaters from production of biodiesel tilapia. *Journal of Chemistry*, *2015*. https://doi.org/10.1155/2015/265160

Brask, J., Damstrup, M. L., Nielsen, P. M., Holm, H. C., Maes, J., & De Greyt, W. (2011). Combining enzymatic esterification with conventional alkaline transesterification in an integrated biodiesel process. *Applied Biochemistry and Biotechnology*, *163*(7), 918–927. https://doi.org/10.1007/s12010-010-9095-9

Brennan, L., & Owende, P. (2010). Biofuels from microalgae—A review of technologies for production, processing, and extractions of biofuels and co-products. *Renewable and Sustainable Energy Reviews*, *14*(2), 557–577. https://doi.org/10.1016/J.RSER.2009.10.009

Brethauer, S., & Studer, M. H. (2015). Biochemical conversion processes of lignocellulosic biomass to fuels and chemicals - A review. *Chimia*, *69*(10), 572–581. https://doi.org/10.2533/chimia.2015.572

Buasri, A., Chaiyut, N., Loryuenyong, V., Rodklum, C., Chaikwan, T., Kumphan, N., Jadee, K., Klinklom, P., & WittayaWittayarounayut. (2012). Transesterification of waste frying oil for synthesizing biodiesel by KOH supported on coconut shell activated carbon in packed bed reactor. *ScienceAsia*, *38*(3), 283–288. https://doi.org/10.2306/scienceasia1513-1874.2012.38.283

Buasri, A., Chaiyut, N., Loryuenyong, V., Wongweang, C., & Khamsrisuk, S. (2013). *Application of Eggshell Wastes as a Heterogeneous Catalyst for Biodiesel Production*. *1*(2), 7–13. https://doi.org/10.12691/rse-1-2-1

Busca, G., Paula, A., Dias, S., Pedra, I., Salvador, É., Rijo, B., Francisco, M., Pereira, C., Serralha, F., & Nogueira, I. (2024). *Biodiesel Production over Banana Peel Biochar as a Sustainable Catalyst*. https://doi.org/10.3390/catal14040266

Büyükoğlu, M., Tuba, ·, Doğan, H., Orhan Arpa, ·, Nadaroğlu, H., İlhan, ·, & Öner, V. (123 C.E.). Experimental investigation of engine performance and emissions, and characterization, of waste transformer oils and diesel blends with biodiesel produced from olive oil wastes in a CI engine. *Journal of Thermal Analysis and Calorimetry*, *149*, 5381–5398. https://doi.org/10.1007/s10973-024-13207-3

Calero, J., Luna, D., Sancho, E. D., Luna, C., Bautista, F. M., Romero, A. A., Posadillo, A., & Verdugo, C. (2014). Development of a new biodiesel that integrates glycerol, by using CaO as heterogeneous catalyst, in the partial methanolysis of sunflower oil. *Fuel*, *122*, 94–102. https://doi.org/10.1016/J.FUEL.2014.01.033

Canakci, M. , & V. G. J. (1999). Biodiesel production via acid catalysis. *Transactions of the ASAE*, *42*(5), 1203–1210.

Chakraborty, R., Bepari, S., & Banerjee, A. (2011a). Application of calcined waste fish (Labeo rohita) scale as low-cost heterogeneous catalyst for biodiesel synthesis. *Bioresource Technology*, *102*(3), 3610–3618. https://doi.org/10.1016/J.BIORTECH.2010.10.123

Chakraborty, R., Bepari, S., & Banerjee, A. (2011b). Application of calcined waste fish (Labeo rohita) scale as low-cost heterogeneous catalyst for biodiesel synthesis. *Bioresource Technology*, *102*(3), 3610–3618. https://doi.org/10.1016/J.BIORTECH.2010.10.123

Changmai, B., Sudarsanam, P., & Rokhum, S. L. (2020). Biodiesel production using a renewable mesoporous solid catalyst. *Industrial Crops and Products*, *145*, 111911. https://doi.org/10.1016/J.INDCROP.2019.111911

Chen, R., Qin, Z., Han, J., Wang, M., Taheripour, F., Tyner, W., O'Connor, D., & Duffield, J. (2018). Life cycle energy and greenhouse gas emission effects of biodiesel in the United States with induced land use change impacts. *Bioresource Technology*, *251*, 249–258. https://doi.org/10.1016/j.biortech.2017.12.031

Chen, Y., Xiao, B., Chang, J., Fu, Y., Lv, P., & Wang, X. (2009). Synthesis of biodiesel from waste cooking oil using immobilized lipase in fixed bed reactor. *Energy Conversion and Management*, *50*(3), 668–673. https://doi.org/10.1016/J.ENCONMAN.2008.10.011

Cherubini, F., Jungmeier, G., Cherubini, F., & Jungmeier, G. (2010). LCA FOR AGRICULTURE PRACTICES AND BIOBASED INDUSTRIAL PRODUCTS LCA of a biorefinery concept producing bioethanol, bioenergy, and chemicals from switchgrass. *Int J Life Cycle Assess*, *15*, 53–66. https://doi.org/10.1007/s11367-009-0124-2

Chhetri, A. B., Watts, K. C., & Islam, M. R. (2008). Waste cooking oil as an alternate feedstock for biodiesel production. *Energies*, *1*(1), 3–18. https://doi.org/10.3390/en1010003

Chisti, Y. (2007a). Biodiesel from microalgae. *Biotechnology Advances*, *25*(3), 294–306. https://doi.org/10.1016/J.BIOTECHADV.2007.02.001

Chisti, Y. (2007b). Biodiesel from microalgae. *Biotechnology Advances*, *25*(3), 294–306. https://doi.org/10.1016/J.BIOTECHADV.2007.02.001

Christopher, L. P., Hemanathan Kumar, & Zambare, V. P. (2014). Enzymatic biodiesel: Challenges and opportunities. *Applied Energy*, *119*, 497–520. https://doi.org/10.1016/J.APENERGY.2014.01.017

Dalena, F., Senatore, A., Tursi, A., & Basile, A. (2017). Bioenergy production from second- and third-generation feedstocks. *Bioenergy Systems for the Future: Prospects for Biofuels and Biohydrogen*, 559–599. https://doi.org/10.1016/B978-0-08-101031-0.00017-X

Dalvand, P., & Mahdavian, L. (2018). Calculation of the properties of biodiesel produced from castor seed by eggshell catalyst. *Biofuels*, *9*(6), 705–710. https://doi.org/10.1080/17597269.2017.1302668

De Boer, K. (2010). *Optimised Small Scale Reactor Technology, a new approach for the Australian Biodiesel Industry*.

Degfie, T. A., Mamo, T. T., & Mekonnen, Y. S. (2019). Optimized Biodiesel Production from Waste Cooking Oil (WCO) using Calcium Oxide (CaO) Nano-catalyst. *Scientific Reports*, *9*(1). https://doi.org/10.1038/s41598-019-55403-4

Demirbas, A. (2004). Pyrolysis of municipal plastic wastes for recovery of gasoline-range hydrocarbons. *Journal of Analytical and Applied Pyrolysis*, *72*(1), 97–102. https://doi.org/10.1016/J.JAAP.2004.03.001

Demirbas, A. (2007a). Effect of temperature on pyrolysis products from biomass. *Energy Sources, Part A: Recovery, Utilization and Environmental Effects*, *29*(4), 329–336. https://doi.org/10.1080/009083190965794

Demirbas, A. (2007b). Importance of biodiesel as transportation fuel. *Energy Policy*, *35*(9), 4661–4670. https://doi.org/10.1016/J.ENPOL.2007.04.003

Demirbas, M. F., Balat, M., & Balat, H. (2009). Potential contribution of biomass to the sustainable energy development. *Energy Conversion and Management*, *50*(7), 1746–1760. https://doi.org/10.1016/J.ENCONMAN.2009.03.013

Díaz, O., González, E., Vera, L., Luis, ·, Fernández, J., Díaz-Marrero, A. R., & Fernández, J. J. (n.d.). Recirculating packed-bed biofilm photobioreactor combined with membrane ultrafiltration as advanced wastewater treatment. *Environmental Science and Pollution Research*, *1*, 3. https://doi.org/10.1007/s11356-023-27309-2

Dong, Z., Liu, Z., Shi, J., Tang, H., Xiang, X., Huang, F., & Zheng, M. (2019). Carbon Nanoparticle-Stabilized Pickering Emulsion as a Sustainable and High-Performance Interfacial Catalysis Platform for Enzymatic Esterification/Transesterification. *ACS Sustainable Chemistry and Engineering*, *7*(8), 7619–7629. https://doi.org/10.1021/acssuschemeng.8b05908

Du, L., Li, Z., Ding, S., Chen, C., Qu, S., Yi, W., Lu, J., & Ding, J. (2019). Synthesis and characterization of carbon-based MgO catalysts for biodiesel production from castor oil. *Fuel*, *258*, 116122. https://doi.org/10.1016/J.FUEL.2019.116122

El Sherbiny, S. A., Refaat, A. A., & El Sheltawy, S. T. (2010a). Production of biodiesel using the microwave technique. *Journal of Advanced Research*, *1*(4), 309–314. https://doi.org/10.1016/J.JARE.2010.07.003

El Sherbiny, S. A., Refaat, A. A., & El Sheltawy, S. T. (2010b). Production of biodiesel using the microwave technique. *Journal of Advanced Research*, *1*(4), 309–314. https://doi.org/10.1016/J.JARE.2010.07.003

El yaakouby, I., Rhrissi, I., Abouliatim, Y., Hlaibi, M., & Kamil, N. (2023). Moroccan sardine scales as a novel and renewable source of heterogeneous

catalyst for biodiesel production using palm fatty acid distillate. *Renewable Energy*, *217*, 119223. https://doi.org/10.1016/J.RENENE.2023.119223

Enweremadu, C. C., & Mbarawa, M. M. (2009). Technical aspects of production and analysis of biodiesel from used cooking oil—A review. *Renewable and Sustainable Energy Reviews*, *13*(9), 2205–2224. https://doi.org/10.1016/J.RSER.2009.06.007

Epa, U., & Change Division, C. (1990). *Inventory of U.S. Greenhouse Gas Emissions and Sinks: 1990-2022 – Main Text*. https://www.epa.gov/ghgemissions/inventory-us-greenhouse-gas-emissions-and-

Fan, M., Wu, H., Shi, M., Zhang, P., & Jiang, P. (2019a). Well-dispersive K2OKCl alkaline catalyst derived from waste banana peel for biodiesel synthesis. *Green Energy & Environment*, *4*(3), 322–327. https://doi.org/10.1016/J.GEE.2018.09.004

Fan, M., Wu, H., Shi, M., Zhang, P., & Jiang, P. (2019b). Well-dispersive K2OKCl alkaline catalyst derived from waste banana peel for biodiesel synthesis. *Green Energy & Environment*, *4*(3), 322–327. https://doi.org/10.1016/J.GEE.2018.09.004

Farooq, M., & Ramli, A. (2015). Biodiesel production from low FFA waste cooking oil using heterogeneous catalyst derived from chicken bones. *Renewable Energy*, *76*, 362–368. https://doi.org/10.1016/J.RENENE.2014.11.042

Farooq, M., Ramli, A., & Subbarao, D. (2013). Biodiesel production from waste cooking oil using bifunctional heterogeneous solid catalysts. *Journal of Cleaner Production*, *59*, 131–140. https://doi.org/10.1016/J.JCLEPRO.2013.06.015

Fernandes, U., & Costa, M. (2012). Particle emissions from a domestic pellets-fired boiler. *Fuel Processing Technology*, *103*, 51–56. https://doi.org/10.1016/J.FUPROC.2011.08.020

Fernández, Y., & Menéndez, J. A. (2011). Influence of feed characteristics on the microwave-assisted pyrolysis used to produce syngas from biomass wastes. *Journal of Analytical and Applied Pyrolysis*, *91*(2), 316–322. https://doi.org/10.1016/J.JAAP.2011.03.010

Feyzi, M., Rafiee, H. R., & Jafari, F. (2014). Preparation and characterization of Fe-V/TiO 2-SiO 2 nanocatalyst modified by zinc. In *Bull. Mater. Sci* (Vol. 37, Issue 6).

Flynn, J. H., & Wall, L. A. (n.d.). *General Treatment of the Thermogravimetry of Polymers*.

Foust, T. D., Aden, A., Abhijit, A. E., Ae, D., & Phillips, S. (n.d.). *An economic and environmental comparison of a biochemical and a thermochemical lignocellulosic ethanol conversion processes*. https://doi.org/10.1007/s10570-009-9317-x

Fukuda, H., Kondo, A., & Noda, H. (2001a). Biodiesel fuel production by transesterification of oils. *Journal of Bioscience and Bioengineering*, *92*(5), 405–416. https://doi.org/10.1016/S1389-1723(01)80288-7

Fukuda, H., Kondo, A., & Noda, H. (2001b). Biodiesel fuel production by transesterification of oils. *Journal of Bioscience and Bioengineering*, *92*(5), 405–416. https://doi.org/10.1016/S1389-1723(01)80288-7

Fukuda, H., Kondo, A., & Noda, H. (2001c). Biodiesel fuel production by transesterification of oils. *Journal of Bioscience and Bioengineering*, *92*(5), 405–416. https://doi.org/10.1016/S1389-1723(01)80288-7

Galadima, A., & Muraza, O. (2014). Biodiesel production from algae by using heterogeneous catalysts: A critical review. *Energy*, *78*, 72–83. https://doi.org/10.1016/J.ENERGY.2014.06.018

Gebara, C. H., & Laurent, A. (2023). National SDG-7 performance assessment to support achieving sustainable energy for all within planetary limits. *Renewable and Sustainable Energy Reviews*, *173*. https://doi.org/10.1016/j.rser.2022.112934

Ghenai, C. (n.d.). *Life Cycle Analysis of Wind Turbine; Life Cycle Analysis of Wind Turbine*.

GLOBAL BIOENERGY STATISTICS REPORT. (2023a).

GLOBAL BIOENERGY STATISTICS REPORT. (2023b).

Gog, A., Roman, M., Toşa, M., Paizs, C., & Irimie, F. D. (2012). Biodiesel production using enzymatic transesterification – Current state and perspectives. *Renewable Energy*, *39*(1), 10–16. https://doi.org/10.1016/J.RENENE.2011.08.007

Gohain, M., Devi, A., & Deka, D. (2017a). Musa balbisiana Colla peel as highly effective renewable heterogeneous base catalyst for biodiesel production. *Industrial Crops and Products*, *109*, 8–18. https://doi.org/10.1016/J.INDCROP.2017.08.006

Gohain, M., Devi, A., & Deka, D. (2017b). Musa balbisiana Colla peel as highly effective renewable heterogeneous base catalyst for biodiesel production. *Industrial Crops and Products*, *109*, 8–18. https://doi.org/10.1016/J.INDCROP.2017.08.006

Gohain, M., Devi, A., & Deka, D. (2017c). Musa balbisiana Colla peel as highly effective renewable heterogeneous base catalyst for biodiesel production.

Industrial Crops and Products, *109*, 8–18. https://doi.org/10.1016/J.INDCROP.2017.08.006

Goldberg, M. A., Torresani, E., Safronova, T., Vorobyov, V., Kildeeva, N., Shatalova, T., Toshev, O., Filippov, Y., Dmitrienko, A., Gavlina, O., Chernega, O., Nizhnikova, E., Akhmedov, M., Kukueva, E., & Lyssenko, K. (2022). *Inorganic Powders Prepared from Fish Scales*. https://doi.org/10.3390/ceramics5030037

Gollakota, A. R. K., Kishore, N., & Gu, S. (2018). A review on hydrothermal liquefaction of biomass. *Renewable and Sustainable Energy Reviews*, *81*, 1378–1392. https://doi.org/10.1016/J.RSER.2017.05.178

Gollakota, A. R. K., Volli, V., & Shu, C. M. (2019). Transesterification of waste cooking oil using pyrolysis residue supported eggshell catalyst. *Science of The Total Environment*, *661*, 316–325. https://doi.org/10.1016/J.SCITOTENV.2019.01.165

Guldhe, A., Moura, C. V. R., Singh, P., Rawat, I., Moura, E. M., Sharma, Y., & Bux, F. (2017). Conversion of microalgal lipids to biodiesel using chromium-aluminum mixed oxide as a heterogeneous solid acid catalyst. *Renewable Energy*, *105*, 175–182. https://doi.org/10.1016/J.RENENE.2016.12.053

Gumahin, A. C., Galamiton, J. M., Allerite, M. J., Valmorida, R. S., Laranang, J. R. L., Mabayo, V. I. F., Arazo, R. O., & Ido, A. L. (2019). Response surface optimization of biodiesel yield from pre-treated waste oil of rendered pork from a food processing industry. *Bioresources and Bioprocessing*, *6*(1). https://doi.org/10.1186/s40643-019-0284-2

Hamamci, C., Saydut, A., Tonbul, Y., Kaya, C., & Kafadar, A. B. (2011). Biodiesel production via transesterification from safflower (Carthamus tinctorius L.) seed

oil. *Energy Sources, Part A: Recovery, Utilization and Environmental Effects*, *33*(6), 512–520. https://doi.org/10.1080/15567030903096964

Horan, N., Zahrim, A., Newati, Y., & Editors, W. (n.d.). *Green Energy and Technology Applications and Effluent Treatment Anaerobic Digestion Processes*. http://www.springer.com/series/8059

Hussain, F., Alshahrani, S., Abbas, M. M., Khan, H. M., Jamil, A., Yaqoob, H., Elahi, M., Soudagar, M., Imran, M., Ahmad, M., Munir, M., Cambra Ibáñez, J. F., Laura, V., Cagigal, B., & Pk, A. J. (2021). *catalysts Waste Animal Bones as Catalysts for Biodiesel Production; A Mini Review*. https://doi.org/10.3390/catal11050630

Hussain, F., Alshahrani, S., Abbas, M. M., Khan, H. M., Jamil, A., Yaqoob, H., Soudagar, M. E. M., Imran, M., Ahmad, M., & Munir, M. (2021). Review waste animal bones as catalysts for biodiesel production; a mini review. In *Catalysts* (Vol. 11, Issue 5). MDPI. https://doi.org/10.3390/catal11050630

Hybrid, & Graphics. (n.d.). *World Energy Outlook 2023*. www.iea.org/terms

Issariyakul, T., & Dalai, A. K. (2014). Biodiesel from vegetable oils. *Renewable and Sustainable Energy Reviews*, *31*, 446–471. https://doi.org/10.1016/J.RSER.2013.11.001

Istadi, I., Prasetyo, S. A., & Nugroho, T. S. (2015). Characterization of K2O/CaO-ZnO Catalyst for Transesterification of Soybean Oil to Biodiesel. *Procedia Environmental Sciences*, *23*, 394–399. https://doi.org/10.1016/J.PROENV.2015.01.056

Jacobson, K., Gopinath, R., Meher, L. C., & Dalai, A. K. (2008). Solid acid catalyzed biodiesel production from waste cooking oil. *Applied Catalysis B: Environmental*, *85*(1–2), 86–91. https://doi.org/10.1016/J.APCATB.2008.07.005

Jain, S., & Sharma, M. P. (2010). Prospects of biodiesel from Jatropha in India: A review. *Renewable and Sustainable Energy Reviews*, *14*(2), 763–771. https://doi.org/10.1016/J.RSER.2009.10.005

Jaiswal, K. K., Dutta, S., Banerjee, I., Jaiswal, K. S., Renuka, N., Ratha, S. K., & Jaiswal, A. K. (2024). Valorization of fish processing industry waste for biodiesel production: Opportunities, challenges, and technological perspectives. *Renewable Energy*, *220*, 119601. https://doi.org/10.1016/J.RENENE.2023.119601

Jeswani, H. K., Chilvers, A., & Azapagic, A. (2020). Environmental sustainability of biofuels: A review: Environmental sustainability of biofuels. In *Proceedings of the Royal Society A: Mathematical, Physical and Engineering Sciences* (Vol. 476, Issue 2243). Royal Society Publishing. https://doi.org/10.1098/rspa.2020.0351

Kargbo, D. M. (2010). Biodiesel Production from Municipal Sewage Sludges. *Energy Fuels*, *24*, 2791–2794. https://doi.org/10.1021/ef1001106

Katrin Thommes, V. S. (2014). *Biomass Processing Technologies*. CRC Press.

Kaur, M., Malhotra, R., & Ali, A. (2018). Tungsten supported Ti/SiO2 nanoflowers as reusable heterogeneous catalyst for biodiesel production. *Renewable Energy*, *116*, 109–119. https://doi.org/10.1016/J.RENENE.2017.09.065

Kesserwan, F., Ahmad, M. N., Khalil, M., & El-Rassy, H. (2020). Hybrid CaO/Al2O3 aerogel as heterogeneous catalyst for biodiesel production. *Chemical Engineering Journal*, *385*, 123834. https://doi.org/10.1016/J.CEJ.2019.123834

Khan, H. M., Iqbal, T., Ali, C. H., Yasin, S., & Jamil, F. (2020). Waste quail beaks as renewable source for synthesizing novel catalysts for biodiesel production.

Renewable Energy, *154*, 1035–1043. https://doi.org/10.1016/J.RENENE.2020.03.079

Khatibi, M., Khorasheh, F., & Larimi, A. (2021). Biodiesel production via transesterification of canola oil in the presence of Na–K doped CaO derived from calcined eggshell. *Renewable Energy*, *163*, 1626–1636. https://doi.org/10.1016/J.RENENE.2020.10.039

Knothe, G., & Steidley, K. R. (2009). A comparison of used cooking oils: A very heterogeneous feedstock for biodiesel. *Bioresource Technology*, *100*(23), 5796–5801. https://doi.org/10.1016/J.BIORTECH.2008.11.064

Koh, M. Y., & Tinia, T. I. (2011). A review of biodiesel production from Jatropha curcas L. oil. *Renewable and Sustainable Energy Reviews*, *15*(5), 2240–2251. https://doi.org/10.1016/J.RSER.2011.02.013

Komintarachat, C., & Chuepeng, S. (2010). Methanol-Based Transesterification Optimization of Waste Used Cooking Oil over Potassium Hydroxide Catalyst. *American Journal of Applied Sciences*, *7*(8), 1073–1078.

Kulkarni, M. G., & Dalai, A. K. (2006). Waste cooking oil - An economical source for biodiesel: A review. In *Industrial and Engineering Chemistry Research* (Vol. 45, Issue 9, pp. 2901–2913). https://doi.org/10.1021/ie0510526

Kumar, G., Kumar, D., Singh, S., Kothari, S., Bhatt, S., & Singh, C. P. (2010). Continuous low cost transesterification process for the production of coconut biodiesel. *Energies*, *3*(1), 43–56. https://doi.org/10.3390/en3010043

Kynčlová, P., Upadhyaya, S., & Nice, T. (2020). Composite index as a measure on achieving Sustainable Development Goal 9 (SDG-9) industry-related targets: The SDG-9 index. *Applied Energy*, *265*, 114755. https://doi.org/10.1016/J.APENERGY.2020.114755

Lam, M. K., Jamalluddin, N. A., & Lee, K. T. (2019). Production of Biodiesel Using Palm Oil. *Biomass, Biofuels, Biochemicals: Biofuels: Alternative Feedstocks and Conversion Processes for the Production of Liquid and Gaseous Biofuels*, 539–574. https://doi.org/10.1016/B978-0-12-816856-1.00023-3

Lappi, H., & Alén, R. (2009). Production of vegetable oil-based biofuels—Thermochemical behavior of fatty acid sodium salts during pyrolysis. *Journal of Analytical and Applied Pyrolysis*, *86*(2), 274–280. https://doi.org/10.1016/J.JAAP.2009.07.005

Lappi, H., & Alén, R. (2011). Pyrolysis of vegetable oil soaps—Palm, olive, rapeseed and castor oils. *Journal of Analytical and Applied Pyrolysis*, *91*(1), 154–158. https://doi.org/10.1016/J.JAAP.2011.02.003

Latchubugata, C. S., Kondapaneni, R. V., Patluri, K. K., Virendra, U., & Vedantam, S. (2018). Kinetics and optimization studies using Response Surface Methodology in biodiesel production using heterogeneous catalyst. *Chemical Engineering Research and Design*, *135*, 129–139. https://doi.org/10.1016/J.CHERD.2018.05.022

Lee, C. Y., Sun, W. C., & Li, Y. H. (2022). Biodiesel Economic Evaluation and Biomass Planting Allocation Optimization in Global Supply Chain. *IEEE Transactions on Engineering Management*, *69*(3), 602–615. https://doi.org/10.1109/TEM.2019.2900033

Leung, D. Y. C., Wu, X., & Leung, M. K. H. (2010a). A review on biodiesel production using catalyzed transesterification. *Applied Energy*, *87*(4), 1083–1095. https://doi.org/10.1016/J.APENERGY.2009.10.006

Leung, D. Y. C., Wu, X., & Leung, M. K. H. (2010b). A review on biodiesel production using catalyzed transesterification. *Applied Energy*, *87*(4), 1083–1095. https://doi.org/10.1016/J.APENERGY.2009.10.006

Leung, D. Y. C., Wu, X., & Leung, M. K. H. (2010c). A review on biodiesel production using catalyzed transesterification. *Applied Energy*, *87*(4), 1083–1095. https://doi.org/10.1016/J.APENERGY.2009.10.006

Li, F., Hülsey, M. J., Yan, N., Dai, Y., & Wang, C. H. (2021). Co-transesterification of waste cooking oil, algal oil and dimethyl carbonate over sustainable nanoparticle catalysts. *Chemical Engineering Journal*, *405*, 127036. https://doi.org/10.1016/J.CEJ.2020.127036

Liew, W. H., Hassim, M. H., & Ng, D. K. S. (2014). Review of evolution, technology and sustainability assessments of biofuel production. *Journal of Cleaner Production*, *71*, 11–29. https://doi.org/10.1016/J.JCLEPRO.2014.01.006

Lim, B. Y., Shamsudin, R., Baharudin, B. T. H. T., & Yunus, R. (2015). A review of processing and machinery for Jatropha curcas L. fruits and seeds in biodiesel production: Harvesting, shelling, pretreatment and storage. *Renewable and Sustainable Energy Reviews*, *52*, 991–1002. https://doi.org/10.1016/J.RSER.2015.07.077

Lima, D. G., Soares, V. C. D., Ribeiro, E. B., Carvalho, D. A., Cardoso, É. C. V., Rassi, F. C., Mundim, K. C., Rubim, J. C., & Suarez, P. A. Z. (2004). Diesel-like fuel obtained by pyrolysis of vegetable oils. *Journal of Analytical and Applied Pyrolysis*, *71*(2), 987–996. https://doi.org/10.1016/J.JAAP.2003.12.008

Limmanee, S., Naree, T., Bunyakiat, K., & Ngamcharussrivichai, C. (2013). Mixed oxides of Ca, Mg and Zn as heterogeneous base catalysts for the synthesis of

palm kernel oil methyl esters. *Chemical Engineering Journal*, *225*, 616–624. https://doi.org/10.1016/J.CEJ.2013.03.093

Lin, Y. C., Amesho, K. T. T., Chen, C. E., Cheng, P. C., & Chou, F. C. (2020). A cleaner process for green biodiesel synthesis from waste cooking oil using recycled waste oyster shells as a sustainable base heterogeneous catalyst under the microwave heating system. *Sustainable Chemistry and Pharmacy*, *17*, 100310. https://doi.org/10.1016/J.SCP.2020.100310

Linan, A. and F. A. W. (1993). *Fundamental Aspects of Combustion*. Oxford Academic.

Liu, X., He, H., Wang, Y., Zhu, S., & Piao, X. (2008). Transesterification of soybean oil to biodiesel using CaO as a solid base catalyst. *Fuel*, *87*(2), 216–221. https://doi.org/10.1016/J.FUEL.2007.04.013

López Barreiro, D., Zamalloa, C., Boon, N., Vyverman, W., Ronsse, F., Brilman, W., & Prins, W. (2013). Influence of strain-specific parameters on hydrothermal liquefaction of microalgae. *Bioresource Technology*, *146*, 463–471. https://doi.org/10.1016/J.BIORTECH.2013.07.123

Lotero, E., Liu, Y., Lopez, D. E., Suwannakarn, K., Bruce, D. A., & Goodwin, J. G. (2005). Synthesis of biodiesel via acid catalysis. *Industrial and Engineering Chemistry Research*, *44*(14), 5353–5363. https://doi.org/10.1021/ie049157g

Lotti, M., Pleiss, J., Valero, F., & Ferrer, P. (2018). Enzymatic Production of Biodiesel: Strategies to Overcome Methanol Inactivation. In *Biotechnology Journal* (Vol. 13, Issue 5). Wiley-VCH Verlag. https://doi.org/10.1002/biot.201700155

Ludin, N. A., Mustafa, N. I., Hanafiah, M. M., Ibrahim, M. A., Asri Mat Teridi, M., Sepeai, S., Zaharim, A., & Sopian, K. (2018). Prospects of life cycle assessment

of renewable energy from solar photovoltaic technologies: A review. In *Renewable and Sustainable Energy Reviews* (Vol. 96, pp. 11–28). Elsevier Ltd. https://doi.org/10.1016/j.rser.2018.07.048

Ma, F., & Hanna, M. A. (1999a). Biodiesel production: a review. *Bioresource Technology*, *70*(1), 1–15. https://doi.org/10.1016/S0960-8524(99)00025-5

Ma, F., & Hanna, M. A. (1999b). Biodiesel production: a review. *Bioresource Technology*, *70*(1), 1–15. https://doi.org/10.1016/S0960-8524(99)00025-5

Ma, F., & Hanna, M. A. (1999c). Biodiesel production: a review. *Bioresource Technology*, *70*(1), 1–15. https://doi.org/10.1016/S0960-8524(99)00025-5

Ma, Y., Wang, Q., Sun, X., Wu, C., & Gao, Z. (2017). Kinetics studies of biodiesel production from waste cooking oil using FeCl3-modified resin as heterogeneous catalyst. *Renewable Energy*, *107*, 522–530. https://doi.org/10.1016/J.RENENE.2017.02.007

Maceiras, R., Cancela, A., Vega, M., & Márquez, M. C. (n.d.). *Enzymatic Alholysis For Biodiesel Production From Waste Cooking Oil*.

Magner, E. (2013). Immobilisation of enzymes on mesoporous silicate materials. *Chemical Society Reviews*, *42*(15), 6213–6222. https://doi.org/10.1039/c2cs35450k

Mahalaxmi, S. , and C. W. (2014). *Biochemical conversion of biomass to fuels." Handbook of climate change mitigation and adaptation*. Springer.

Maher, K. D., & Bressler, D. C. (2007). Pyrolysis of triglyceride materials for the production of renewable fuels and chemicals. *Bioresource Technology*, *98*(12), 2351–2368. https://doi.org/10.1016/J.BIORTECH.2006.10.025

Majhi, S., & Ray, S. (2016). A study on production of biodiesel using a novel solid oxide catalyst derived from waste. *Environmental Science and Pollution Research*, *23*(10), 9251–9259. https://doi.org/10.1007/s11356-015-4824-9

Marchetti, J. M., Miguel, V. U., & Errazu, A. F. (2007). Possible methods for biodiesel production. *Renewable and Sustainable Energy Reviews*, *11*(6), 1300–1311. https://doi.org/10.1016/J.RSER.2005.08.006

Mardhiah, H. H., Ong, H. C., Masjuki, H. H., Lim, S., & Lee, H. V. (2017). A review on latest developments and future prospects of heterogeneous catalyst in biodiesel production from non-edible oils. *Renewable and Sustainable Energy Reviews*, *67*, 1225–1236. https://doi.org/10.1016/J.RSER.2016.09.036

Mariod, A. A. (2016). Effect of Essential Oils on Organoleptic (Smell, Taste, and Texture) Properties of Food. *Essential Oils in Food Preservation, Flavor and Safety*, 131–137. https://doi.org/10.1016/B978-0-12-416641-7.00013-4

Martínez, G., Sánchez, N., Encinar, J. M., & González, J. F. (2014). Fuel properties of biodiesel from vegetable oils and oil mixtures. Influence of methyl esters distribution. *Biomass and Bioenergy*, *63*, 22–32. https://doi.org/10.1016/J.BIOMBIOE.2014.01.034

Martínez-Patiño, J. C., Ruiz, E., Romero, I., Cara, C., López-Linares, J. C., & Castro, E. (2017). Combined acid/alkaline-peroxide pretreatment of olive tree biomass for bioethanol production. *Bioresource Technology*, *239*, 326–335. https://doi.org/10.1016/J.BIORTECH.2017.04.102

Meher, L. C., Churamani, C. P., Arif, M., Ahmed, Z., & Naik, S. N. (2013). Jatropha curcas as a renewable source for bio-fuels—A review. *Renewable and Sustainable Energy Reviews*, *26*, 397–407. https://doi.org/10.1016/J.RSER.2013.05.065

Mercer, P., & Armenta, R. E. (n.d.). *Review Article Developments in oil extraction from microalgae**. https://doi.org/10.1002/ejlt.201000455

Mercy Nisha Pauline, J., Sivaramakrishnan, R., Pugazhendhi, A., Anbarasan, T., & Achary, A. (2021). Transesterification kinetics of waste cooking oil and its diesel engine performance. *Fuel*, *285*, 119108. https://doi.org/10.1016/J.FUEL.2020.119108

Meriatna, Husin, H., Riza, M., Faisal, M., Ahmadi, & Sulastri. (2023a). Biodiesel production using waste banana peel as renewable base catalyst. *Materials Today: Proceedings*, *87*, 214–217. https://doi.org/10.1016/J.MATPR.2023.02.400

Meriatna, Husin, H., Riza, M., Faisal, M., Ahmadi, & Sulastri. (2023b). Biodiesel production using waste banana peel as renewable base catalyst. *Materials Today: Proceedings*, *87*, 214–217. https://doi.org/10.1016/J.MATPR.2023.02.400

Miladinović, M. R., Zdujić, M. V., Veljović, D. N., Krstić, J. B., Banković-Ilić, I. B., Veljković, V. B., & Stamenković, O. S. (2020). Valorization of walnut shell ash as a catalyst for biodiesel production. *Renewable Energy*, *147*, 1033–1043. https://doi.org/10.1016/j.renene.2019.09.056

Milne, T. A., Evans, R. J., & Abatzoglou, N. (n.d.). *Biomass Gasifier "Tars": Their Nature, Formation, and Conversion*. http://www.doe.gov/bridge/home.html

Mitaphonna, R., Ramli, M., Maulana, I., Novita, D., Zahara, I., & Wardani, R. (2019a). *International Proceeding ASEAN YOUTH CONFERENCE 2018 PPI-MALAYSIA PREPARATION OF HETEROGENOUS CATALYST OF ACEH COW BONE MATERIAL AND ITS CATALYTIC PERFORMANCE FOR BIODIESEL SYNTHESIS*. https://doi.org/10.5281/zenodo.2549060

Mitaphonna, R., Ramli, M., Maulana, I., Novita, D., Zahara, I., & Wardani, R. (2019b). *International Proceeding ASEAN YOUTH CONFERENCE 2018 PPI-*

MALAYSIA PREPARATION OF HETEROGENOUS CATALYST OF ACEH COW BONE MATERIAL AND ITS CATALYTIC PERFORMANCE FOR BIODIESEL SYNTHESIS. https://doi.org/10.5281/zenodo.2549060

Mokhtar, M. , et al. (2017). Thermochemical characterization of lignocellulosic biomass for sustainable bioenergy production. *Renewable Energy*, *103*, 676–683.

Moraes, P. S., Engelmann, J. I., Igansi, A. V., Sant'Anna Cadaval, T. R., & Antonio de Almeida Pinto, L. (2021). Nile tilapia industrialization waste: Evaluation of the yield, quality and cost of the biodiesel production process. *Journal of Cleaner Production*, *287*, 125041. https://doi.org/10.1016/J.JCLEPRO.2020.125041

Moriarty, P., & Honnery, D. (2019a). Ecosystem maintenance energy and the need for a green EROI. *Energy Policy*, *131*, 229–234. https://doi.org/10.1016/J.ENPOL.2019.05.006

Moriarty, P., & Honnery, D. (2019b). Global renewable energy resources and use in 2050. *Managing Global Warming: An Interface of Technology and Human Issues*, 221–235. https://doi.org/10.1016/B978-0-12-814104-5.00006-5

Mouiya, M., Bouazizi, A., Abourriche, A., El Khessaimi, Y., Benhammou, A., El hafiane, Y., Taha, Y., Oumam, M., Abouliatim, Y., Smith, A., & Hannache, H. (2019). Effect of sintering temperature on the microstructure and mechanical behavior of porous ceramics made from clay and banana peel powder. *Results in Materials*, *4*, 100028. https://doi.org/10.1016/J.RINMA.2019.100028

Mustafa, N., Ibrahim, M. H. I., Asmawi, R., & Amin, A. M. (2015). Hydroxyapatite Extracted from Waste Fish Bones and Scales via Calcination Method. *Applied Mechanics and Materials*, *773–774*, 287–290. https://doi.org/10.4028/www.scientific.net/amm.773-774.287

Muthu, K., & Priya, S. (2017). Green synthesis, characterization and catalytic activity of silver nanoparticles using Cassia auriculata flower extract separated fraction. *Spectrochimica Acta Part A: Molecular and Biomolecular Spectroscopy*, *179*, 66–72. https://doi.org/10.1016/J.SAA.2017.02.024

Najafpour, G., Mohammadi, M., Hassani, M., Najafpour, G. D., & Mohammadi, M. (2016). Transesterification of Waste Cooking Oil to Biodiesel using γ-alumina Coated on Zeolite Pellets. *J. Mater. Environ. Sci*, *7*(4), 1193–1203. https://www.researchgate.net/publication/297704437

Nasreen, S. , N. M. , Q. L. A. , A. M. S. , S. A. , & A. S. D. (2018). Review of catalytic transesterification methods for biodiesel production. *Biofuels: State of Development*, *6*, 93–119.

Nath, B., Kalita, P., Das, B., & Basumatary, S. (2020). Highly efficient renewable heterogeneous base catalyst derived from waste Sesamum indicum plant for synthesis of biodiesel. *Renewable Energy*, *151*, 295–310. https://doi.org/10.1016/J.RENENE.2019.11.029

Navarro, R. M., Guil-Lopez, R., Fierro, J. L. G., Mota, N., Jiménez, S., Pizarro, P., Coronado, J. M., & Serrano, D. P. (2018). Catalytic fast pyrolysis of biomass over Mg-Al mixed oxides derived from hydrotalcite-like precursors: Influence of Mg/Al ratio. *Journal of Analytical and Applied Pyrolysis*, *134*, 362–370. https://doi.org/10.1016/J.JAAP.2018.07.001

Niju, S., Begum, M. M. M. S., & Anantharaman, N. (2014a). Modification of egg shell and its application in biodiesel production. *Journal of Saudi Chemical Society*, *18*(5), 702–706. https://doi.org/10.1016/J.JSCS.2014.02.010

Niju, S., Begum, M. M. M. S., & Anantharaman, N. (2014b). Modification of egg shell and its application in biodiesel production. *Journal of Saudi Chemical Society*, *18*(5), 702–706. https://doi.org/10.1016/J.JSCS.2014.02.010

Norjannah, B., Ong, H. C., Masjuki, H. H., Juan, J. C., & Chong, W. T. (2016). Enzymatic transesterification for biodiesel production: A comprehensive review. In *RSC Advances* (Vol. 6, Issue 65, pp. 60034–60055). Royal Society of Chemistry. https://doi.org/10.1039/c6ra08062f

Obadiah, A., Swaroopa, G. A., Kumar, S. V., Jeganathan, K. R., & Ramasubbu, A. (2012a). Biodiesel production from Palm oil using calcined waste animal bone as catalyst. *Bioresource Technology*, *116*, 512–516. https://doi.org/10.1016/J.BIORTECH.2012.03.112

Obadiah, A., Swaroopa, G. A., Kumar, S. V., Jeganathan, K. R., & Ramasubbu, A. (2012b). Biodiesel production from Palm oil using calcined waste animal bone as catalyst. *Bioresource Technology*, *116*, 512–516. https://doi.org/10.1016/J.BIORTECH.2012.03.112

Okullo, A. A., & Temu, A. K. (2015). Modelling the Kinetics of Jatropha Oil Transesterification. *Energy and Power Engineering*, *07*(04), 135–143. https://doi.org/10.4236/epe.2015.74013

Oladipo, B., & Betiku, E. (2020). Optimization and kinetic studies on conversion of rubber seed (Hevea brasiliensis) oil to methyl esters over a green biowaste catalyst. *Journal of Environmental Management*, *268*, 110705. https://doi.org/10.1016/J.JENVMAN.2020.110705

Osman, A. I., Mehta, N., Elgarahy, A. M., Al-Hinai, A., Ala', ·, Al-Muhtaseb, H., David, ·, & Rooney, W. (2021). *Conversion of biomass to biofuels and life cycle*

assessment: a review. *19*, 4075–4118. https://doi.org/10.1007/s10311-021-01273-0

Otori, A. A., Jimoh, A. A., Mathew, J. T., Otori, A. A., Jimoh, A. A., & Mathew, J. T. (2021). Development of Heterogeneous Catalyst from Waste Cow Bone Using Parinarium Macrophylum Seed Oil for Biodiesel Production. In *Communication in Physical Sciences* (Vol. 7, Issue 3).

Our world in data. (2024, June 20). *World energy consumption by source*. Our World in Data.

Owusu, P. A., & Asumadu-Sarkodie, S. (2016). A review of renewable energy sources, sustainability issues and climate change mitigation. In *Cogent Engineering* (Vol. 3, Issue 1). Cogent OA. https://doi.org/10.1080/23311916.2016.1167990

Ozbay, N., Yargic, A. S., Yarbay Sahin, R. Z., & Yaman, E. (2019). Valorization of banana peel waste via in-situ catalytic pyrolysis using Al-Modified SBA-15. *Renewable Energy*, *140*, 633–646. https://doi.org/10.1016/J.RENENE.2019.03.071

Pandit, P. R., & Fulekar, M. H. (2019). Biodiesel production from microalgal biomass using CaO catalyst synthesized from natural waste material. *Renewable Energy*, *136*, 837–845. https://doi.org/10.1016/J.RENENE.2019.01.047

Perea-Moreno, A.-J., & Kalak, T. (2023). *Citation: Kalak, T. Potential Use of Industrial Biomass Waste as a Sustainable Energy Source in the Potential Use of Industrial Biomass Waste as a Sustainable Energy Source in the Future*. https://doi.org/10.3390/en16041783

Pradhan, P., & Chakraborty, R. (2018). Optimal efficient biodiesel synthesis from used oil employing low-cost ram bone supported Cr catalyst: Engine

performance and exhaust assessment. *Energy*, *164*, 35–45. https://doi.org/10.1016/J.ENERGY.2018.08.181

Prag, A. (2017). *ADBI Working Paper Series TRADE AND SDG 13-ACTION ON CLIMATE CHANGE Asian Development Bank Institute*. https://www.adb.org/publications/trade-

Prasetyo, J., Kusmardini, D., Sa'adah, T. N., Sari, D. P., Dahnum, D., Adelia, N., Kurniati, E., Wibisana, A., Hidayat, H., & Ndruru, S. T. C. L. (2024). Optimization of used cooking oil for biodiesel using CaO-derived of bovine bone catalyst. *South African Journal of Chemical Engineering*, *48*, 95–102. https://doi.org/10.1016/j.sajce.2024.01.008

Puna, J. F., Gomes, J. F., Bordado, J. C., Correia, M. J. N., & Dias, A. P. S. (2014). Biodiesel production over lithium modified lime catalysts: Activity and deactivation. *Applied Catalysis A: General*, *470*, 451–457. https://doi.org/10.1016/J.APCATA.2013.11.022

Rabaçal, M., Ferreira, A. F., & Silva, C. A. M. (n.d.-a). *Lecture Notes in Energy 57 Biorefineries Targeting Energy, High Value Products and Waste Valorisation*. http://www.springer.com/series/8874

Rabaçal, M., Ferreira, A. F., & Silva, C. A. M. (n.d.-b). *Lecture Notes in Energy 57 Biorefineries Targeting Energy, High Value Products and Waste Valorisation*. http://www.springer.com/series/8874

Rashtizadeh, E., Farzaneh, F., & Talebpour, Z. (2014). Synthesis and characterization of Sr3Al2O6 nanocomposite as catalyst for biodiesel production. *Bioresource Technology*, *154*, 32–37. https://doi.org/10.1016/J.BIORTECH.2013.12.014

Rezania, S., Mahdinia, S., Oryani, B., Cho, J., Kwon, E. E., Bozorgian, A., Rashidi Nodeh, H., Darajeh, N., & Mehranzamir, K. (2022). Biodiesel production from

wild mustard (Sinapis Arvensis) seed oil using a novel heterogeneous catalyst of LaTiO3 nanoparticles. *Fuel*, *307*, 121759. https://doi.org/10.1016/J.FUEL.2021.121759

Rezania, S., Oryani, B., Park, J., Hashemi, B., Yadav, K. K., Kwon, E. E., Hur, J., & Cho, J. (2019a). Review on transesterification of non-edible sources for biodiesel production with a focus on economic aspects, fuel properties and by-product applications. *Energy Conversion and Management*, *201*, 112155. https://doi.org/10.1016/J.ENCONMAN.2019.112155

Rezania, S., Oryani, B., Park, J., Hashemi, B., Yadav, K. K., Kwon, E. E., Hur, J., & Cho, J. (2019b). Review on transesterification of non-edible sources for biodiesel production with a focus on economic aspects, fuel properties and by-product applications. *Energy Conversion and Management*, *201*, 112155. https://doi.org/10.1016/J.ENCONMAN.2019.112155

Risso, R., Ferraz, P., Meireles, S., Fonseca, I., & Vital, J. (2018). Highly active Cao catalysts from waste shells of egg, oyster and clam for biodiesel production. *Applied Catalysis A: General*, *567*, 56–64. https://doi.org/10.1016/J.APCATA.2018.09.003

Rizwanul Fattah, I. M., Ong, H. C., Mahlia, T. M. I., Mofijur, M., Silitonga, A. S., Ashrafur Rahman, S. M., & Ahmad, A. (2020a). State of the Art of Catalysts for Biodiesel Production. In *Frontiers in Energy Research* (Vol. 8). Frontiers Media S.A. https://doi.org/10.3389/fenrg.2020.00101

Rizwanul Fattah, I. M., Ong, H. C., Mahlia, T. M. I., Mofijur, M., Silitonga, A. S., Ashrafur Rahman, S. M., & Ahmad, A. (2020b). State of the Art of Catalysts for Biodiesel Production. In *Frontiers in Energy Research* (Vol. 8). Frontiers Media S.A. https://doi.org/10.3389/fenrg.2020.00101

Roschat, W., Siritanon, T., Kaewpuang, T., Yoosuk, B., & Promarak, V. (2016). Economical and green biodiesel production process using river snail shells-derived heterogeneous catalyst and co-solvent method. *Bioresource Technology*, *209*, 343–350. https://doi.org/10.1016/J.BIORTECH.2016.03.038

Roschat, W., Siritanon, T., Yoosuk, B., & Promarak, V. (2016). Biodiesel production from palm oil using hydrated lime-derived CaO as a low-cost basic heterogeneous catalyst. *Energy Conversion and Management*, *108*, 459–467. https://doi.org/10.1016/J.ENCONMAN.2015.11.036

s11746-997-0254-2-2. (n.d.).

Saadatkhah, N., Adrián, |, Garcia, C., Ackermann, S., Leclerc, P., Latifi, | Mohammad, Samih, | Said, Patience, G. S., Chaouki, | Jamal, & Chaouki, J. (2019). *Experimental methods in chemical engineering: Thermogravimetric analysis-TGA*. https://doi.org/10.1002/cjce.23673

Saini, J. K., Saini, R., & Tewari, L. (2015). Lignocellulosic agriculture wastes as biomass feedstocks for second-generation bioethanol production: concepts and recent developments. In *3 Biotech* (Vol. 5, Issue 4, pp. 337–353). Springer Verlag. https://doi.org/10.1007/s13205-014-0246-5

Sait, H. H., Hussain, A., Salema, A. A., & Ani, F. N. (2012). Pyrolysis and combustion kinetics of date palm biomass using thermogravimetric analysis. *Bioresource Technology*, *118*, 382–389. https://doi.org/10.1016/J.BIORTECH.2012.04.081

Sarkar, N., Ghosh, S. K., Bannerjee, S., & Aikat, K. (2012). Bioethanol production from agricultural wastes: An overview. *Renewable Energy*, *37*(1), 19–27. https://doi.org/10.1016/J.RENENE.2011.06.045

Schlögl, R. (2009). Chapter 5 X-ray Diffraction: A Basic Tool for Characterization of Solid Catalysts in the Working State. *Advances in Catalysis*, *52*(C), 273–338. https://doi.org/10.1016/S0360-0564(08)00005-9

Schuchardt, U., Sercheli, R., & Vargas, R. M. (1998). *Transesterification of Vegetable Oils: a Review*.

Schwab, A. W., Bagby, M. O., & Freedman, B. (1987). Preparation and properties of diesel fuels from vegetable oils. *Fuel*, *66*(10), 1372–1378. https://doi.org/10.1016/0016-2361(87)90184-0

Scotchford, C. A. , ; A. S. Y. (1995). Magnesium whitlockite deposition in articular cartilage: a study of 80 specimens from 70 patients. *Annals of the Rheumatic Diseases*, *54(5)*, *54*(5), 339–344.

Semwal, S., Arora, A. K., Badoni, R. P., & Tuli, D. K. (2011). Biodiesel production using heterogeneous catalysts. *Bioresource Technology*, *102*(3), 2151–2161. https://doi.org/10.1016/J.BIORTECH.2010.10.080

Serio, M. Di, Tesser, R., Pengmei, L., & Santacesaria, E. (n.d.). *Heterogeneous Catalysts for Biodiesel Production*. https://doi.org/10.1021/ef700250g

Sharma, M. K., & Kazmi, A. A. (2015). Anaerobic onsite treatment of black water using filter-based packaged system as an alternative of conventional septic tank. *Ecological Engineering*, *75*, 457–461. https://doi.org/10.1016/J.ECOLENG.2014.12.014

Sharma, Y. C., & Singh, B. (2009). Development of biodiesel: Current scenario. *Renewable and Sustainable Energy Reviews*, *13*(6–7), 1646–1651. https://doi.org/10.1016/J.RSER.2008.08.009

Sivabalan, K. ; H. S. ; Y. H. ; P. J. (2021). A review on the characteristic of biomass and classification of bioenergy through direct combustion and gasification as an alternative power supply. *J. Phys. Conf. Ser.*, 1831.

Soares, O. S. G. P., Órfão, J. J. M., Ruiz-Martínez, J., Silvestre-Albero, J., Sepúlveda-Escribano, A., & Pereira, M. F. R. (2010). Pd–Cu/AC and Pt–Cu/AC catalysts for nitrate reduction with hydrogen: Influence of calcination and reduction temperatures. *Chemical Engineering Journal*, *165*(1), 78–88. https://doi.org/10.1016/J.CEJ.2010.08.065

Sobczak, A., Kowalski, Z., & Wzorek, Z. (2009). Preparation of hydroxyapatite from animal bones. In *Acta of Bioengineering and Biomechanics Original Paper* (Vol. 11, Issue 4).

Sreekrishnan, T., Santosh, S., & Kohli, S. (2007). Effect of HRT and Slurry Concentration on Biogas Production in Cattle Dung Based Anaerobic Bioreactors. *Environmental Technology*, *28*(4), 433–442. https://doi.org/10.1080/09593332808618804

Stout, B. A. (n.d.). *Handbook of Energy for World Agriculture*. Elsevier Applied Science: London, UK.

Tada, A. (1975). Basic properties of metal phosphates and their catalytic activity in the decomposition of diacetone alcohol. *Bulletin of the Chemical Society of Japan*, *5*, 1391–1393.

Taherzadeh, M. J., & Karimi, K. (2008). Pretreatment of lignocellulosic wastes to improve ethanol and biogas production: A review. In *International Journal of Molecular Sciences* (Vol. 9, Issue 9, pp. 1621–1651). https://doi.org/10.3390/ijms9091621

Takase, M. (2022). Biodiesel Yield and Conversion Percentage from Waste Frying Oil Using Fish Shell at Elmina as a Heterogeneous Catalyst and the Kinetics of the Reaction. *International Journal of Chemical Engineering*, *2022*. https://doi.org/10.1155/2022/8718638

Talebian-Kiakalaieh, A., Amin, N. A. S., & Mazaheri, H. (2013). A review on novel processes of biodiesel production from waste cooking oil. *Applied Energy*, *104*, 683–710. https://doi.org/10.1016/J.APENERGY.2012.11.061

Tan, Y. H., Abdullah, M. O., Nolasco-Hipolito, C., & Taufiq-Yap, Y. H. (2015a). Waste ostrich- and chicken-eggshells as heterogeneous base catalyst for biodiesel production from used cooking oil: Catalyst characterization and biodiesel yield performance. *Applied Energy*, *160*, 58–70. https://doi.org/10.1016/J.APENERGY.2015.09.023

Tan, Y. H., Abdullah, M. O., Nolasco-Hipolito, C., & Taufiq-Yap, Y. H. (2015b). Waste ostrich- and chicken-eggshells as heterogeneous base catalyst for biodiesel production from used cooking oil: Catalyst characterization and biodiesel yield performance. *Applied Energy*, *160*, 58–70. https://doi.org/10.1016/J.APENERGY.2015.09.023

Tanger, P., Field, J. L., Jahn, C. E., Defoort, M. W., Leach, J. E., Hazen, S. P., Debolt, S., & Allison, G. G. (2013). *Biomass for thermochemical conversion: targets and challenges*. https://doi.org/10.3389/fpls.2013.00218

Tariq, M., Ali, S., & Khalid, N. (2012). Activity of homogeneous and heterogeneous catalysts, spectroscopic and chromatographic characterization of biodiesel: A review. *Renewable and Sustainable Energy Reviews*, *16*(8), 6303–6316. https://doi.org/10.1016/J.RSER.2012.07.005

Teo, S. H., Rashid, U., Thomas Choong, S. Y., & Taufiq-Yap, Y. H. (2017). Heterogeneous calcium-based bimetallic oxide catalyzed transesterification of Elaeis guineensis derived triglycerides for biodiesel production. *Energy Conversion and Management*, *141*, 20–27. https://doi.org/10.1016/J.ENCONMAN.2016.03.042

Terza Anokye-Poku Regina, B. (2022). *CO2 EMISSIONS REDUCTION THROUGH CATALYTIC PRODUCTION & USE OF FUELS DERIVED FROM BIOMASS*.

Tursi, A. (2019a). A review on biomass: Importance, chemistry, classification, and conversion. In *Biofuel Research Journal* (Vol. 6, Issue 2, pp. 962–979). Green Wave Publishing of Canada. https://doi.org/10.18331/BRJ2019.6.2.3

Tursi, A. (2019b). A review on biomass: Importance, chemistry, classification, and conversion. In *Biofuel Research Journal* (Vol. 6, Issue 2, pp. 962–979). Green Wave Publishing of Canada. https://doi.org/10.18331/BRJ2019.6.2.3

Uddin, M. N., Techato, K., Taweekun, J., Rahman, M., Rasul, M. G., Mahlia, T. M. I., & Ashrafur, S. M. (2018). *An Overview of Recent Developments in Biomass Pyrolysis Technologies*. https://doi.org/10.3390/en11113115

Uğuz, G., Musafer, M., & Alwahidhawi, O. (2021). *An Alternative Heterogeneous Catalyst Synthesis From Seabass (Dicentrarchus Labrax) Scales for Biodiesel Production*. https://doi.org/10.21203/rs.3.rs-678657/v1

Valladares-Diestra, K. , de S. V. L. P. , & S. C. R. (2020). Oilseed enzymatic pretreatment for efficient oil recovery in biodiesel production industry: A review. *BioEnergy Research*, *13*, 1016–1030.

Venkatesan, J., & Kim, S. K. (1996). Effect of Temperature on Isolation and Characterization of Hydroxyapatite from Tuna (Thunnus obesus) Bone. *Materials*, *3*, 4761–4772. https://doi.org/10.3390/ma3104761

Viriya-Empikul, N., Krasae, P., Nualpaeng, W., Yoosuk, B., & Faungnawakij, K. (2012). Biodiesel production over Ca-based solid catalysts derived from industrial wastes. *Fuel*, *92*(1), 239–244. https://doi.org/10.1016/J.FUEL.2011.07.013

Vitidsant, R., Kodama, S., & Sekiguchi, H. (2021). Transesterification using ultrasonic spray of triolein containing CaO particles into methanol vapor in a 3-phase reactor. *Processes*, *9*(1), 1–11. https://doi.org/10.3390/pr9010181

Vyazovkin, S., Burnham, A. K., Criado, J. M., Pérez-Maqueda, L. A., Popescu, C., & Sbirrazzuoli, N. (2011). ICTAC Kinetics Committee recommendations for performing kinetic computations on thermal analysis data. *Thermochimica Acta*, *520*(1–2), 1–19. https://doi.org/10.1016/J.TCA.2011.03.034

Wang, Y., Ou, S., Liu, P., Xue, F., & Tang, S. (2006). Comparison of two different processes to synthesize biodiesel by waste cooking oil. *Journal of Molecular Catalysis A: Chemical*, *252*(1–2), 107–112. https://doi.org/10.1016/J.MOLCATA.2006.02.047

Wei, Z., Xu, C., & Li, B. (2009). Application of waste eggshell as low-cost solid catalyst for biodiesel production. *Bioresource Technology*, *100*(11), 2883–2885. https://doi.org/10.1016/J.BIORTECH.2008.12.039

Wu, S., Li, H., Zhou, X., Liang, P., Zhang, X., Jiang, Y., & Huang, X. (2016). A novel pilot-scale stacked microbial fuel cell for efficient electricity generation and wastewater treatment. *Water Research*, *98*, 396–403. https://doi.org/10.1016/J.WATRES.2016.04.043

Yang, H., Yan, R., Chen, H., Lee, D. H., & Zheng, C. (2007). Characteristics of hemicellulose, cellulose and lignin pyrolysis. *Fuel*, *86*(12–13), 1781–1788. https://doi.org/10.1016/J.FUEL.2006.12.013

Yaşar, F. (2019). Biodiesel production via waste eggshell as a low-cost heterogeneous catalyst: Its effects on some critical fuel properties and comparison with CaO. *Fuel*, *255*, 115828. https://doi.org/10.1016/J.FUEL.2019.115828

Yoo, S. J., Lee, H. shik, Veriansyah, B., Kim, J., Kim, J. D., & Lee, Y. W. (2010). Synthesis of biodiesel from rapeseed oil using supercritical methanol with metal oxide catalysts. *Bioresource Technology*, *101*(22), 8686–8689. https://doi.org/10.1016/J.BIORTECH.2010.06.073

Yu, G. Y. Z. L. S. T. F. and Z. W. (2011). Distributions of carbon and nitrogen in the products from hydrothermal liquefaction of low-lipid microalgae. *Energy & Environmental Science* , *4*, 4587–4595.

Yusuf, N. N. A. N., Kamarudin, S. K., & Yaakub, Z. (2011). Overview on the current trends in biodiesel production. *Energy Conversion and Management*, *52*(7), 2741–2751. https://doi.org/10.1016/J.ENCONMAN.2010.12.004

Zabeti, M., Daud, W. M. A. W., & Aroua, M. K. (2010). Biodiesel production using alumina-supported calcium oxide: An optimization study. *Fuel Processing Technology*, *91*(2), 243–248. https://doi.org/10.1016/J.FUPROC.2009.10.004

Zabeti, M., Wan Daud, W. M. A., & Aroua, M. K. (2009). Activity of solid catalysts for biodiesel production: A review. *Fuel Processing Technology*, *90*(6), 770–777. https://doi.org/10.1016/J.FUPROC.2009.03.010

Zaki, M. I., Knözinger, † H, & Tesche, B. (2006). *Structural and Morphological Consequences of High-Temperature Treatments of Hydroxyapatite in the Absence or Presence of HCl Vapor*. https://doi.org/10.1021/la051644t

Zamani Abyaneh, E., Zarghami, R., Krühne, U., Rosinha Grundtvig, I. P., Ramin, P., & Mostoufi, N. (2022). Mixing assessment of an industrial anaerobic digestion

reactor using CFD. *Renewable Energy*, *192*, 537–549. https://doi.org/10.1016/J.RENENE.2022.04.147

Zamani, N., Ganjifar, A., Karrabi, M., Shahnavaz, B., & Dewil, R. (n.d.). *Bioconversion of Lignocellulosic Biomass Wastes to Energy through Anaerobic Co-2 Digestion with Sewage Sludge (An Experimental and Kinetic-based Study) 3 4*. https://ssrn.com/abstract=4807776

Zhang, S., Wang, H., Liu, J., & Bao, C. (2020). Measuring the specific surface area of monolayer graphene oxide in water. *Materials Letters*, *261*, 127098. https://doi.org/10.1016/J.MATLET.2019.127098

Zhang, Y., Dubé, M. A., McLean, D. D., & Kates, M. (2003). Biodiesel production from waste cooking oil: 2. Economic assessment and sensitivity analysis. *Bioresource Technology*, *90*(3), 229–240. https://doi.org/10.1016/S0960-8524(03)00150-0

Zhang, Z., & Verykios, X. E. (1996). Carbon dioxide reforming of methane to synthesis gas over Ni/La2O3 catalysts. *Applied Catalysis A: General*, *138*(1), 109–133. https://doi.org/10.1016/0926-860X(95)00238-3

Zhao, C., Yang, L., Xing, S., Luo, W., Wang, Z., & Lv, P. (2018). Biodiesel production by a highly effective renewable catalyst from pyrolytic rice husk. *Journal of Cleaner Production*, *199*, 772–780. https://doi.org/10.1016/J.JCLEPRO.2018.07.242

APPENDICES

Appendix A: Calculation of amounts or reactants, catalyst, biodiesel yield and acid value

A 200g fixed amount of waste cooking oil was used for all experimental runs. The amount of ethanol was then calculated based on the required ethanol to oil ratio. For an x:1 ethanol to il ratio the required ethanol mass is calculated as follows.

$$n_{oil} = \frac{m_{oil}}{MW_{oil}}$$

$$n_{ethanol} = \frac{m_{ethanol}}{MW_{ethanol}}$$

$$\frac{n_{ethanol}}{n_{oil}} = \frac{x}{1} = \frac{m_{ethanol} * MW_{oil}}{MW_{ethanol} * m_{oil}}$$

$$m_{ethanol} = \frac{x * MW_{ethanol} * m_{oil}}{MW_{oil}}$$

For a 95% ethanol concentration the require mass is given by

$$m_{ethanol} = \frac{100 * x * MW_{ethanol} * m_{oil}}{95 * MW_{oil}}$$

Where MW is the molar mass, n is number of moles and m is the mass.

The molar mass of ethanol is 46.068g/mol and that of the waste cooking oil is 848.6621g/mol.

Therefore, for a 15:1 ethanol to oil ratio, the required mass of ethanol is,

$$m_{ethanol} = \frac{100 * x * MW_{ethanol} * m_{oil}}{95 * MW_{oil}}$$

$$m_{ethanol} = \frac{100 * 15 * 46.068 * 200}{95 * 848.6621}$$

$$m_{ethanol} = 171.42g\ of\ ethanol$$

The amount of catalyst for each run was calculated as a percentage of the mass of waste cooking oil. For an x wt% catalyst dosage, the mass of catalyst used is.

$$m_{catalyst} = \frac{x}{100} * m_{oil}$$

For a 2wt% catalyst dosage, and 200g waste cooking oil amount, the actual mass of catalyst is.

$$m_{catalyst} = \frac{x}{100} * m_{oil}$$

$$m_{catalyst} = \frac{2}{100} * 200$$

$$m_{catalyst} = 4g\ of\ catalyst$$

The biodiesel yield is calculated using the equation below.

$$Biodiesesl\ yield = \frac{m_{biodiesel}}{m_{oil}} * 100\%$$

For an obtained biodiesel mass of 153.067g the biodiesel yields is.

$$Biodiesesl\ yield = \frac{m_{biodiesel}}{m_{oil}} * 100\%$$

$$Biodiesesl\ yield = \frac{153.067}{200} * 100\%$$

$$Biodiesesl\ yield = 76.53\%$$

The acid value was obtained by using the average titre value of two titrations.

The acid values were calculated using the equation below.

$$Acid\ value = \frac{Concentration\ of\ KOH * Molar\ mass\ of\ KOH * Titre\ value\ (ml)}{mass\ of\ oil\ (g)}$$

A 0.1M KOH concentration was used and the molar mass of KOH is 56.1g/mol. For a biodiesel sample with 0.1ml and 0.1ml recorded titre values and a 5.0145g average sample mass, the avid values obtained are calculated as.

$$Acid\ value = \frac{Concentration\ of\ KOH * Molar\ mass\ of\ KOH * Titre\ value\ (ml)}{mass\ of\ oil\ (g)}$$

$$Acid\ value = \frac{0.1 * 56.1 * 0.1}{5.0145}$$

$$Acid\ value = 0.1119 mgKOH/g$$

Appendix B: Calculation of the amounts of precursors for Inorganic equivalent of banana peel synthesis

BPIn 3 catalyst was prepared via co-impregnation of 10 precursors. The amount of each precursor required to prepare 10g of catalyst is outlined below.

Table B-1: Amount summary

Component	Literature amount (%)	Amount in this work (%)	Mass in catalyst
K_2O	65.11	68.737	6.87g
SiO_2	10.864	11.469	1.15g
CaO	7.787	8.221	0.82g
P_2O_5	6.068	6.406	0.64g
MgO	2.472	2.610	0.26g
Fe_2O_3	1.152	1.216	0.12g
Al_2O_3	0.737	0.778	0.08g
MnO	0.227	0.240	0.02g
CuO	0.192	0.203	0.02g
ZnO	0.114	0.120	0.02g
Total	94.723	100	10g

1. *K_2O precursor (KNO_3) amount calculation*

$$2KNO_3 + {}^1/_2\, O_2 \rightarrow K_2O + 2NO_3$$

$$\frac{n(K_2O)}{n(KNO_3)} = \frac{1}{2}$$

$$m(KNO_3) = \frac{2 * m(K_2O) * M(KNO_3)}{M(K_2O)}$$

$$m(KNO_3) = \frac{2 * 6.87 * 101.10}{94.196}$$

$$m(KNO_3) = 14.7471g$$

2. *SiO_2 precursor (SiO_2) amount calculation*

   Since the precursor used is already in the actual expected final catalyst and does not undergo any reaction during the preparation stages the amount required is 1.15g

3. *CaO precursor ($Ca(NO_3)_2.4H_2O$) amount calculation*

$$Ca(NO_3)_2.4H_2O \rightarrow CaO + 2NO_2 + 4H_2O + {}^1/_2\, O_2$$

$$m(Ca(NO_3)_2.4H_2O) = \frac{m(CaO) * M(Ca(NO_3)_2.4H_2O)}{M(CaO)}$$

$$m(Ca(NO_3)_2.4H_2O) = \frac{0.82 * 236.15}{56.0774}$$

$$m(Ca(NO_3)_2.4H_2O) = 3.45g$$

4. *P_2O_5 precursor (H_3PO_4) amount calculation*

$$m(H_3PO_4) = \frac{2 * m(P_2O_5) * M(H_3PO_4)}{M(P_2O_5)}$$

$$m(H_3PO_4) = \frac{2 * 0.64 * 98}{141.9445}$$

$$m(H_3PO_4) = 0.8837g$$

5. *MgO precursor ($Mg(NO_3)_2.6H_2O$) amount calculation*

$$Mg(NO_3)_2.6H_2O \rightarrow MgO + 2NO_2 + 6H_2O + {}^1/_2\, O_2$$

$$m(Mg(NO_3)_2.6H_2O) = \frac{m(MgO) * M(Mg(NO_3)_2.6H_2O)}{M(MgO)}$$

$$m(Mg(NO_3)_2.6H_2O) = \frac{0.26 * 256.41}{40.3044}$$

$$m(Mg(NO_3)_2.6H_2O) = 1.6541g$$

6. *Fe_2O_3 precursor (Fe_2O_3) amount calculation*

Since the precursor used is already in the actual expected final catalyst and does not undergo any reaction during the preparation stages the amount required is 0.12g

7. *Al_2O_3 precursor ($Al(NO_3)_3.9H_2O$) amount calculation*

$$2Al(NO_3)_3.9H_2O \rightarrow Al_2O_3 + 6NO_2 + 9H_2O + {}^3/_2\, O_2$$

$$m(Al(NO_3)_3.9H_2O) = \frac{2 * m(Al_2O_3) * M(Al(NO_3)_3.9H_2O)}{M(Al_2O_3)}$$

$$m(Al(NO_3)_3.9H_2O) = \frac{2 * 0.08 * 375.134}{101.96}$$

$$m(Al(NO_3)_3.9H_2O) = 0.5887g$$

8. *MnO precursor (MnO) amount calculation*

Since the precursor used is already in the actual expected final catalyst and does not undergo any reaction during the preparation stages the amount required is 0.02g

9. *CuO precursor ($Cu(NO_3)_2.H_2O$) amount calculation*

$$Cu(NO_3)_2.H_2O \rightarrow CuO + 2NO_2 + H_2O + {}^1/_2\, O_2$$

$$m(Cu(NO_3)_2.H_2O) = \frac{m(CuO) * M(Cu(NO_3)_2.H_2O)}{M(CuO)}$$

$$m(Cu(NO_3)_2.H_2O) = \frac{0.02 * 232.59}{79.545}$$

$$m(Cu(NO_3)_2.H_2O) = 0.0585g$$

10. *ZnO precursor ($Zn(NO_3)_2.6H_2O$) amount calculation*

$$Zn(NO_3)_2.6H_2O \rightarrow ZnO + 2NO_2 + 6H_2O + {}^1/_2\, O_2$$

$$m(Zn(NO_3)_2.6H_2O) = \frac{m(ZnO) * M(Zn(NO_3)_2.6H_2O)}{M(CuO)}$$

$$m(Zn(NO_3)_2.6H_2O) = \frac{0.02 * 297.49}{81.38}$$

$$m(Zn(NO_3)_2.6H_2O) = 0.0731g$$

Appendix C: Calculation of kinetic parameters

The kinetic regression was carried out using NLReg software with data and results resented below.

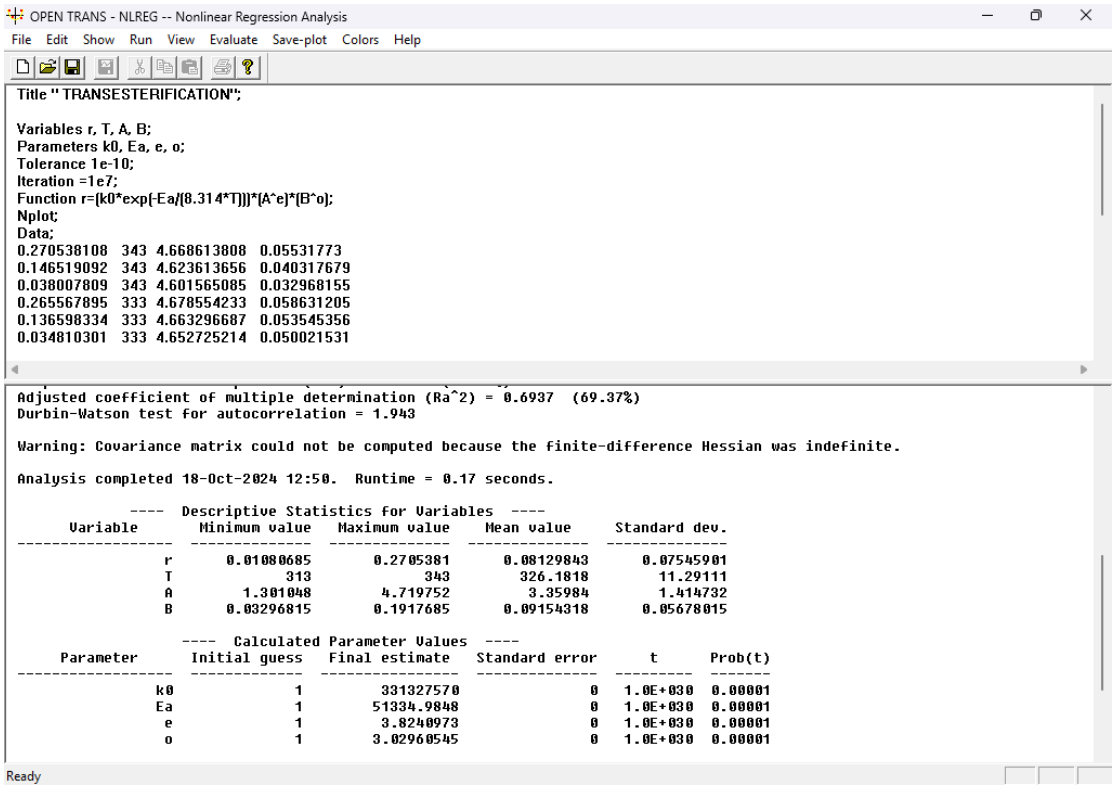

Figure C-1: Data for NLReg analysis

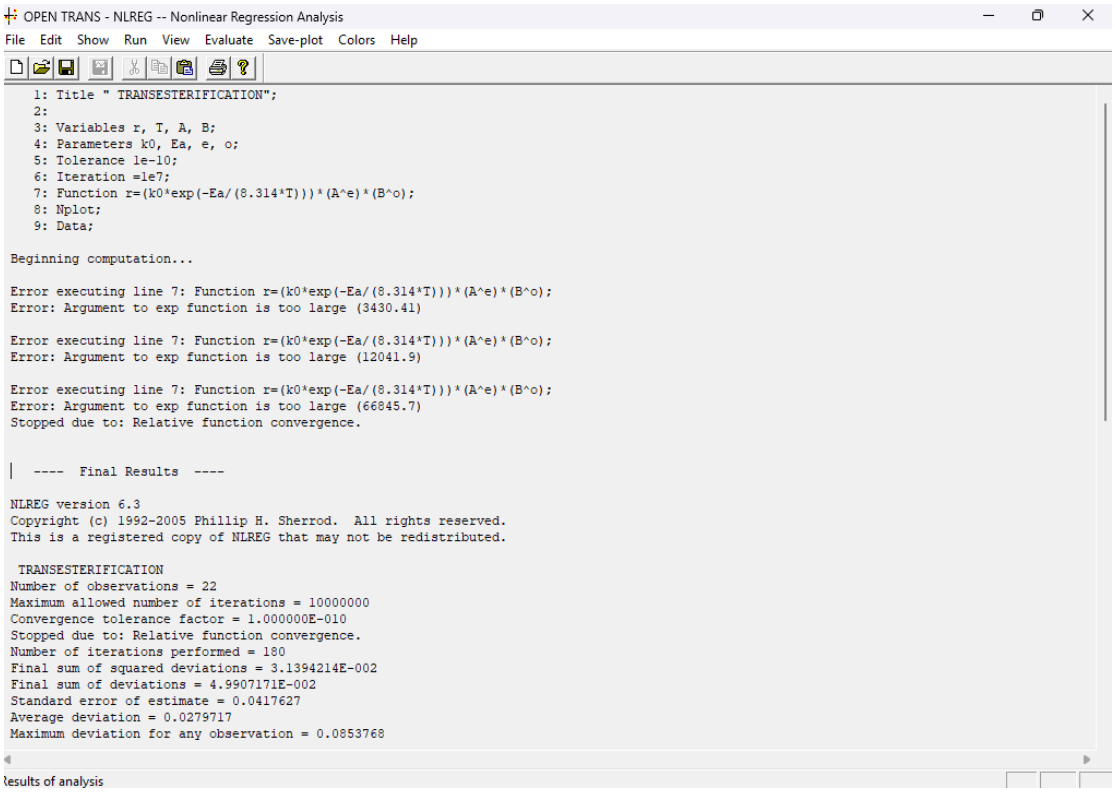

Figure C-2: NLReg result sheet 1

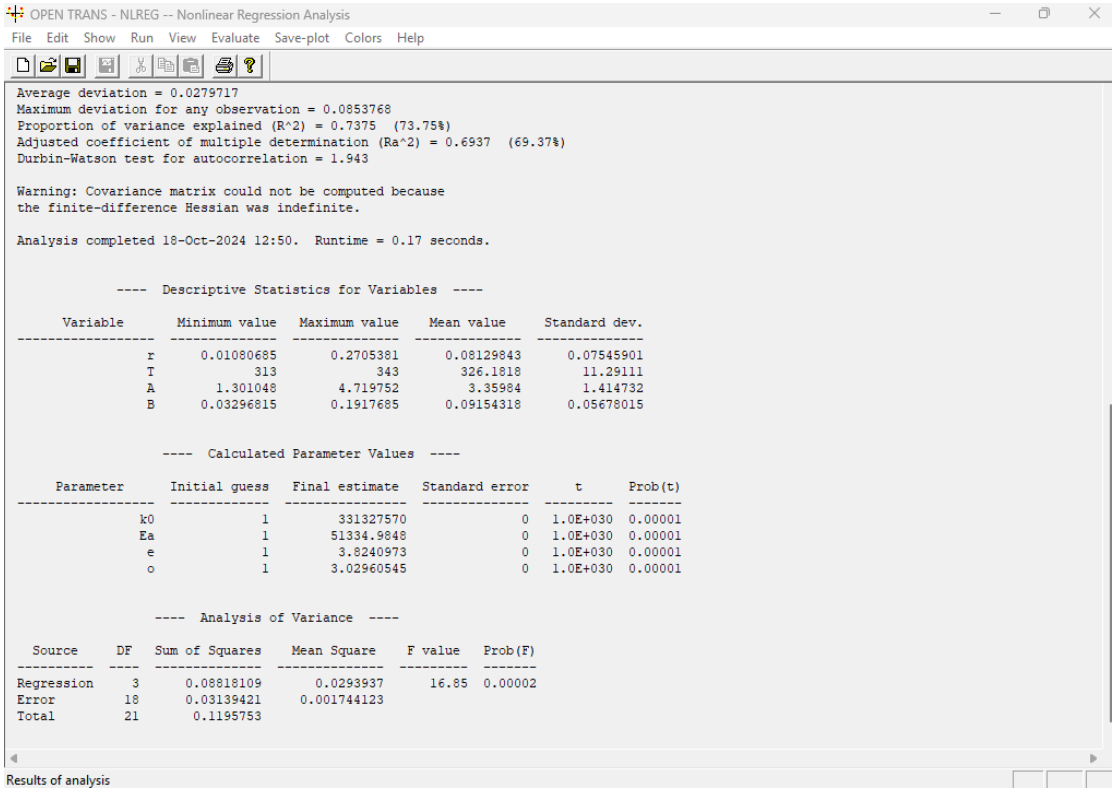

Figure C-3: NLReg results sheet 2

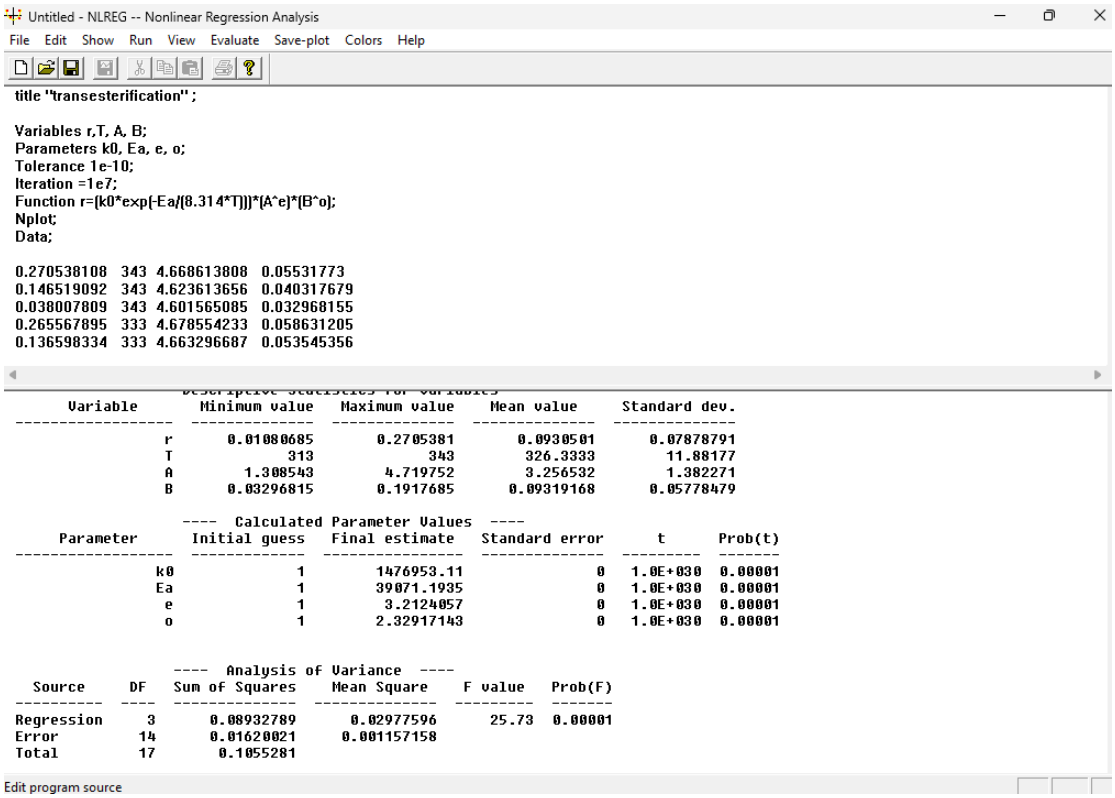

Figure C-4: NLReg results for Model 2

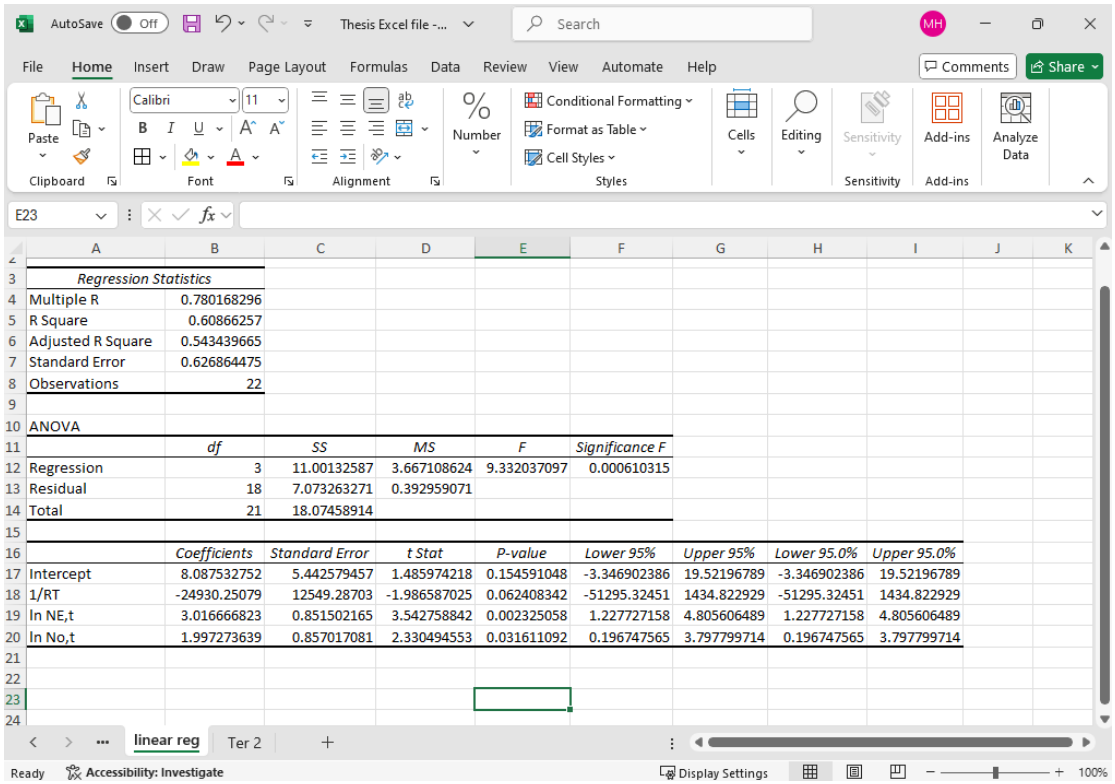

Figure C-5: MS excel obtained Linear regression results